AD-A122 940 MATHEMATICAL STRUCTURE OF ELECTROMAGNETIC TERRAIN FEATURE CANOPY MODELS(U) COLORADO STATE UNIV FORT COLLINS COLL OF FORESTRY AND NATURAL.. J A SMITH

1/2

UNCLASSIFIED NOV 82 ARO-16628.5-GS DAAG29-79-C-0199 F/G 12/1 NL

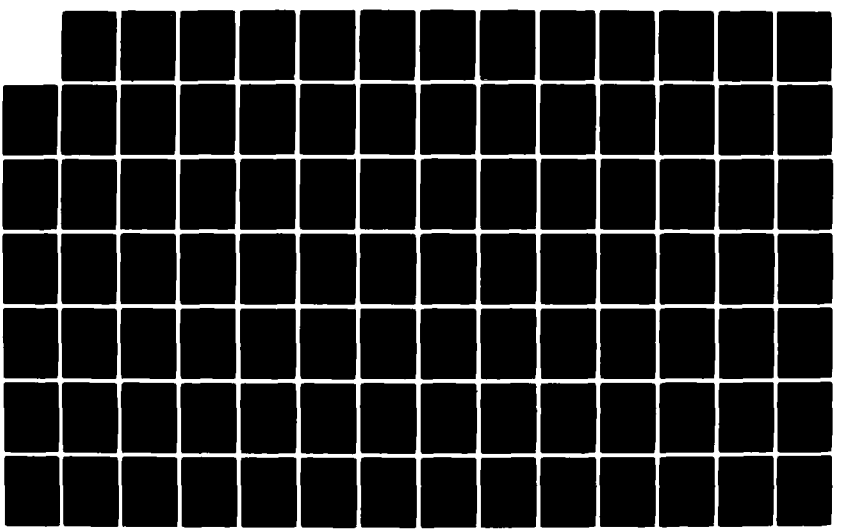

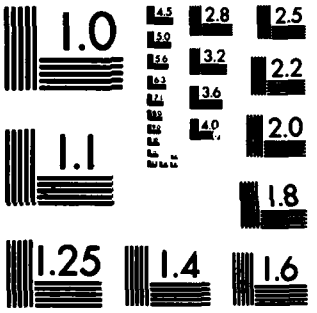

MATHEMATICAL STRUCTURE OF ELECTROMAGNETIC TERRAIN

FEATURE CANOPY MODELS

FINAL REPORT

J. A. Smith

November, 1982

U.S. ARMY RESEARCH OFFICE

Grant Number: DAAG29-79-C-0199

College of Forestry and Natural Resources

Colorado State University

Fort Collins, Colorado 80523

APPROVED FOR PUBLIC RELEASE;
DISTRIBUTION UNLIMITED

THE VIEW, OPINIONS, AND/OR FINDINGS CONTAINED IN THIS REPORT ARE THOSE OF THE AUTHOR(S) AND SHOULD NOT BE CONSTRUED AS AN OFFICIAL DEPARTMENT OF THE ARMY POSITION, POLICY, OR DECISION, UNLESS SO DESIGNATED BY OTHER DOCUMENTATION.

UNCLASSIFIED

SECURITY CLASSIFICATION OF THIS PAGE (When Data Entered)

REPORT DOCUMENTATION PAGE		READ INSTRUCTIONS BEFORE COMPLETING FORM
1. REPORT NUMBER	2. GOVT ACCESSION NO. AD-A122940	3. RECIPIENT'S CATALOG NUMBER
4. TITLE (and Subtitle) Mathematical Structure of Electrogagnetic Terrain Feature Canopy Models		5. TYPE OF REPORT & PERIOD COVERED Final Report 09/79 - 09/82
		6. PERFORMING ORG. REPORT NUMBER
7. AUTHOR(s) J. A. Smith		8. CONTRACT OR GRANT NUMBER(s) DAAG 29-79-C-0199
9. PERFORMING ORGANIZATION NAME AND ADDRESS College of Forestry and Natural Resources Colorado State University Fort Collins, Colorado 80523		10. PROGRAM ELEMENT, PROJECT, TASK AREA & WORK UNIT NUMBERS
11. CONTROLLING OFFICE NAME AND ADDRESS U.S. Army Research Office Post Office Box 12211 Research Triangle Park, N.C . 27709		12. REPORT DATE November 1982
		13. NUMBER OF PAGES 90
14. MONITORING AGENCY NAME & ADDRESS(if different from Controlling Office)		15. SECURITY CLASS. (of this report) Unclassified
		15a. DECLASSIFICATION/DOWNGRADING SCHEDULE NA

16. DISTRIBUTION STATEMENT (of this Report)

Approved for public release; distribution unlimited

17. DISTRIBUTION STATEMENT (of the abstract entered in Block 20, if different from Report)

NA

18. SUPPLEMENTARY NOTES The view, opinions, and/or findings contained in this report are those of the author(s) and should not be construed as an official department of the Army position, policy, or decision, unless so designated by other documentation.

19. KEY WORDS (Continue on reverse side if necessary and identify by block number)

Remote sensing, thermal terrain modeling, radiative transfer calculations, reflectance, background electromagnetic signatures.

20. ABSTRACT (Continue on reverse side if necessary and identify by block number)

The primary objective of the work undertaken in this project was to review the mathematical structure and physical concepts inherent in optical electrogagnetic vegetation canopy models. New formulations of both reflective and thermal exitance models were developed which factor canopy geometric dependent-terms from basic optical properties. A computationally efficient

DD FORM 1 JAN 73 1473 EDITION OF 1 NOV 65 IS OBSOLETE

UNCLASSIFIED

SECURITY CLASSIFICATION OF THIS PAGE (When Data Entered)

implementation of the Adding Method for canopy reflectance was effected as well as tractible solutions to the Duntley equations which incorporate the complete leaf slope distribution in the calculation of the direct flux extinction coefficients.

Several comparisons between various models are made both for theoretical canopies and field data. In addition several issues related to such comparisons are addressed. The report directs the reader to the reviewed literature for several of the major conclusions of the study. Within the body of the report, a detailed discussion of reflective modeling for plane parallel vegetation canopies is presented with particular attention to the calculation of media scattering properties in terms of the distribution of canopy scattering facets.

FOREWORD

The three-year effort described in this report and other publications (Appendix A) was funded by the U.S. Army Research Office under Grant Number DAAG29-79-C-0199 and directed by Dr. James A. Smith, Principal Investigator, Colorado State University. Dr. Steve Mock of the Terrestrial Sciences Branch, was the Technical Monitor.

Dr. S. Youkhana received the Doctor of Philosophy degree, in part, for the work reported here. Other project personnel included Dr. C. Nikolopoulos and Mr. Herb Randolph, Graduate Research Assistants in the Department of Mathematics and Forest and Wood Sciences. In addition, cooperative assistance was provided by Mr. Kevin Cooper, Graduate Research Assistant, Department of Forest and Wood Sciences, who was funded under a NASA Graduate Researchers Fellowship.

Also during this reporting period, Dr. Lee Balick from the Department of Forest and Wood Sciences was on an Intergovernmental Personnel Assignment at the U.S. Army Waterways Experiment Station where he provided cooperative assistance relative to our thermal modeling work.

TABLE OF CONTENTS

LIST OF SYMBOLS

Symbol	Unit	Explanation
A, LAI		Leaf area index
$\bar{A}$, $\hat{n}$		Vector area of individual canopy element
A_h	m^2	Mean projection of actual leaf area index on horizontal surface
A_s	m^2	Soil surface area above which foliage area measured
b	m	Canopy bottom
E	$w \cdot m^{-2}$	Irradiance (incident flux density on unit area)
E_s	$w \cdot m^{-2}$	Incident direct solar irradiance
E(+d)	$w \cdot m^{-2}$	Upward diffuse irradiance
E(-d)	$w \cdot m^{-2}$	Downward diffuse irradiance
$f(\theta_a)$, $S(\theta_n)$		Leaf slope distribution function
H		Leaf area index projected in horizontal plane
I	$w \cdot Sr^{-1}$	Downward isotropic light intensity at leaf area index A(x)
I_o	$w \cdot Sr^{-1}$	Isotropic light intensity on horizontal surface at the canopy top
K, K´, α_{33}	m^{-1}	Direct flux extinction coefficient
$\hat{K}'$		Vector of reflected light
L_{E_S}	$w \cdot m^{-2} \cdot Sr^{-1}$	Direct incident (reflected) radiance
L_E(+d)	$w \cdot m^{-2} \cdot Sr^{-1}$	Apparent radiance from the canopy due to upward diffuse flux
L_E(-d)	$w \cdot m^{-2} \cdot Sr^{-1}$	Apparent radiance from the canopy due to downward diffusion flux

Symbol	Unit	Explanation
ΔL	$w \cdot m^{-2} \cdot Sr^{-1}$	Change in radiance
P_+, P_-	$w \cdot m^{-2} \cdot Sr^{-1}$	Average of upward and downard (power)
$\bar{R}$, $\hat{K}$	m^{-1}	Unit vector in the direction of source
u, u_1	m^{-1}	Scattering coefficient for conversion of upward diffuse flux into directional radiance
V		Leaf area index projected in vertical Cartesian coordinates
v, v_1	m^{-1}	Scattering coefficient for conversion downward diffuse flux into directional radiance
w, w_1, w'	m^{-1}	Bidirectional scattering coefficent for conversion of direct solar flux into directional radiance
α_{11}, α_{22}	m^{-1}	Attenuation coefficient for diffuse fluxes
α_{12}, α_{21}	m^{-1}	Scattering coefficient for diffuse fluxes
α_{13}	m^{-1}	Scattering coefficient for conversion of direct flux into upward diffuse flux
α_{23}	m^{-1}	Scattering coefficient for conversion of direct flux into downward diffuse flux
α_c, α_c'	radian	Azimuth of a ray for which the sine of incidence and scattering is zero respectively
β	radian	Leaf inclination angle
$\vec{\varepsilon}$		Unit vector in the x, y, and z directions
$\varepsilon(o)$, $\varepsilon(s)$		Model constant, following from boundary conditions at canopy top and soil level respectively
η', ℓ'		Transformed cosine directions
θ	radian	Arbitrary angle
θ_a, θ_n	radian	Foliage polar (zenith) angle
θ_o	radian	Observation polar angle

Symbol	Unit	Explanation
θ_r, θ_s	radian	Source zenith angle
$\rho, \rho_\ell, \rho_\mu$		Leaf hemispherical reflectance in general, from lower side, and from upper side respectively
ρ_s		Soil hemispherical reflectance
$\tau, \tau_\ell, \tau_\mu$		Leaf hemispherical transmittance in general, from lower side, and from upper side respectively
ϕ	radian	Azimuthal angle difference between canopy element and source direction
ϕ_o, ϕ_c, δ_o	radian	Critical azimuthal angle difference between source and canopy element

LIST OF TABLES

LIST OF FIGURES

Chapter 1

(J. A. Smith)

EXECUTIVE SUMMARY

The primary objective of the work undertaken in this project was to review the mathematical structure and physical concepts inherent in electromagnetic terrain feature canopy models. One goal of such a review was to determine if a factoring of canopy electromagnetic interactions into separate geometric and radiative terms could be achieved. A second goal was the extension of modeling concepts to multidimensional problems either spatially (for the reflective regime) or temporally (for the thermal regime).

We have been successful in the primary objective of the project and in the analysis of the factoring of geometric dependent terms from individual optical properties. In addition we have expanded our repertoire of calculational procedures for general terrain radiative transfer calculations and have addressed several issues related to the comparison of models and experiments. We have been partially successful in the analysis of multidimensional problems.

For the most part, the major results of this study have been presented in the reviewed literature. However, Chapters 2-4, discussed below, present a detailed discussion of the mathematical treatment of canopy biophysical attributes relative to the calculation of canopy element scattering properties. In addition, our analysis of the time-dependent thermal canopy problem has not yet been documented.

Our basic modeling approaches in both the thermal and reflective regime are given in Smith (1980), Appendix A1, Kimes and Smith (1980),

Appendix A2, Kimes, Smith and Link, (1981) Appendix A3 and Cooper, Smith and Pitts (1982), Appendx A5.

The factorization of the thermal model into geometrical and optical-dependent terms is given in Smith, Ranson, Nguyen, Balick, Link, Fritschen, and Hutchison (1981), Appendix A4. This paper also indicates a method for the inverse problem relative to canopy geometry. The respective factorization for the reflective problem is given in Cooper, Smith, and Pitts (1982), Appendix A5.

Several issues relative to the comparison of models with field data and vice-versa are documented in Kimes, Smith, and Ranson (1980), Appendix A6, Kirchner, Youkhana, and Smith (1982), Appendix A7, and Smith (1982), Appendix A8.

Finally, in collaborative fashion our thermal modeling work has been used in the comparison of various modeling abstractions for soil and soil/vegetation composites in Balick, Scoggins, and Link (1981), Appendix A9, and in three dimensional modeling concepts incorporated in Kimes and Kirchner (1982), Appendix A10.

The remaining chapters of the report all deal with reflective modeling of plane parallel vegetation canopies with particular attention to calculation of media scattering properties in terms of the distribution of canopy scattering facets. The general problem studied is the application of the Duntley equations to solution of the vegetation radiative transfer problem. Chapter 4 presents a rather exhaustive analysis of the problem. Expressions are derived for all five of the Duntley equation coefficients in terms of general biophysical attributes of the canopy and, in particular, the complete leaf slope distribution. A general solution approach is outlined, but a more simplified analysis

is presented for the special case of a canopy with symmetrical upper and lower leaf optical properties. The results of Chapter 4 are of theoretical interest but of limited practical application because of the general complexity of the analysis and lack of explicit analytic solutions. We have, however, used some of the expressions in more tractible formulations, e.g., The Adding Method of Appendix A5.

Of more practical consideration is a simplified analysis of the problem presented in Chapter 2 where only the Duntley equation coefficients dealing with the direct flux components are analysed in detail. Tractible expressions are formulated and evaluated for a number of standard theoretical canopy geometries. A Suits prime model incorporating the extinction coefficient calculated using the complete leaf slope distribution is formulated and compared with the standard Suits model which assumes only horizontal and vertical canopy projections in Chapter 3. Comparisons with both theoretical and field collected data as well as with the Monte Carlo SRVC model developed under previous Army Research Office funding are presented. The new Suits prime model yields results comparable to the Monte Carlo solution but with corresponding execution times reduced by a factor of several hundred.

At various times the following individuals participated in the project:

Dr. James A. Smith, Principal Investigator

Dr. R. Laven

Mr. S. Youkhana, Graduate Research Assistant. Mr. Youkhana received the degree Doctor of Philosophy for work related to project objectives.

Mr. H. Randolph, Graduate Research Assistant.

Mr. C. Nikolopoulos, Graduate Research Assistant. Mr. Nikolopoulos received the degree Doctor of Philosophy but for thesis research unrelated to project objectives.

A list of all publications related to project objectives is given in Appendix A together with copies of journal abstracts.

Chapter 2

(S. Youkhana and J. A. Smith)

DIRECT FLUX EXTINCTION COEFFICIENT

Introduction

Light is one of the important environmental condition parameters and to some degree a critical factor to the green plant growth and its distribution. Plant growth and productivity depend on the quality of solar radiation available and the plant's ability to utilize visible light.

Shading caused by upperstory (interception of light by dominant plants) will affect the understory growth (saplings, seedlings, and grasses). Thus, a decrease in the amount of light for understory is mainly due to absorption of light by leaves. Absorption of light is the main factor governing plant photosynthesis and transpiration. Norman (1980) stated that vegetation leaves absorb about 85 percent of incident visible radiation for photosynthesis. Understanding the relation between photosynthesis and light intensity will be an important factor to understand and relate dry matter to other community characteristics. One of the most important parameters for analysis of production rates of plant communities is the photosynthetic rate (McCree and Loomis, 1969).

As mentioned, interception and absorption will attenuate light as it passes through the canopy. Many researchers experimentally examined

light depletion in a plant community as a function of plant height to examine the following:

- community productivity
- morphology of understory
- species that dominate as succession proceeds toward climax
- invasion and
- for the purpose of planning and vegetation management.

Community productivity was the main purpose of investigators since it has been known that photosynthetic rate (CO_2 uptake) is proportional to the amount of light absorbed up to a compensation point (Donhoe, 1981). Some effort has been made to examine leaf morphology at different positions in plant canopy. Understanding the relationship between light intensity and community characteristics, a proper management decision can be made. With proper light models, one can make decisions as to the ideal planting pattern, the best leaf arrangement and the plant properties which should be changed to achieve the greatest increase in water-use efficiency of a given plant species (Lemeur and Blad, 1974). Thus, all field data previously collected was by instantaneous readings inside and outside plant communities, and then correlating light intensity at different levels to photosynthetic rate.

Beginning in 1950, many investigators explained light attenuation at different canopy heights mathematically. A mathematical model is an abstraction of the real world. In general, for the model to be applicable, it should be simple to understand and easy to handle. However, in order that the mathematical model approximate the real system behavior, it should include the important parameters. This means that the model cannot be realistic if it is too simple and its adequacy can only be judged in terms of the purpose for which it has been created.

Mathematical models for the extinction coefficient of light through a plant canopy have been developed over a period of time by many investigators to consider both diffuse and direct light, effects due to solar zenith angles, and canopy characteristics. One of the main problems in modeling the extinction coefficient is the abstraction of canopy structure. In this chapter, the extinction coefficient will be formulated by projecting canopy elements in the direction of light and weighting these projections by the leaf distribution function. This approach is new and forms the basis for Suits prime (Suits') canopy reflectance model discussed later.

Background

Definitions and expressions for the extinction coefficient of light through vegetation canopies have been changed and progressed over a period of time. Projection of foliage area has been used as the basis in almost all mathematical models derived for the extinction coefficient.

Monsi and Saeki (1953) were the first to develop theoretical and experimental methods to explain and understand the depletion of isotropic diffuse light through a plant community. Their experimental field method "stratifying clip technique" related observed field data of canopy characteristics (accumulation of leaf index area) to light intensities at different canopy levels. The plotted field data showed that the light intensity decreases exponentially as leaf index area increases above a certain level. Based on the observed relationship between light intensity and leaf area index accumulation, they formulated their expression in the general form analogous to

Beer's-Lambert law of monochromatic flux extinction through homogeneous absorbing medium

$$I = I_o\, e^{-KA}$$

where

I is the downward intensity of isotropic light at leaf area index A

I_o is the light intensity on a horizontal surface at the canopy top

K is the extinction coefficient of light.

Leaf area index is downward accumulation of leaf area

(i.e. $A = \int_t^b A(x)dx$

t, b, x are canopy top, canopy bottom and increment in leaf area respectively. The coefficient of light attenuation is given by the authors as:

$$K = \frac{A_s}{A_h} \ln\left(1 - \frac{A_h}{A_s}\right)$$

where

A_h is the mean projection of actual leaf area index (A) on horizontal surface

A_s is the soil surface area above which foliage area is measured.

The mean projection of leaf area on a horizontal surface is estimated as:

$$A_h = \begin{cases} A \cdot \sin\theta_a & \theta_r \leq \theta_a \\ \frac{2}{\pi} A\{\sin\theta_a \sin^{-1}(\tan\theta_a \cot\theta_r) + \cos\theta_a \tan\theta_r (1 - \tan^2\theta_a \cot^2\theta_r)^{\frac{1}{2}}\} & \theta_r > \theta_a \end{cases}$$

They claimed that there was an agreement between measured field data and model prediction of extinction coefficient.

Dewit (1965) extended and generalized Monsi and Saeki's theory of light attenuation to include canopy geometry. His definition of the extinction coefficient for a canopy of randomly oriented leaves is the ratio of foliage unit area to the soil unit area both projected in the direction of light.

Isobe (1962) used cosine direction to introduce the effect of source position in his model for predicting the extinction coefficient of light. He also proposed a distinct model for leaves and for stems in the same canopy. The average of light attenuation through canopy is the sum of the contributions from both leaves and stems. As in Monsi and Saeki's work (1953), the author's model will predict an extinction coefficient ranging from zero to unity for horizontally oriented leaves when the energy source is at horizon and at nadir respectively.

$$K = \begin{cases} -\eta' \sin\theta_a & \theta_r \leq \theta_a \\ -\frac{2}{\pi}\{(\phi - \frac{\pi}{2})\eta' \sin\theta_a + \ell' \cos\theta_a \sin\phi\} & \theta_r > \theta_a \end{cases}$$

$$\phi = \cos^{-1}(-\frac{\eta'}{\ell'} \tan\theta_a) \text{ and } \frac{\pi}{2} \leq \phi < \pi$$

where ℓ' and n' are transformed direction cosines.

Anderson (1966) reviewed previous work on light attenuation through plant canopies and also modified the definition of the extinction coefficient to include the source illumination angle. She defined the extinction coefficient in terms of mean foliage area projected onto a plane normal to the direction making an angle β with the horizontal and the actual leaf area index. Both Anderson (1966) and Warren Wilson (1967) showed the extinction coefficient of light for a stand of uniform (constantly) inclined leaves to be of the following relation:

$$K = \begin{cases} \sin\theta_a & \theta_r \leqq \theta_a \\ \sin\theta_a\{1+\frac{2}{\pi}(\tan\phi-\phi)\} & \theta_r > \theta_a \end{cases}$$

$$\phi = \cos^{-1}(\tan\theta_a \cot\theta_r)$$

This result has also been shown by Lupton (1972). In 1969, Anderson derived the extinction coefficient for randomly oriented vertical leaves as:

$$K = \frac{2}{\pi}\tan\theta_r \qquad \theta_a = 0$$

Cowan (1968) expressed the extinction coefficient as the projection mean of leaf area in a plane perpendicular to incident radiation. The author extended Anderson's (1966) idea to introduce three different idealized abstract plant community "stands" as follows:

$$K = \begin{cases} 1.0 & \text{Canopy with horizontally oriented leaves} \\ \frac{1}{2}\sec\theta_r & \text{Canopy with randomly oriented leaves} \\ \frac{2}{\pi}\tan\theta_r & \text{Canopy with vertical leaves randomly oriented} \end{cases}$$

Recently, investigators have collected field data to examine the variation in extinction coefficient with different cover types. Miller (1967) and Landesberg (1973) collected field data under forest type cover to examine the relation between the extinction coefficient and source elevation and mean leaf inclination angles. Similar work has been done for agricultural crops (oats, beans, sunflower, and corn) by Impens and Lemeur (1969).

Suits (1972) utilized an extinction coefficient as a function of source angle θ_r and canopy characteristics in his reflectance model. He approximated canopy elements by projecting them orthogonally in horizontal and vertical planes.

$$K = H + \frac{2}{\pi} V \tan\theta_r$$

$$H = A \int_o^{\frac{\pi}{2}} f(\theta_a) \cos\theta_a d\theta_a$$

$$V = A \int_o^{\frac{\pi}{2}} f(\theta_a) \sin\theta_a d\theta_a$$

H and V are orthogonal projections of canopy components in horizontal and vertical planes.

In this chapter a more complete development of the extinction coefficient incorporating the complete leaf angle distribution is developed and contrasted with Suits results for several theoretical and measured canopies. The new coefficient, termed K', is subsequently incorporated into the Suits model to yield a so-called, Suits' model. Model comparisons are made in the next chapter.

Approach

The direct flux extinction coefficient K can be defined as the amount of power (flux) absorbed (attenuated) per unit path length. The amount of energy absorbed by canopy leaves is proportional to the amount intercepted by those elements. The amount of power intercepted by individual canopy elements is proportional to the projection of the leaf segment in the direction of the beam. Projection of the foliage area in the direction of the source will be considered as the basis in this approach. Mathematical equations will be derived to predict the direct flux extinction coefficient as a function of illumination source and leaf distribution function.

Let $\bar{A}$ be the vector area of an individual canopy element and $\bar{R}$ be the unit vector in the direction of energy source. These two vectors can be written in cartesian coordinates as following:

$$\bar{A} = \sum_{i=1}^{3} A_i \vec{\varepsilon}_i$$

$$\bar{R} = \sum_{i} R_i \vec{\varepsilon}_i$$

where

$$\bar{A} \cdot \bar{A} = A^2$$

$$\bar{R} \cdot \bar{R} = \text{unity}$$

i is the X, Y, and Z direction respectively and $\vec{\varepsilon}_i$ is a unit vector in the X, Y, and Z directions. Both vectors $\bar{A}$ and $\bar{R}$ can be written in the spherical polar (system) coordinates (Fig. 1) where

$$X = \sin\theta \cos\phi$$

$$Y = \sin\theta \sin\phi \text{ and}$$

$$Z = \cos\theta$$

$$\bar{A} = A_x \vec{\varepsilon}_x + A_y \vec{\varepsilon}_y + A_z \vec{\varepsilon}_z$$

$$\left.\begin{aligned} \bar{A} &= A \{\sin\theta_a \cos\phi_a \vec{\varepsilon}_x + \sin\theta_a \sin\phi_a \vec{\varepsilon}_y + \cos\theta_a \vec{\varepsilon}_z\} \\ \bar{R} &= \{\sin\theta_r \cos\phi_r \vec{\varepsilon}_x + \sin\theta_r \sin\phi_r \vec{\varepsilon}_y + \cos\theta_r \vec{\varepsilon}_z\} \end{aligned}\right\} \quad (1)$$

Where θ and ϕ are zenith and azimuth angles respectively of each vector.

The power intercepted by an individual canopy element A from the source in the direction R is proportional to

$$\bar{A} \cdot \bar{R} = A \cos(\bar{A} \cdot \bar{R})$$

$$\bar{A} \cdot \bar{R} = \sum_{i} A_i R_i$$

$$\bar{A} \cdot \bar{R} = A_x R_x + A_y R_y + A_z R_z \quad (2)$$

Substituting equation 1 into 2 will yield

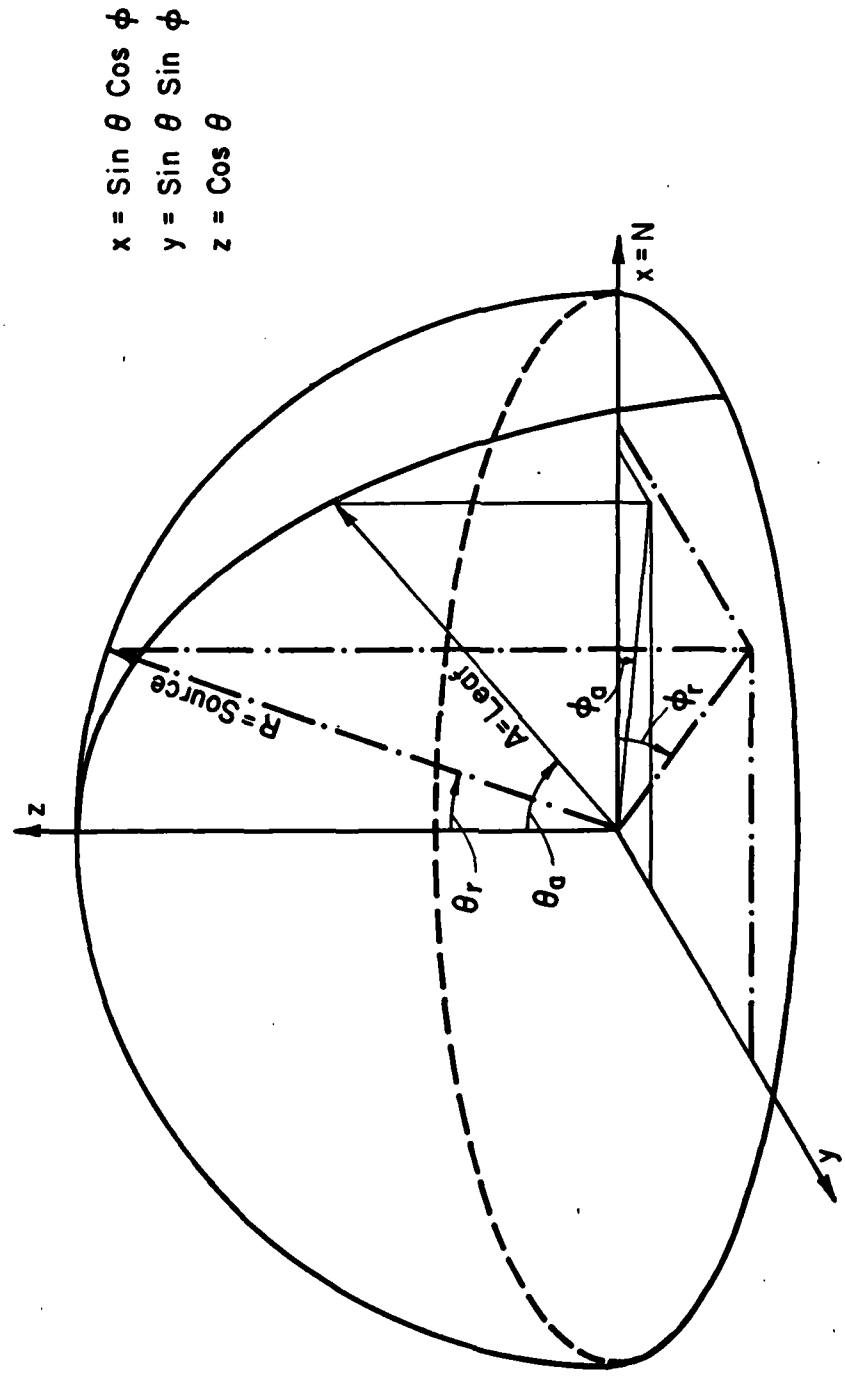

Fig. 1. Projection of Foliage Element in Spherical Polar Coordinates.

$$\bar{A} \cdot \bar{R} = |A| \{\sin\theta_a \cos\phi_a \sin\theta_r \cos\phi_r + \sin\theta_a \sin\phi_a \sin\theta_r \sin\phi_r + \cos\theta_a \cos\theta_r\}$$

$$\bar{A} \cdot \bar{R} = |A| \{\sin\theta_a \sin\theta_r (\cos\phi_a \cos\phi_r + \sin\phi_a \sin\phi_r) + \cos\theta_a \cos\theta_r\}$$

from trigonometry $\cos(\phi_a - \phi_r) = \cos\phi_a \cos\phi_r + \sin\phi_a \sin\phi_r$

$$\bar{A} \cdot \bar{R} = |A| \{\sin\theta_a \sin\theta_r \cos(\phi_a - \phi_r) + \cos\theta_a \cos\theta_r\} \qquad (3)$$
$$= F(\phi_a - \phi_r)$$

For simplicity, let $\phi = \phi_a - \phi_r$ which is the azimuthal angle difference between source direction and canopy element.

The average power intercepted per canopy element A (denoted $\langle \bar{A} \cdot \bar{R} \rangle_\phi$) can be determined from the total interception by collection of elements randomly distributed, all of which are characterized by the same element zenith angle and assuming azimuthally isotropic leaves. Thus

$$\langle \bar{A} \cdot \bar{R} \rangle_\phi = \int_o^\pi \bar{A} \cdot \bar{R} d\phi / \int_o^\pi d\phi \qquad \text{where } 0 \leq \phi < \pi$$

The integral will be broken down into two parts based on a critical azimuthal angle difference between energy source and canopy element. This angle determines when the illumination angle is greater than the foliage angle. When azimuthal angle difference ϕ is smaller than the critical angle ϕ_o, the beam will strike the upper side of the element. The beam will hit the lower part of the foliage element when ϕ is greater than ϕ_o, and the beam will be parallel to the foliage element when $\phi = \phi_o$.

$$\langle \bar{A}\cdot\bar{R} \rangle_{\phi} = \frac{1}{\pi} A\{\int_{o}^{\phi_o} \bar{A}\cdot\bar{R}d\phi - \int_{\phi_o}^{\pi} \bar{A}\cdot\bar{R}d\phi\}$$

$$= \frac{2}{\pi} A \{\int_{o}^{\phi_o}(\sin\theta_a \sin\theta_r \cos\phi + \cos\theta_a\cos\theta_r)d\phi$$

$$- \int_{\phi_o}^{\pi}(\sin\theta_a\sin\theta_r\cos\phi + \cos\theta_a\cos\theta_r)d\phi$$

$$= \frac{2}{\pi} A \{\sin\theta_a\sin\theta_r\sin\phi_o + (\phi_o - \frac{\pi}{2}) \cos\theta_a\cos\theta_r\} \qquad (4)$$

The complication arises because the critical azimuth angle ϕ_o depends on both θ_a and θ_r (foliage and source zenith angles). ϕ_o can be found by investigating the sign of $F(\phi_a - \phi_r)$, assuming that both θ_a and θ_r are in the range between zero and $\frac{\pi}{2}$ ($0 \leqq \theta_a$ or $\theta_r \leqq \frac{\pi}{2}$) as following:

a. If $\frac{\pi}{2} \leqq \theta_a + \theta_r < \pi$

$$\cos(\theta_a + \theta_r) \leqq 0$$

$$F(\phi_a - \phi_r) = \sin\theta_a\sin\theta_r\cos\phi_o + \cos\theta_a\cos\theta_r \leqq 0$$

$$\cos\phi_o \leqq -\cot\theta_a\cot\theta_r$$

$$\phi_o = \cos^{-1}(-\cot\theta_a\cot\theta_r)$$

b. If $0 < \theta_a + \theta_r \leqq \frac{\pi}{2}$

$$\cos(\theta_a + \theta_r) \geqq 0$$

$$F(\phi_a - \phi_r) = \sin\theta_a\sin\theta_r\cos\phi_o + \cos\theta_a\cos\theta_r \geqq 0$$

$$\cos\phi_o = -\cot\theta_a\cot\theta_r \leqq -1$$

$$\cos\phi_o \cong -1 \text{ and } \phi_o = \pi$$

For $\phi > \phi_o \Rightarrow F(\phi) \leqq 0$ and for $\phi \leqq \phi_o \Rightarrow F(\phi) \geqq 0$

One of the main problems in this formulation is how to introduce canopy abstraction and how to project the foliage area index. Suits

(1972) approximated component leaf areas by the sum of orthogonally projected areas in horizontal and vertical planes. More generally, however, normalized leaf distribution functions (Fig. 2) should be introduced to predict the average power intercepted by the collection of leaves over their inclination angles. The proportion of leaves having a slope between θ_a and $\theta_a + d\theta_a$ is given by $f(\theta_a)d\theta_a$ then

$$\langle \bar{A}\cdot\bar{R} \rangle_{\phi,\theta_a} = (\tfrac{2}{\pi})^2 A \{\int_o^{\frac{\pi}{2} - \theta_r} \langle \bar{A}\cdot\bar{R} \rangle_{\phi} f(\theta_a)d\theta_a + \int_{\frac{\pi}{2} - \theta_r}^{\frac{\pi}{2}} \langle \bar{A}\cdot\bar{R} \rangle_{\phi} f(\theta_a)d\theta_a\}$$

$$= (\tfrac{2}{\pi})^2 A \{\int_o^{\frac{\pi}{2} - \theta_r} \sin\theta_a \sin\theta_r \sin\phi_o f(\theta_a)d\theta_a$$

$$+ \int_o^{\frac{\pi}{2} - \theta_r} (\phi_o - \tfrac{\pi}{2}) \cos\theta_a \cos\theta_r f(\theta_a)d\theta_a + \int_{\frac{\pi}{2} - \theta_r}^{\frac{\pi}{2}} \sin\theta_a$$

$$\sin\theta_r \sin\phi_o f(\theta_a)d\theta_a + \int_{\frac{\pi}{2} - \theta_r}^{\frac{\pi}{2}} (\phi_o - \tfrac{\pi}{2}) \cos\theta_a \cos\theta_r f(\theta_a)d\theta_a\}$$

The critical azimuthal difference angle ϕ_o is equal to π in the range where foliage inclinations are between zero and $\frac{\pi}{2} - \theta_r$. This means the first term in the above relation will approach zero and the last three terms will predict the average power intercepted by a single element.

$$\langle \bar{A}\cdot\bar{R} \rangle_{\phi,\theta_a} = \tfrac{2}{\pi} A \cos\theta_r \int_o^{\frac{\pi}{2} - \theta_r} \cos\theta_a f(\theta_a)d\theta_a + (\tfrac{2}{\pi})^2 A \sin\theta_r \int_{\frac{\pi}{2} - \theta_r}^{\frac{\pi}{2}} \sin\theta_a$$

$$\sin\phi_o f(\theta_a)d\theta_a + (\tfrac{2}{\pi})^2 A \cos\theta_r \int_{\frac{\pi}{2} - \theta_r}^{\frac{\pi}{2}} (\phi_o - \tfrac{\pi}{2}) \cos\theta_a f(\theta_a)d\theta_a \quad (5)$$

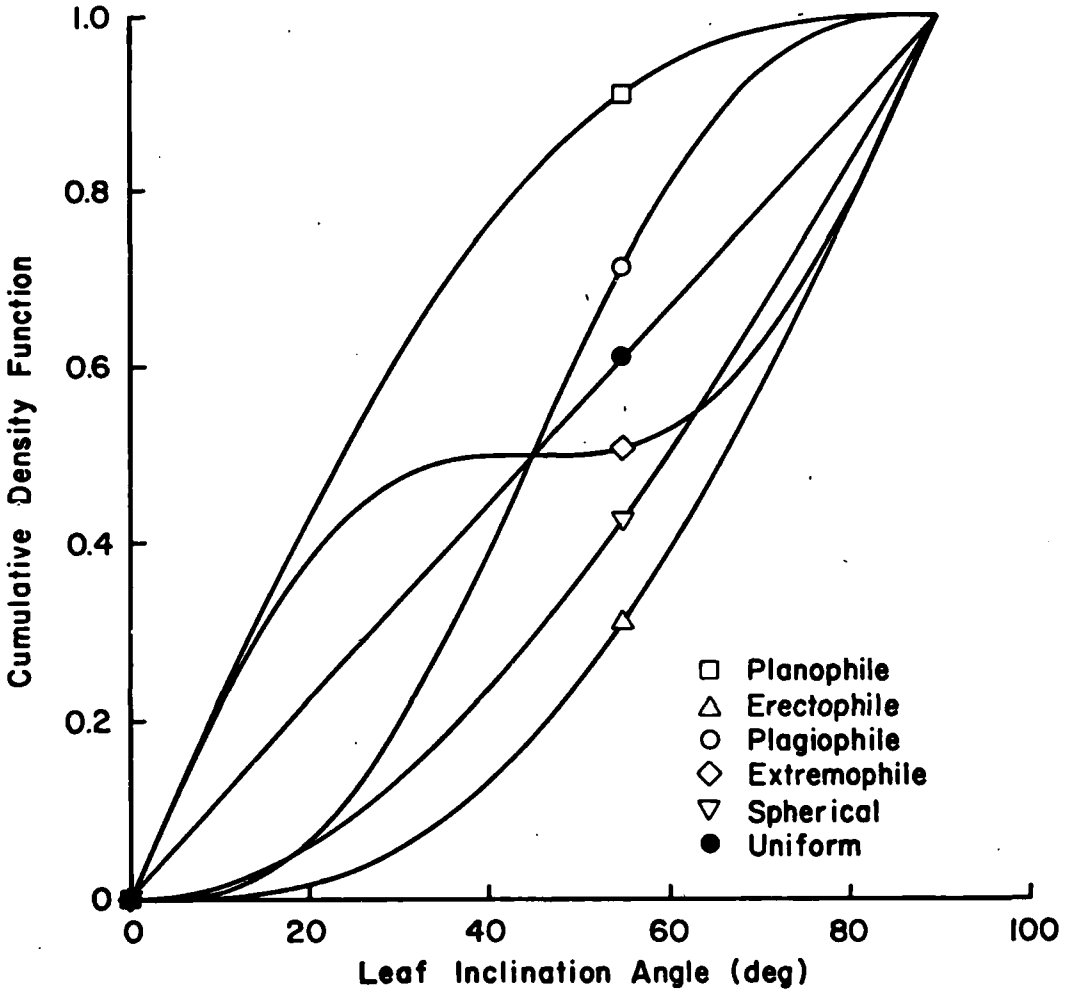

Fig. 2. Leaf Distribution Functions.

The extinction coefficient is given by:

$$K = \frac{\text{Average power intercepted (absorbed)}}{\text{unit path length}}$$

The cosine of the source zenith angle will correct for increased path lengths at varying sun elevations thus the general form is given by:

$$K' = \frac{2}{\pi} A \int_{o}^{\frac{\pi}{2} - \theta_r} \cos\theta_a \, f(\theta_a) d\theta_a + (\frac{2}{\pi})^2 A \tan\theta_r \int_{\frac{\pi}{2} - \theta_r}^{\frac{\pi}{2}} \sin\theta_a \sin\phi_o$$

$$f(\theta_a) d\theta_a + (\frac{2}{\pi})^2 A \int_{\frac{\pi}{2} - \theta_r}^{\frac{\pi}{2}} (\phi_o - \frac{\pi}{2}) \cos\theta_a \, f(\theta_a) d\theta_a \qquad (6)$$

Results

Normalized leaf-slope distribution functions should be introduced in equation (6) to evaluate direct flux extinction coefficient. The following theoretical abstractions have been used to calculate attenuation coefficient:

Planophile - horizontal leaves are most frequent

$$f(\theta_a) = \frac{2}{\pi} (1 + \cos 2\theta_a)$$

Erectophile - vertical leaves are most frequent

$$f(\theta_a) = \frac{2}{\pi} (1 - \cos 2\theta_a)$$

Plagiophile - oblique leaves are most frequent

$$f(\theta_a) = \frac{2}{\pi} (1 - \cos 4\theta_a)$$

Extremophile - oblique leaves are less frequent

$$f(\theta_a) = \frac{2}{\pi} (1 + \cos 4\theta_a)$$

Uniform - same proportion leaves at any angle

$$f(\theta_a) = \frac{2}{\pi}$$

Spherical - Relative frequency of leaf inclination is the same as relative frequency of inclination of surface element of a sphere.

$$f(\theta_a) = \sin\theta_a$$

Measured leaf-slope distributions for a variety of canopies were also used.

Direct flux extinction coefficient derived by Suit (1972) using orthogonal projection approximation is of the following relation

$$K = \{\langle \bar{A}_v \cdot \bar{R} \rangle_{\phi,\theta_a} + \langle \bar{A}_h \cdot \bar{R} \rangle_{\phi,\theta_a}\}/\cos\theta_r$$

$$K = LAI\{\int_o^{\frac{\pi}{2}} \cos\theta_a \, f(\theta_a)d\theta_a + \frac{2}{\pi}\tan\theta_r \int_o^{\frac{\pi}{2}} \sin\theta_a \, f(\theta_a)d\theta_a\} \qquad (7)$$

and the expression for attenuation coefficeint using projection of elements in the direction of beam approach is as following:

$$K' = \{\langle \bar{A} \cdot \bar{R} \rangle_{\theta,\phi_a}\}/\cos\theta_a$$

$$K' = LAI\{\frac{2}{\pi}\int_o^{\frac{\pi}{2} - \theta_r} (\phi_o - \frac{\pi}{2}) \cos\theta_a \, f(\theta_a)d\theta_a + \frac{2}{\pi}\tan\theta_r \int_o^{\frac{\pi}{2} - \theta_r} \sin\theta_a$$

$$\sin\phi_o \, f(\theta_a)d\theta_a + \frac{2}{\pi}\int_{\frac{\pi}{2} - \theta_r}^{\frac{\pi}{2}} (\phi_o - \frac{\pi}{2}) \cos\theta_a \, f(\theta_a)d\theta_a$$

$$+ \frac{2}{\pi}\tan\theta_r \int_{\frac{\pi}{2} - \theta_r}^{\frac{\pi}{2}} \sin\theta_a \sin\phi_o \, f(\theta_a)d\theta_a\} \qquad (8)$$

The first and third terms in equation (8) account for the first term in equation (7) which is leaf area projected in the horizontal plane X-Y

coordinate. The second and fourth terms in equation (8) account for the second term in equation (7) which is the sum of leaf area projected in vertical cartesian coordinates Y-Z and X-Z planes.

The critical azimuthal angle difference between source and leaf plane ϕ_o is equal to the π when leaf zenith angle is in the range between zero and $\frac{\pi}{2} - \theta_r$ ($0 < \theta_a \leq \frac{\pi}{2} - \theta_r$). This implies that part of the contribution due to vertical components (second term in equation (8) will approach zero, while this contribution exists in orthogonal projection. In the region where $\theta_a > \frac{\pi}{2} - \theta_r$, the critical azimuthal angle difference ϕ_o will be in the range $\frac{\pi}{2}$ and π ($\frac{\pi}{2} < \phi_o < \pi$). In this range, $\sin\phi_o$ will take values less than unity and the contribution will be minimized proportional to the value of $\sin\phi_o$. It should be noted that this reduction does not exist in orthogonal method. Over all, the orthogonal projection technique overestimates the average amount of power received by canopy elements compared to what will actually be intercepted.

To calculate specific extinction coefficients for different canopy geometries, equation (8) must be solved. Integration of equation (8) over leaf inclination angles is quite difficult because of the dependence of ϕ_o on both θ_a and θ_r respectively, $\phi_o = \cos^{-1}(-\cot\theta_a \cot\theta_r)$. To perform the integration and to obtain fairly accurate results, numerical solutions are needed. Simpson's composite algorithm numerical method (Burden et. al., 1978) over 2m subinterval of [a,b] was used to solve the problem and evaluate $I = \int_a^b f(x)dx$ where

$$\int_a^b f(x)dx = \frac{h}{3}\{f(a) + 2 \sum_{j=1}^{m-1} f(x_{2j}) + 4 \sum_{j=1}^{m} f(x_{2j-1}) + f(b)\}$$

Extinction coefficients have been calculated using both approaches for different theoretical vegetation architectures having a leaf area index of unity (Table 1) and for different field crops (wheat/May, wheat/June, blue grama, and sorghum) having different leaf area indices (Table 2). The percentage differences in predicted K values between both approaches have been plotted versus source zenith angles for the four theoretical canopy geometries (Fig. 3) and for measured blue grama grass, wheat and sorghum shown in Fig. 4.

From Figures 3 and 4, it is clear that the percentage differences in K is a function of two factors:

a. Canopy abstraction

In general the percentage difference in K between the two methods is a minimum for extremophile canopy because most of canopy leaves are not inclined but are at both extreme ends (vertical and horizontal). Thus, the orthogonal projection method can approximate this canopy fairly well due to the presence of a higher proportion of leaves in vertical and horizontally oriented planes. Bunnik (1978) stated that the Suits canopy model is an extreme example of an extremophile canopy. On the other hand, the greatest percentage differences in K is found for plagiophile canopies because inclined leaves in this abstraction are more frequent.

For a spherical abstraction which approximates most grasses and crops (e.g. blue grama, Smith and Oliver 1972; soybeans, Ranson 1981; sorghum, agronomy field data 1981), the percentage difference in K values ranges from 7 to 43 with an average of 25 perent. The difference is mainly due

Table 1. Suits and Suits' model predictions of K and percentage difference between model predictions for four theoretical canopy abstractions.

θ_s	Planophile	Extremophile	Plagiophile	Spherical
		K'		
5	0.848	0.597	0.769	0.502
15	0.849	0.616	0.680	0.518
25	0.850	0.655	0.685	0.552
35	0.855	0.715	0.703	0.610
45	0.870	0.799	0.749	0.707
55	0.908	0.926	0.852	0.872
65	1.008	1.146	1.086	1.183
75	1.317	1.668	1.703	1.932
85	3.229	4.448	4.970	5.737
		K		
5	0.872	0.627	0.717	0.544
15	0.921	0.696	0.795	0.634
25	0.975	0.771	0.881	0.733
35	1.038	0.859	0.982	0.850
45	1.119	0.972	1.111	1.000
55	1.235	1.134	1.296	1.214
65	1.428	1.405	1.606	1.572
75	1.857	2.006	2.292	2.366
85	3.937	4.918	5.620	6.215
		$\lvert(K' - K)\rvert/K' \times 100$		
5	2.8	5.0	6.8	8.4
15	8.5	13.0	16.9	22.4
25	14.7	17.7	28.6	32.8
35	21.4	20.1	39.7	39.3
45	28.6	21.7	48.3	41.4
55	36.0	22.5	52.1	39.2
65	41.7	22.6	47.9	32.9
75	41.0	20.3	34.6	22.5
85	21.9	10.6	13.1	8.3

Table 2. Suits and Suits' model predictions of K and percentage difference between model predictions for three different crops.

θ_s	May/Wheat	June/Wheat	B. Grama	Sorghum
		K'		
5	0.7346	0.4836	3.6595	4.259
15	0.7482	0.4900	3.6993	4.316
25	0.7727	0.5091	3.8386	4.507
35	0.8179	0.5417	4.1249	4.941
45	0.8993	0.5965	4.6392	5.766
55	1.0433	0.6911	5.5791	7.218
65	1.3270	0.8320	7.4021	10.017
75	2.0446	1.3260	11.8477	16.610
85	5.7912	3.7142	34.7030	49.822
		K		
5	0.8003	0.5283	3.9694	4.653
15	0.8937	0.5887	4.5182	5.448
25	0.9963	0.6551	5.1214	6.321
35	1.1174	0.7335	5.8328	7.352
45	1.2726	0.8339	6.7445	8.672
55	1.4942	0.9772	8.0466	10.557
65	1.8649	1.2171	10.2252	13.712
75	2.6866	1.7487	15.0532	20.703
85	6.6709	4.3265	38.4643	54.604
		$\lvert(K' - K)\rvert/K' \times 100$		
5	8.9	9.2	8.5	9.3
15	19.4	20.1	22.1	26.2
25	28.9	28.7	33.4	40.2
35	36.6	35.4	41.4	48.8
45	41.5	39.8	45.4	50.4
55	43.2	41.4	44.2	46.3
65	40.5	39.4	38.1	36.9
75	31.4	31.9	27.1	24.6
85	15.2	16.5	10.8	9.6

LAI for May/Wheat = 1.28
LAI for June/Wheat = 0.82
LAI for B. Grama = 6.51
LAI for Sorghum = 8.50

to an overestimate in vertical projections. Verhoef and Bunnik (1981) stated that Suits model overpredicts K mainly due to drastic simplifications of vertical projection leaf area.

b. Sun zenith angles

The percentage differences are minimum at low and high source angles as shown in Figs. 3 and 4. This is due to contributions of projection canopy elements into horizontal plane at low energy source zenith angles and projection into vertical planes at higher zenith angles. Also, the difference is less when the source is at nadir than at the horizon. This result is expected because of the overestimate arising from vertical components by the orthogonal projection method at low sun elevations.

Conclusions

A mathematical relationship based on projection of a single foliage element in the direction of an energy source has been derived to calculate the direct flux extinction coefficient. Calculation of light attenuation through the canopy has been performed for different standard vegetation canopy architectures (planophile, extremophile, plagiophile, and spherical) and for blue gramma grass, wheat and sorghum, using both the Suits orthogonal projection method and the projection in the direction of source methods.

In general, the orthogonal projection method overestimates the light attenuation coefficient for all canopy abstractions. The extra contribution is mainly due to an overestimation of foliage elements projected in the vertical planes. The largest differences between the

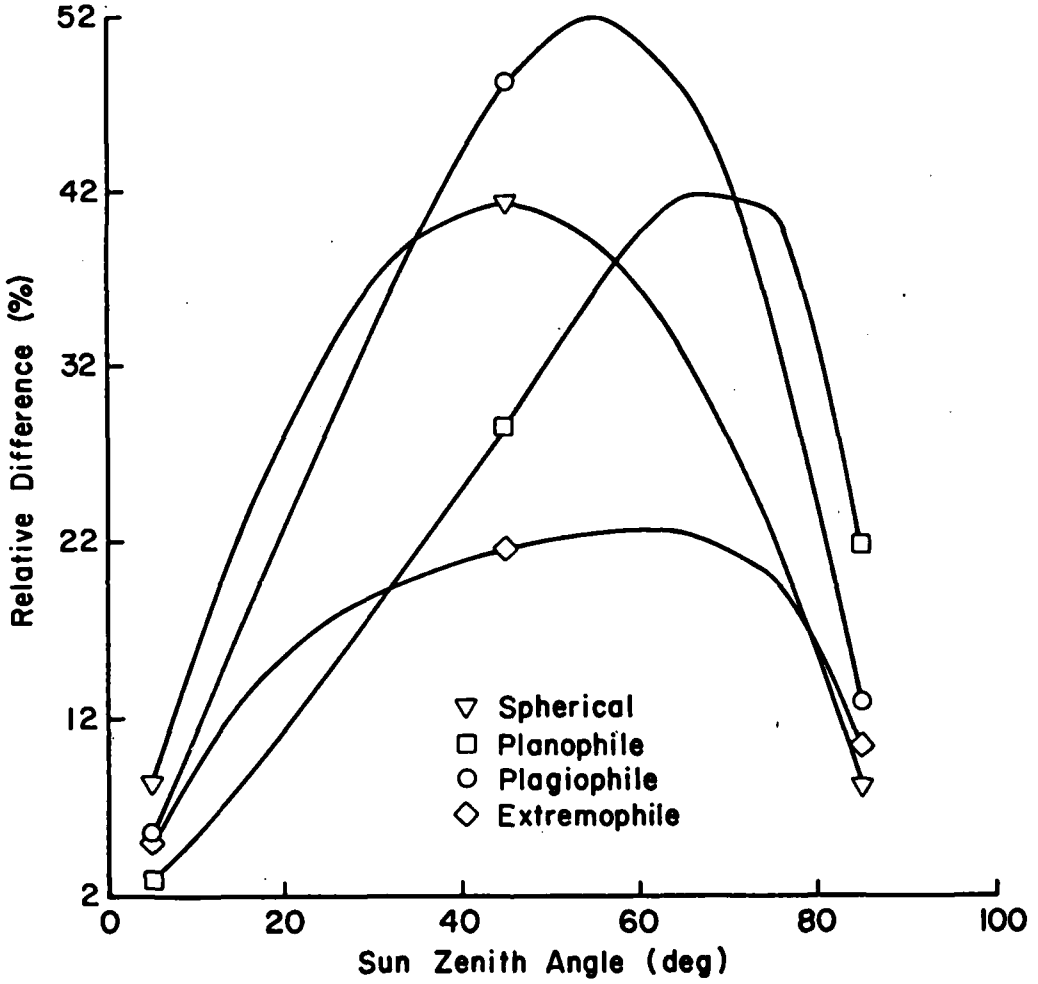

Fig. 3. Percentage Difference in K given by $(K-K')/K' \times 100$.

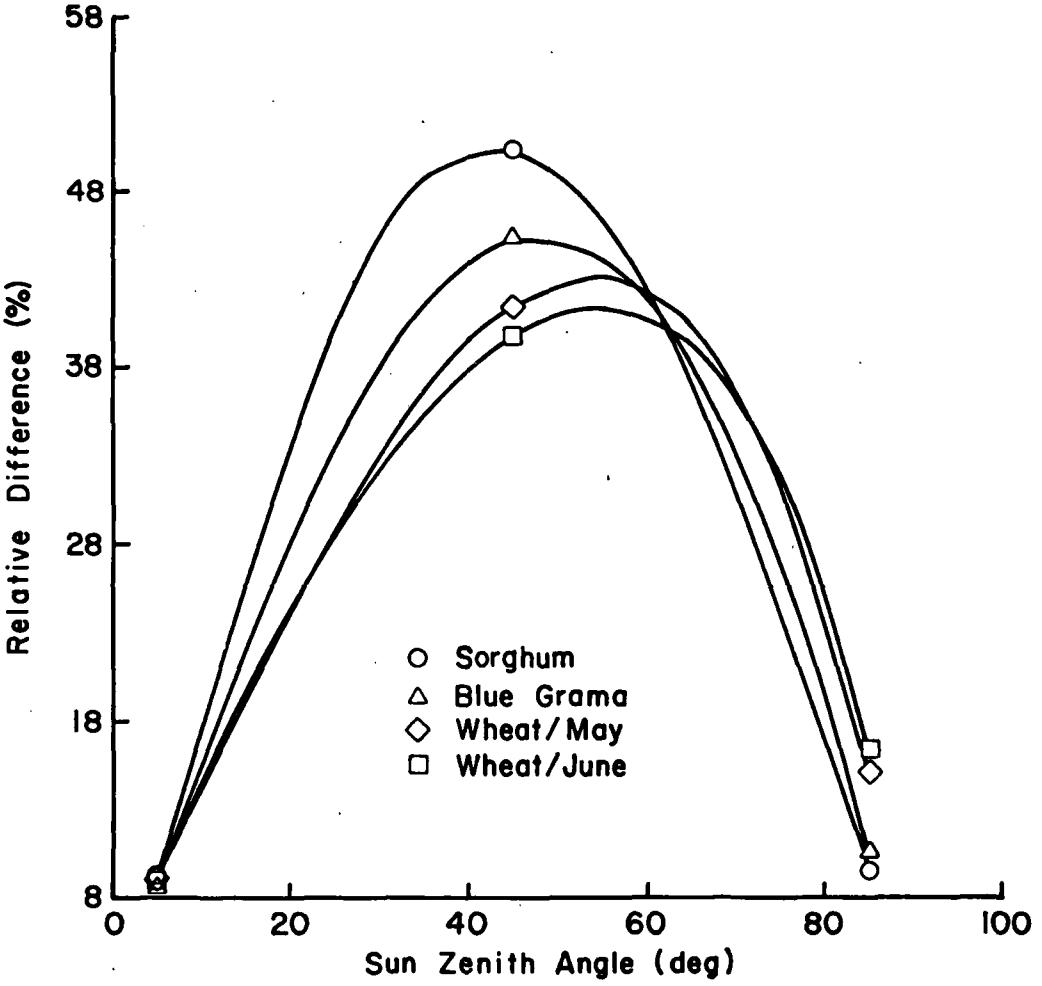

Fig. 4. Percentage Difference in K given by $(K-K')/K' \times 100$.

two approaches was found to be for the canopy whose leaves are mostly inclined (plagiophile) and the smallest differences was found to be for the canopy in which most of its leaves are not inclined, but are at extreme angles (extremophile).

The extinction coefficient of light through vegetation canopy will determine how the beam will be depleted with depth. The intensity of light reaching the soil surface under the canopy will be inversely proportional to the light extinction coefficient. This means, the contribution to overall canopy reflectance from the soil surface under the canopy will be underestimated in the orthogonal projection method because the light will fall off in the canopy faster as compared to the leaf angle distribution method. As will be seen later, when the K' extinction coefficient is inserted into the Suits radiative transfer equation, agreement of this model with measurements is improved.

Chapter 3

(S. Youkhana and J. A. Smith)

MODEL COMPARISONS

Three models were analyzed in this study including the original Suits model (Suits, 1972), the modified Suits prime developed as part of this study (Chapter 2) and the SRVC model developed by Smith and Oliver (1972). Complete descriptions of the original Suits and SRVC models are given in the original literature citations. Briefly, the models differ as follows:

The Suits model is an extension of the Duntly equation approach in which the coefficients of the differential equations are expressed in terms of the optical and geometric properties of the canopy. The optical properties are taken to be the soil reflectance and the leaf reflectance and transmittance as a function of wavelength. The geometry of the canopy is described in terms of its leaf area index and the average horizontal and vertical leaf area projections. A direct solar source is assumed with the capture of solar energy governed by the direct solar extinction coefficient. The model predicts the flux reflected from the canopy as a function of sensor view angle.

The Suits' model developed in this study is virtually identical with the Suits model except in one very important detail; namely, the calculation of the direct flux extinction coefficient as derived in Chapter 2. The key canopy abstraction which is modified for the Suits' model is the consideration of the complete leaf angle distribution rather than only the projected horizontal and vertical components.

The SRVC model uses a stochastic approach to simulate the light interactions within a canopy and the subsequent reflection from it. Identical canopy optical properties are used as in the previous two models, i.e., soil reflectance and leaf reflectance and transmittance; however, the complete leaf angle distribution is used. Since leaves in a vegetation canopy do not form a systematic pattern, the model permits the utilization of user specified statistical rules. The model differs from the Suits model then in two respects: the use of a leaf angle distribution and it is not an analytical solution. It differs from the Suits' model only by its Monte Carlo nature rather than its conceptual abstraction. Consequently, it was hypothesized that the modified Suits model, the Suits' model, would agree more closely with the SRVC model.

To evaluate this hypothesis several sets of measured field data were used in which both the model input parameters and the model predicted values were estimated. The complete set of input data are given in Tables 3 and 4, and used to drive all the model siumlations used in this study. The wheat data were collected by a Colorado State University/Texas A & M University experimental team during April 17, May 16, and June 13, 1976 as part of the National Aeronautics and Space Administration Large Area Crop Inventory Experiment (LACIE) and extracted from Smith, Berry, and Heimes (1976). The study site was in Finney County, Kansas.

Similarly, the blue grama data set was collected during August, 1972 by Colorado State University personnel at the Pawnee National Grasslands at the Intensive Study Site of the International Biological Program and were extracted from Smith and Oliver (1972). An additional advantage of using both this and the previous data set was that the

Table 3. Vegetation canopy characteristics (leaf area index and orthogonal projection), leaf optical properties and soil reflectance.

Vegetation	LAI	H	V	λ	ρ	τ	ρ_s
Sorghum	8.50	4.27	6.92	660	0.108	0.025	0.085
				830	0.405	0.483	0.263
Wheat/April	0.87	0.51	0.59	550	0.078	0.078	0.156
				650	0.067	0.067	0.218
				750	0.331	0.331	0.256
				950	0.480	0.480	0.311
Wheat/May	1.23	0.76	0.81	550	0.076	0.076	0.156
				650	0.045	0.045	0.218
				750	0.381	0.381	0.256
				950	0.450	0.450	0.311
Wheat/June	0.82	0.50	0.53	550	0.168	0.168	0.156
				650	0.206	0.206	0.218
				750	0.437	0.437	0.256
				950	0.480	0.480	0.311
Blue grama	6.5	3.71	4.78	400	0.038	0.014	0.024
				450	0.047	0.022	0.027
				500	0.059	0.034	0.032
				550	0.098	0.095	0.042
				600	0.074	0.064	0.046
				650	0.053	0.035	0.050
				700	0.116	0.083	0.065
				750	0.501	0.277	0.098

Table 4. Probability distribution for leaves.

	Wheat				
β	April	May	June	Blue grama	Sorghum
0	0.044	0.031	0.050	0.0141	0.0031
5	0.044	0.029	0.050	0.0197	0.0049
10	0.044	0.046	0.057	0.0248	0.0061
15	0.044	0.058	0.055	0.0280	0.0071
20	0.045	0.056	0.047	0.0312	0.0940
25	0.046	0.054	0.047	0.0349	0.0205
30	0.047	0.053	0.047	0.0449	0.0304
35	0.048	0.052	0.047	0.0541	0.0434
40	0.049	0.056	0.052	0.0664	0.0537
45	0.051	0.060	0.053	0.0768	0.0729
50	0.052	0.059	0.048	0.0727	0.0814
55	0.054	0.059	0.050	0.0699	0.0997
60	0.055	0.063	0.052	0.0845	0.1174
65	0.057	0.062	0.054	0.0964	0.1287
70	0.059	0.059	0.055	0.0880	0.1191
75	0.062	0.055	0.051	0.0827	0.0836
80	0.064	0.051	0.060	0.0593	0.0680
85	0.067	0.050	0.064	0.0391	0.0288
90	0.070	0.046	0.060	0.0123	0.0218
Total	1.00	1.000	1.000	1.000	1.000

SRVC model, which is expensive to run, had already been applied to these canopies.

Finally, a third data set was collected by the author over a sorghum field on August 22, 1981 at the Colorado State University Agronomy Farm. The Goddard Space Flight Center Mark-II three band hand-held radiometer was used to obtain canopy reflectance measurements. An ISCO radiometer was used to estimate leaf optical properties. The canopy was sampled to estimate leaf area index using a LICOR-3000 Optical portable area meter. While care was taken to obtain a representative measurement for the homogeneous canopy, an accurate estimate of sampling error could not be obtained since destructive sampling was prohibited. Subsequent sensitivity analysis, indicated that this input parameter was not critical at the visible wavelengths but was of concern at infrared wavelengths. Consequently, the infrared data were dropped from further consideration.

Table 5 summarizes all of the model predictions for each of the three data sets. θ_o is the instrument viewing direction and θ_s the sun angle at the time of measurement. The model predictions are plotted against field measurements for blue grama in Figures 5 and 6 for two different view angles. Figures 7 and 8 summarize the data for the wheat canopy for a vertical view angle, and finally, Figures 9 and 10 show the behavior of the models for two different sun angles and varying view angles for the sorghum canopy at the visible wavelength.

As a general observation it is evident that the Suits' predictions are consistently more in agreement with the measured data and the SRVC model predictions than hypothesized. The Suits model systematically underestimates canopy reflectance as compared to the measured data and

Table 5. SRVC, Suits, and Suits' model predictions versus measured blue grama, sorghum and wheat reflectance.

Vegetation	LAI	Date	λ	θ_o	θ_s	Meas.	SRVC	Suits	Suits'
Blue grama	6.51	1972	400	5	35	0.028	0.021	0.0146	0.0182
			450			0.034	0.026	0.0183	0.0228
			500			0.039	0.033	0.0232	0.0290
			550			0.060	0.057	0.0414	0.0519
			600			0.053	0.039	0.0302	0.0377
			650			0.056	0.027	0.0209	0.0261
			700			0.083	0.058	0.0483	0.0605
		1972	400	40	35	0.024	0.024	0.0144	0.0203
			450			0.037	0.030	0.0182	0.0257
			500			0.059	0.038	0.0234	0.0332
			550			0.105	0.068	0.0438	0.0628
			600			0.093	0.049	0.0315	0.0449
			650			0.065	0.033	0.0213	0.0302
			700			0.091	0.073	0.0499	0.0713
Sorghum	850	1980	660	5	35	0.049	0.051	0.0397	0.0532
					45	0.052	0.049	0.0389	0.0497
					55	0.062	0.046	0.0335	0.0445
					65	0.059	0.045	0.0288	0.0371
Wheat	0.87	4/1976	550	5	46.2	0.072	0.072	0.0644	0.0733
			650			0.090	0.070	0.0768	0.0883
			750			0.199	0.265	0.2234	0.3320
			950			0.296	0.390	0.3793	0.4196
	1.23	5/1976	550	5	40.5	0.119	0.063	0.0513	0.0671
			650			0.120	0.053	0.0477	0.0656
			750			0.302	0.315	0.2688	0.3320
			950			0.396	0.398	0.3717	0.4604
	0.82	6/1976	550	5	38.1	0.149	0.123	0.1067	0.1268
			650			0.187	0.150	0.1463	0.1744
			750			0.304	0.305	0.3112	0.3639
			950			0.373	0.358	0.3855	0.4516

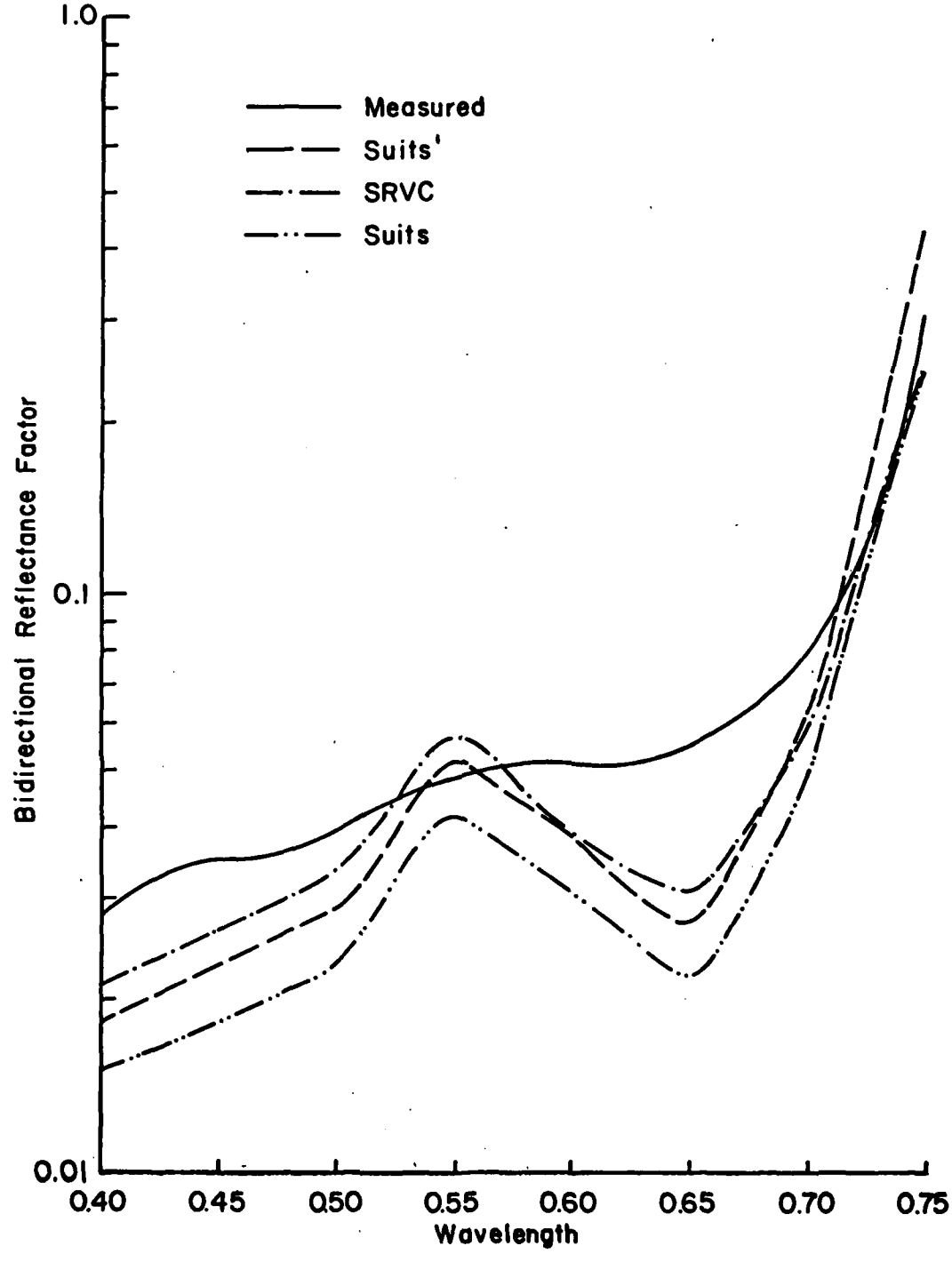

Fig. 5. SRVC, Suits, and Suits' Model Predictions Compared with the Measured Blue Gramma Canopy Reflectance for Sensor Polar Angle of 5° and Sun Zenith Angle of 35°.

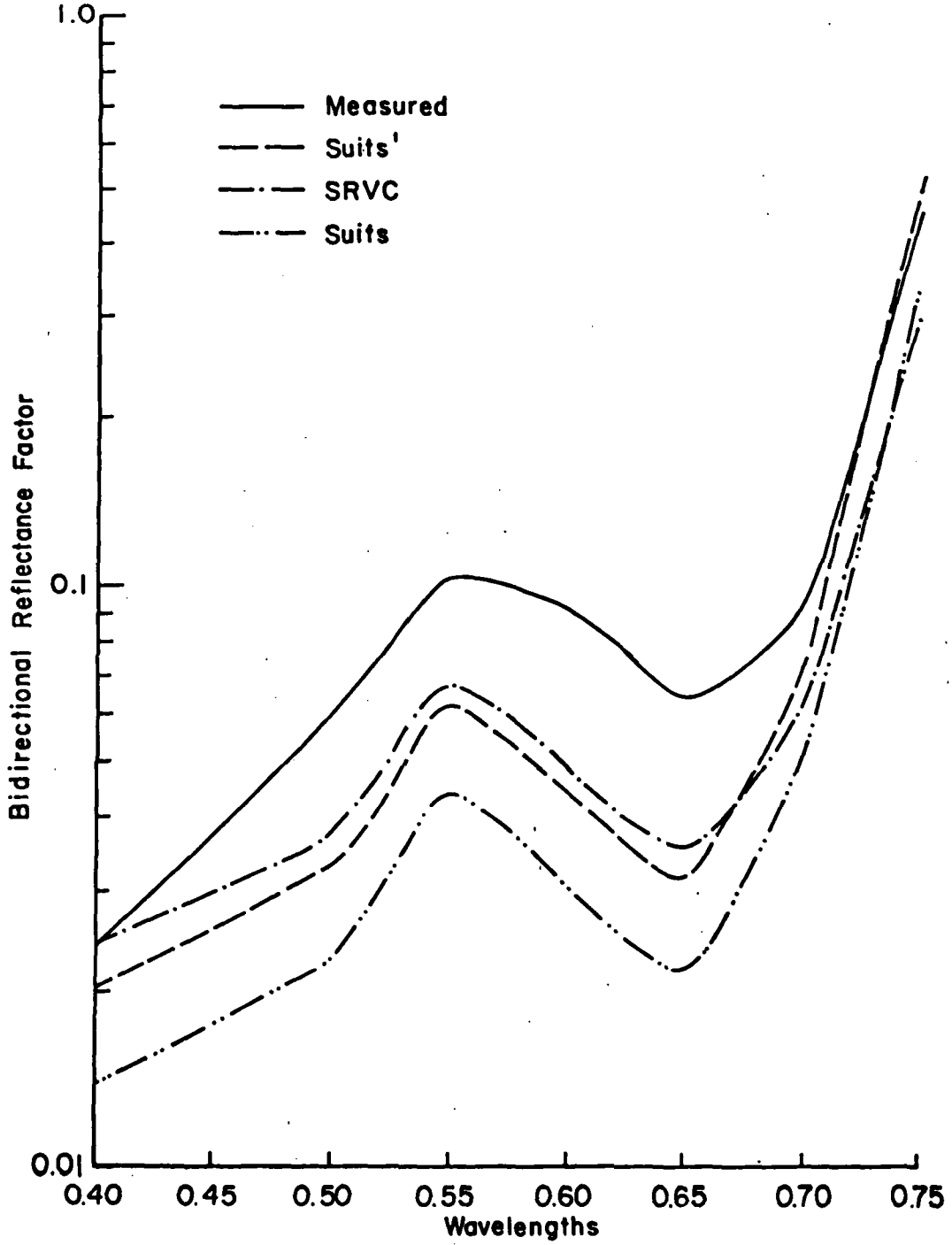

Fig. 6. SRVC, Suits, and Suits' Model Predictions Compared with the Measured Blue Gramma Canopy Reflectance for Sensor Polar Angle of 40° and Sun Zenith Angle of 35°.

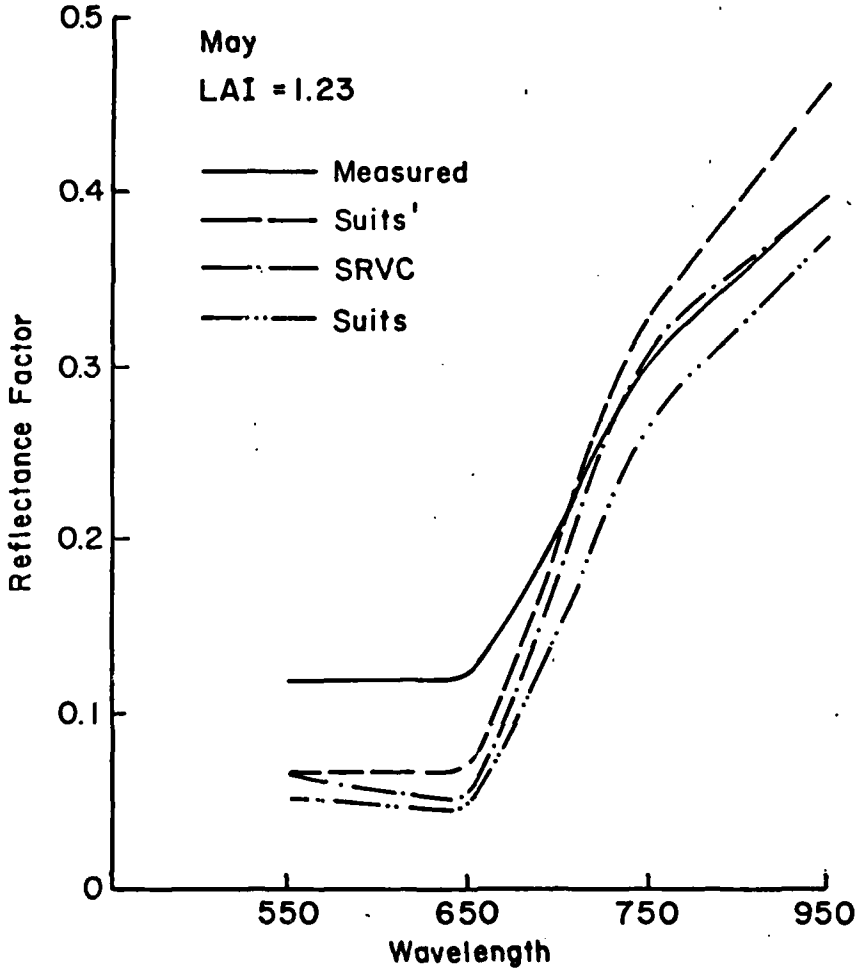

Fig. 7. SRVC, Suits, and Suits' Model Predictions Compared with the Measured Wheat Canopy Reflectance for Sensor Polar Angle of 5° and Sun Zenith Angle of 40.5°.

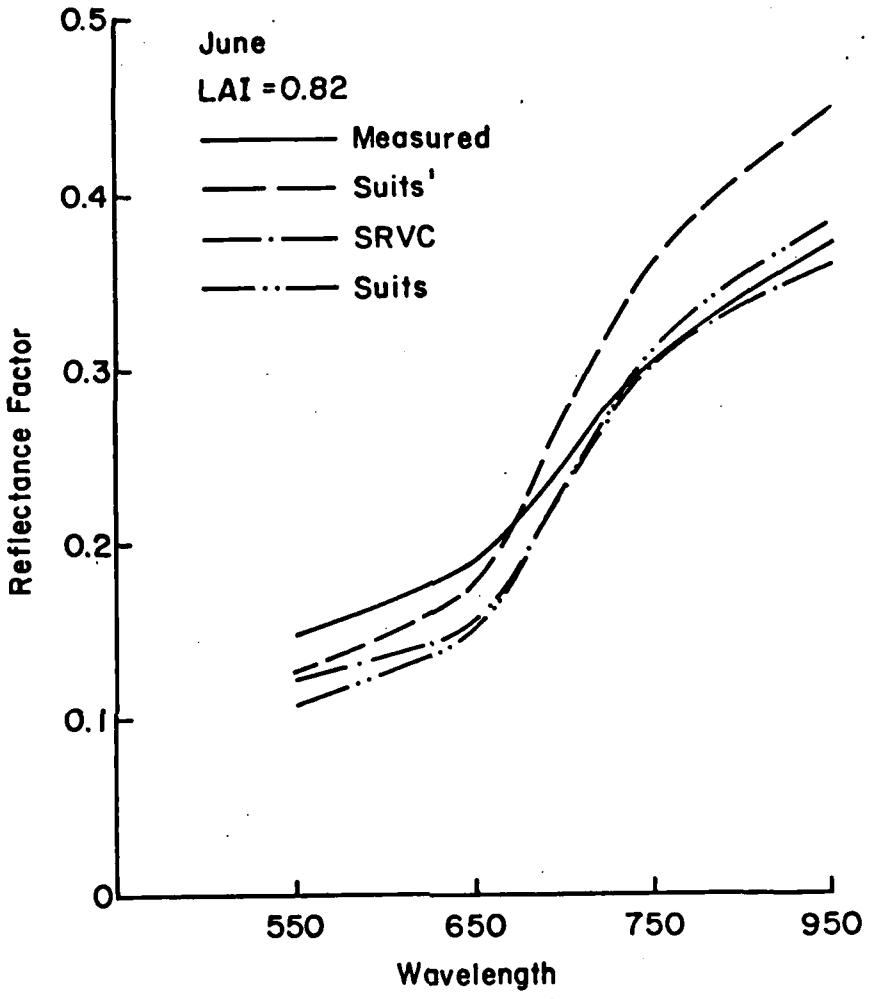

Fig. 8. SRVC, Suits, and Suits' Model Predictions Compared with the Measured Wheat Canopy Reflectance for Sensor Polar Angle of 5° and Sun Zenith Angle of 38.1°.

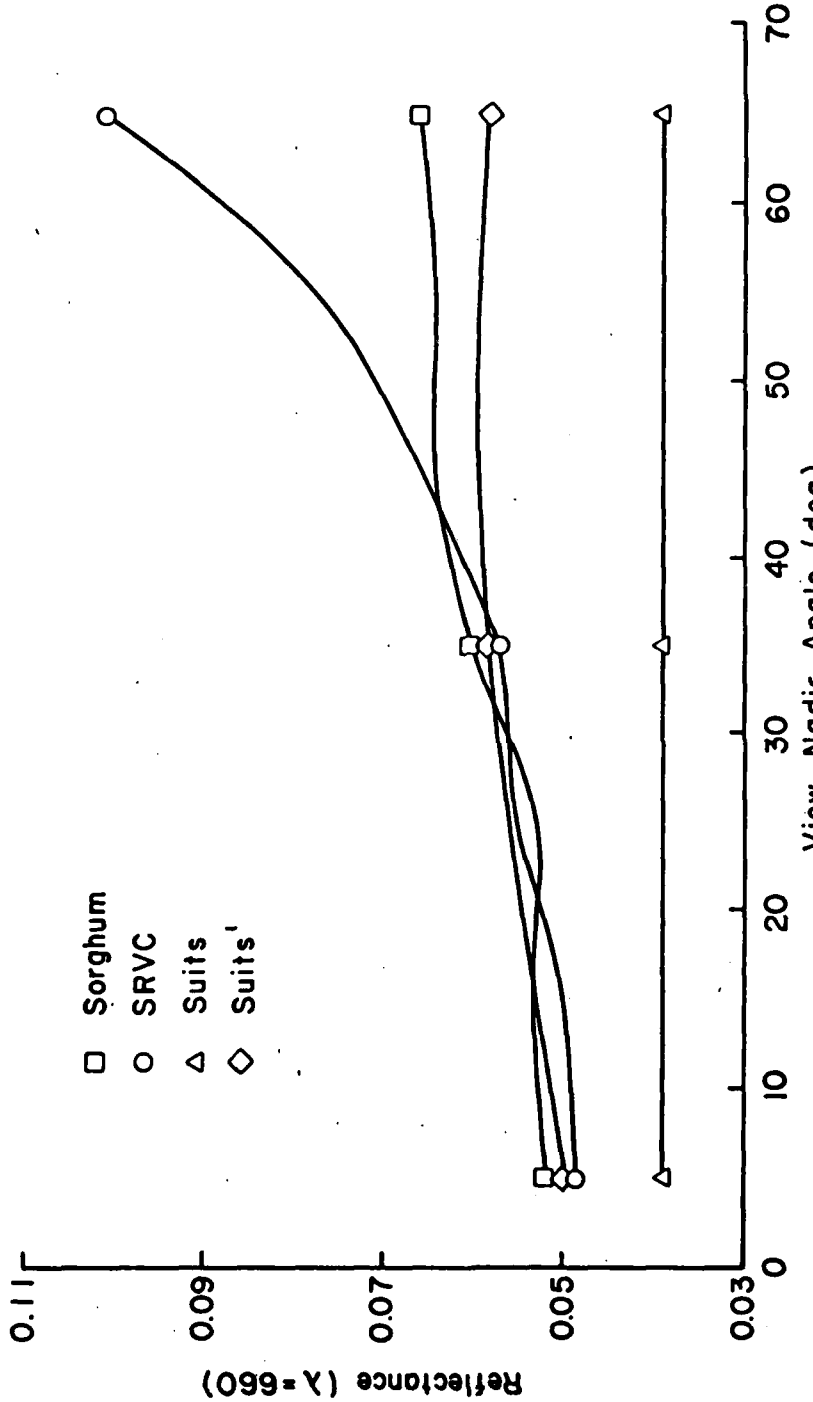

Fig. 9. SRVC, Suits, and Suits' Model Predictions Compared with the Measured Sorghum Canopy Reflectance for Sensor Polar Angle of 5-65° and Sun Zenith Angle of 45°.

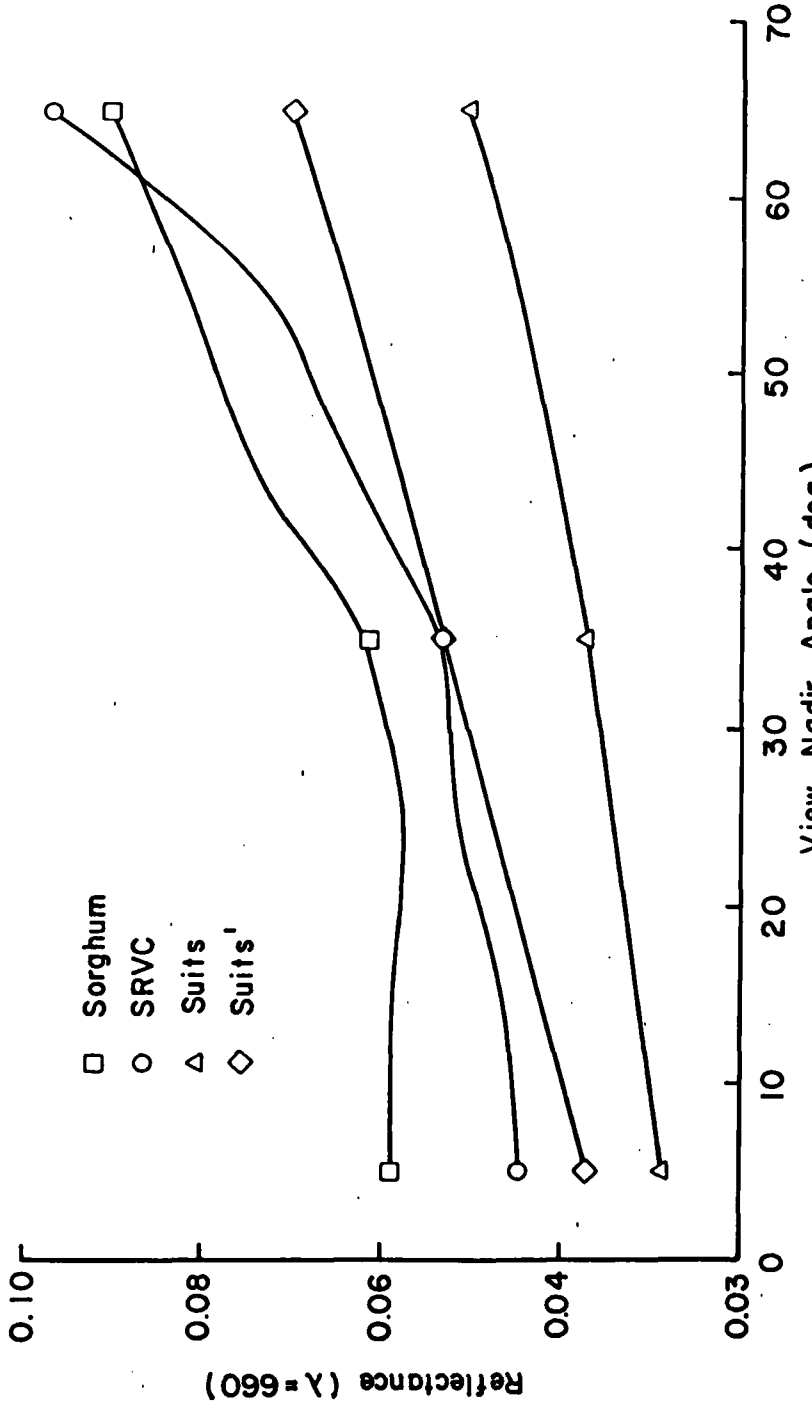

Fig. 10. SRVC, Suits, and Suits' Model Predictions Compared with the Measured Sorghum Canopy Reflectance for Sensor Polar Angle of 5-65° and Sun Zenith Angle of 65°.

this in consistent with the theoretical calculations presented in Tables 1 and 2 of Chapter 2 hich indicate that this model over-estimates the direct flux extinction coefficient. Consequently, less flux will be reflected from the underlying soil layer. Less flux will also be reflected from the leaves since absorption is assumed greater.

More specifically, it is seen from Table 5 that the difference between the Suits and Suits' model for blue for blue grama is between 25 and 40 percent; for wheat the differences are on the order of 20 percent and about 30 percent for sorghum. Generally, the results are insensitive to soil reflectance. Leaf optical properties should be measured to the same degree of precision as the overall canopy reflectance and leaf area index should be determined to within approximately 50 percent of its nominal value. The most stringent requirement experimentally is the estimation of leaf area index for low plant cover situations. This could be a limiting factor, therefore, for the wheat data set.

As a further general comparison test of the three models a simple Chi Square test between each of the model predictions and the measured field data was performed. The value for the SRVC model was 23.6; for the Suits' model, 28.8, and for the original Suits model, 40.3. The corresponding level of significance with 29 degrees of freedom for these values correspond to 75 percent, 50 percent and 10 percent respectively in general agreement with the observations above.

Chapter 4

(C. Nikolopoulos and J. A. Smith)

A MORE COMPLETE ANALYSIS OF THE DUNTLEY EQUATIONS AND THEIR APPLICATION FOR DESCRIBING RADIATIVE TRANSFER IN VEGETATION TERRAIN ELEMENTS

Statement of the Problem and Plan of Attack

The Duntley differential equations for direct and diffuse flux extinction offer a tractible, analytic solution approach, for radiative transfer in plane parallel media whose optical properties can be simply characterized. Diffusing plates are a classic example. Vegetation canopies, however, are more complex in that the individual scattering elements; i.e., leaves, asymmetrically scatter radiation both as a function of their intrinsic optical reflectance and transmittance and their orientations. The original Suits model discussed in Chapter 2 applied the Duntley equations to vegetation media but in order to develop tractible expressions for the Duntley coefficients, abstracted the canopy elements as possessing only vertical and horizontal projections, essentially a Dirac delta function approximation of the leaf slope distribution. The Suits prime (Suits') model developed in Chapter 2 extended the calculations to include consideration of the complete leaf slope distribution in the derivation of the direct flux extinction coefficient and projected view angle. As was seen in Chapter 3, this modification made a considerable change in original Suits model predictions, generally an improvement by a factor between 20 and 40 percent.

In this chapter, the complete analysis of the Duntley equation coefficients is carried out for all five of the original Duntley equation coefficients not just the direct flux extinction coefficient.

Initially, asymmetrical scattering properties of the individual leaves are considered. The analyses presented are of theoretical interest since many of the developments presented are similar to the types of calculations which must be considered in applying classical radiative transfer calculations to vegetation terrain elements, e.g., to calculate appropriate canopy phase functions. However, the complete analysis presented is of limited practical application. Simpler approximations, e.g., Chapter 2, appear more relevant.

The approach is somewhat complex. The general plan of attack is as follows:

First, the solution to the Duntley equations for arbitrary coefficients is given.

Notation and definition of the coordinate system used is then given. The reader should note that the direct flux extinction coefficient of Chapter 2, k, is now represented by α_{33}, and leaf slope distribution by $S(\theta_n)$ rather than $f(\theta_a)$.

Next, the change in the irradiance in the horizontal plane caused by scattering of flux in an infinitestimal plane is calculated. This is accomplished by dividing the coordinate system into four sections, so that the calculation of upwelling and downwelling power emerging from a single component becomes easier. Then an average over all leaf inclinations is performed and the upgoing and downgoing power emerging from a volume element calculated from this power intercepted by both sides of the component due to downwelling and upwelling flux is calculated.

The expressions derived above for the change in the irradiance in the horizontal plane caused by scattering of upwelling and dowwelling flux are then used to derive expressions for α_{ij}, i, j = 1,2. Then a similar analysis used to derive α_{13}, α_{23}.

To evaluate α_{33}, we use the fact that the power intercepted by a component is proportional to the projection of the component in the direction of the beam. So we evaluate the average power intercepted by a component.

An outline of a solution to the problem, by using the classical radiative transfer equation and an iterative procedure to find the radiance emerging from the canopy at a certain direction is then given. However, this approach is shown to be very cumbersome.

Thus, instead certain assumptions that simplify the model are made. More specifically, that the canopy components are assumed uniformly diffuse Lambertian scatterers and the upper reflectance (transmittance) of the component is assumed equal to the lower reflectance (trasmittance). Using these assumptions the formulas of earlier sections are evaluated to find the coefficients α_{ij}.

Finally, the bidirectional reflectance distribution of the canopy is derived.

The Duntley Equations and Their Solution

The Duntley system of differential equations

$$\frac{dE(+d,x)}{dx} = -\alpha_{11}E(+d,x) + \alpha_{12}E(-d,x) + \alpha_{13}E_s(x)$$

$$\frac{dE(-d,x)}{dx} = -\alpha_{21}E(+d,x) + \alpha_{22}E(-d,x) - \alpha_{23}E_s(x) \qquad (1)$$

$$\frac{dE_s(x)}{dx} = \alpha_{33}E_s(x)$$

Subject to the boundary conditions:

$$E(-d,0) = 0$$

$E(+d,1) = \rho_s\{E(-d,-1) + E_s(-1)\}$, where ρ_s is the soil reflectance

has the solutions:

$$E(+d,x) = Ae^{mx} + Be^{-mx} + CE_s(0)\, e^{\alpha_{33}x}$$

$$E(-d,x) = N_1Ae^{mx} + N_2Be^{-mx} + DE_s(0)\, e^{\alpha_{33}x} \qquad (2)$$

$$E_s(x) = E_s(0)\, e^{\alpha_{33}x}$$

where $\alpha = 0.5\ (\alpha_{22} - \alpha_{11})$ and $\sigma = 0.5(\alpha_{12} - \alpha_{21})$

$$m = \sqrt{\alpha^2 - \sigma^2}\ , \quad N_1 = \frac{\alpha + m}{\sigma}\ , \quad N_2 = \frac{\alpha - m}{\sigma}$$

$$C = \frac{\alpha_{23}\sigma - \alpha_{13}(\alpha_{33} - \alpha)}{m^2 - \alpha_{33}^2}$$

$$D = \frac{\alpha_{13}\sigma + \alpha_{23}(\alpha_{33} + \alpha)}{m^2 - \alpha_{33}^2}$$

and A, B are found by $\begin{pmatrix} A \\ B \end{pmatrix} = M^{-1} \cdot \begin{pmatrix} \varepsilon(0) \\ \varepsilon(s) \end{pmatrix}$

where $\varepsilon(0) = E(-d,0) - D\, E_s\,(0)$

$$\varepsilon(s) = [\rho_s\,(D + 1) - C]\, E_s\,(0)\, e^{-\alpha_{33}}$$

$$M = \begin{bmatrix} N_1 & N_2 \\ (1 - \rho_s N_1)\, e^{-m} & (1 - \rho_s N_2)\, e^{m} \end{bmatrix}$$

Establishing Notation, Definitions, and Coordinate System

We consider a single canopy element and its interaction with upwelling and downwelling uniformly diffuse field. Let L_+ denote the upwelling uniformly diffuse radiance of the field, L_- the downwelling uniformly diffuse radiance, E_+ (resp. E_-) the upwelling (resp. downwelling) irradiance evaluated on horizontal plane, I_s the reduced

incident intensity, and E_s the irradiance resulting from reduced incident flow.

Now by definition $\pi L\pm = E\pm$ and $E_s = I_s \cos\theta_s \cdot \Delta\Omega_s$, where $\Delta\Omega_s$ is the solid angle under which the source of specular flux is viewed and θ_s the zenith angle of the source of specular intensity.

The direction $\hat{K}$ of the incoming radiance can be expressed in terms of the polar angles θ and ϕ as $\hat{K} = (|\hat{K}| \sin\theta\cos\phi, |\hat{K}| \sin\theta\sin\phi, |\hat{K}| \cos\theta)$ and if $\hat{K}$ is considered to be a unit vector (i.e., $|\hat{K}| = 1$) $\hat{K} = (\sin\theta\cos\phi, \sin\theta\sin\phi, \cos\theta)$. By $d\vec{A}$ denote the vector down the line of maximum slope of the component of area dA, and by $\hat{n}$ denote the unit vector perpendicular to dA. $I_{\gamma_u}(\hat{K})$ indicates the intensity reflected from upper surface of dA, $I_{\gamma_\ell}(\hat{K})$ the intensity reflected from lower surface of dA, $I_{\tau_u}(\hat{K})$ the intensity transmitted outward from the lower surface and incident on the upper surface, and $I_{\tau_\ell}(\hat{K})$ indicates the intensity transmitted outward from upper surface and incident on the lower surface.

The bidirectional transmisstance and reflectance functions are defined by:

$$I_{\gamma_i}(\hat{K}) := \frac{1}{\pi} \int_i I_{inc}(\hat{K}) \rho_i(\hat{K},\hat{K}') \cdot \hat{K}' \cdot \hat{n}\, d\Omega' \tag{3}$$

$$I_{\tau_i}(\hat{K}) := \frac{1}{\pi} \int_i I_{inc}(\hat{K}') \cdot \tau_i(\hat{K},\hat{K}') \cdot \hat{K}' \cdot \hat{n}\, d\Omega' \tag{4}$$

where $i = u,\ell$, and integration is performed on the upper or lower hemisphere as defined by the plane of dA, $\hat{K}$ is the vector of incidence of light, $\hat{K}'$ the vector of exit of the light, and ρ_i, τ_i the reflectance and trasmittance functions. The trasmittance function of the upper surface is related to that of the lower surface by:

$$\tau_u(\hat{K},\hat{K}') = \tau_\ell(-\hat{K}', -\hat{K})$$

To simplify calculation we choose the coordinate frame as follows: the z-axis is down the line of maximum slope of the canopy component, the y-axis is perpendicular to dA (i.e., $\hat{n} = \hat{\varepsilon}_y$). Thus, if θ is the zenith angle of the incoming radiance vector and ϕ its azimuth angle, then $\hat{n} \cdot \hat{K} = \sin\theta\sin\phi$, since in our coordinate frame $\hat{n} = (0,1,0)$.

It should also be noted that in this chapter leaf angle is denoted by θ_n and leaf slope distribution by $S(\theta_n)$.

Calculation of Total Upwelling and Downwelling Power

Denote the inclination of the canopy element by θ_n. In our coordinate system, partition space into Section A, B, C, D as follows:

$$A = \{(\theta,\phi)/0 < \theta < \pi - \theta_n,\ \pi < \phi < 2\pi\}$$

$$B = \{(\theta,\phi)/0 < \theta < \theta_n,\ 0 < \phi < \pi\}$$

$$C = \{(\theta,\phi)/\pi - \theta_n < \theta < \pi,\ \pi < \phi < 2\pi\}$$

$$D = \{(\theta,\phi)/\theta_n < \theta < \pi,\ 0 < \phi < \pi\}$$

Then all the upwelling intensity emerging from the upper surface is contained in region A. All the downwelling intensity emerging from the upper surface is contained in region C. All upwelling intensity emerging from a lower surface is contained in region B, and all the downwelling intensity emering from lower surface is contained in region D. Therefore, all L_- (resp. L_+) incident on the upper surface is contained in region A (resp. C), and all L_- (resp. L_+) incident on the lower surface is contained in region B (resp. D).

Thus, the scattered intensity caused by downward diffuse intensity L_- is given by:

$$I_{\gamma_u}(\theta,\phi) = \frac{L_-}{\pi} \int_A \rho_u(\theta,\phi;\theta',\phi') \cdot \hat{n} \cdot \hat{K}' \, d\Omega' \tag{5}$$

$$I_{\tau_u}(\theta,\phi) = \frac{L_-}{\pi} \int_A \tau_u(\theta,\phi;\theta',\phi') \, \hat{n} \cdot \hat{K}' \, d\Omega' \tag{6}$$

$$I_{\gamma_\ell}(\theta,\phi) = \frac{L_-}{\pi} \int_B \rho_\ell(\theta,\phi;\theta',\phi') \, \hat{n} \cdot \hat{K}' \, d\Omega' \tag{7}$$

$$I_{\tau_\ell}(\theta,\phi) = \frac{L_-}{\pi} \int_B \tau_\ell(\theta,\phi;\theta',\phi') \, \hat{n} \cdot \hat{K}' \, d\Omega' \tag{8}$$

where (θ,ϕ) is the outgoing direction of I, and (θ',ϕ') is the incoming direction of L.

Let I_+ be the portion of I_{γ_u}, I_{γ_ℓ}, I_{τ_u}, I_{τ_ℓ} directed upward, and I_- be the portion of I_{γ_u}, I_{γ_ℓ}, I_{τ_u}, I_{τ_ℓ} directed downard. Then the power P_+ directed upward is:

$$P_+ = dA \int_o^{\pi} \int_o^{2\pi} I_+ \cdot \hat{n} \cdot \hat{K} \, d\Omega \tag{9}$$

and the power P_- directed downward is:

$$P_- = dA \int_o^{\pi} \int_o^{2\pi} I_- \cdot \hat{n} \cdot \hat{K} \, d\Omega \tag{10}$$

The upwelling intensity emerging from the upper surface is equal to $I_{\tau_\ell} + I_{\gamma_u}$ and is contained in region A. The upwelling intensity emerging from the lower surface is $I_{\gamma_\ell} + I_{\tau_u}$ and is contained in region B. Similarly for downwelling intensity. Therefore (9) and (10) become:

$$P_+ = dA \int_A (I_{\gamma_u}(\theta,\phi) + I_{\tau_\ell}(\theta,\phi)) \, \hat{n} \cdot \hat{K} \, d\Omega$$

$$+ dA \int_B (I_{\gamma_\ell}(\theta,\phi) + I_{\tau_u}(\theta,\phi)) \, \hat{n} \cdot \hat{K} \, d\Omega \tag{11}$$

$$P_- = dA \int_C (I_{\gamma_u}(\theta,\phi) + I_{\tau_\ell}(\theta,\phi))\ \hat{n} \cdot \hat{K}\ d\Omega$$

$$+ dA \int_D (I_{\gamma_\ell}(\theta,\phi) + I_{\tau_u}(\theta,\phi))\ \hat{n} \cdot \hat{K}\ d\Omega \qquad (12)$$

Let $S(\theta_n)$ be the distribution function of the inclination of the canopy components, where $S(\theta_n)$ is normalized by:

$$\frac{2}{\pi} \int_o^{\pi/2} S(\theta_n)\ d\theta_n = 1$$

Then the average of upward and downward power is:

$$\langle P_+ \rangle = \frac{2}{\pi} \int_o^{\pi/2} P_+(\theta_n)\ S(\theta_n)\ d\theta_n \qquad (13)$$

$$\langle P_- \rangle = \frac{2}{\pi} \int_o^{\pi/2} P_-(\theta_n)\ S(\theta_n)\ d\theta_n \qquad (14)$$

Consider a volume element dV, and an element of horizontal area da. Then if x is thickness of dV, $dV = da\ dx$. The number of elements in dV is $ndV = n\ da\ dx$, where n is the number of canopy elements per unit volume. Thus, the upgoing power emerging from dV is $dP_+ = n\ da\ dx \langle P_+ \rangle$ and the downgoing power emerging from a volume element dV is $dP_- = n\ da\ dx \langle P_- \rangle$. Since the irradiance is defined as power over unit area, we have:

$$dE_+ = \frac{dP_+}{da} = n \langle P_+ \rangle dx \quad \text{and} \quad dE_- = \frac{dP_-}{da} = n \langle P_- \rangle dx$$

Hence, the change in the irradiance in the horizontal plane caused by scattering of L_- in a layer of thickness dx is:

$$\frac{dE_+}{dx} = n \langle P_+ \rangle \quad \text{and} \quad \frac{dE_-}{dx} = n \langle P_- \rangle$$

Analogously for the upward diffuse field L_+ we get:

$$I'_{\gamma_u}(\theta,\phi) = \frac{L_+}{\pi} \int_C \rho_u(\theta,\phi;\theta',\phi')\ \hat{n} \cdot \hat{K}\ d\Omega \qquad (15)$$

$$I'_{\tau_\ell}(\theta,\phi) = \frac{L_+}{\pi} \int_D \tau_\ell(\theta,\phi;\theta',\phi') \, \hat{n} \cdot \hat{K} \, d\Omega \tag{16}$$

$$I'_{\gamma_\ell}(\theta,\phi) = \frac{L_+}{\pi} \int_D \rho_\ell(\theta,\phi;\theta',\phi') \, \hat{n} \cdot \hat{K} \, d\Omega \tag{17}$$

$$I'_{\tau_u}(\theta,\phi) = \frac{L_+}{\pi} \int_C \tau_u(\theta,\phi;\theta',\phi') \, \hat{n} \cdot \hat{K} \, d\Omega \tag{18}$$

and using (15) - (18) we get that the power is:

$$P'_+ = dA \int_A [I'_{\gamma_u}(\theta,\phi) + I'_{\tau_\ell}(\theta,\phi)] \, \hat{n} \cdot \hat{K} \, d\Omega$$

$$+ dA \int_B [I'_{\gamma_\ell}(\theta,\phi) + I'_{\tau_u}(\theta,\phi)] \, \hat{n} \cdot \hat{K} \, d\Omega \tag{19}$$

$$P'_- = dA \int_C [I'_{\gamma_u}(\theta,\phi) + I'_{\tau_\ell}(\theta,\phi)] \, \hat{n} \cdot \hat{K} \, d\Omega$$

$$+ dA \int_D [I'_{\gamma_\ell}(\theta,\phi) + I'_{\tau_u}(\theta,\phi)] \, \hat{n} \cdot \hat{K} \, d\Omega \tag{20}$$

and averaging over θ_n we get:

$$\langle P'_+ \rangle = \frac{2}{\pi} \int_o^{\pi/2} P'_+(\theta_n) \, S(\theta_n) \, d\theta_n \tag{21}$$

$$\langle P'_- \rangle = \frac{2}{\pi} \int_o^{\pi/2} P'_-(\theta_n) \, S(\theta_n) \, d\theta_n \tag{22}$$

Thus,

$$\frac{dE'_+}{dx} = n \langle P'_+ \rangle \quad \text{and} \quad \frac{dE'_-}{dx} = n \langle P'_- \rangle$$

where the primes indicate irradiance caused by L_+. We now calculate the total power incident on dA. By definition the incident power P_{inc} is given by:

$$P_{inc} = \int_{I_{inc}} (\theta,\phi) \, \hat{n} \cdot \hat{K} \, d\Omega$$

The downwelling diffuse radiance L_- is nonzero only in the region A and B, and since it is uniformly diffuse it has to be a constant. Also

$d\Omega = \sin\theta d\theta d\phi$, therefore the total power delivered to the upper surface of dA by L_- is:

$$P_U = \int_A dA \cdot L_- \hat{n} \cdot \hat{K}\, d\Omega = dA \cdot L_- \int_A \sin^2\theta\sin\phi d\theta d\phi$$

since the dowelling diffuse radiance L_-, incident on the upper side of dA, is contained in region A.

Evaluating the integral for P_U we get:

$$P_U = dA \cdot L_- \int_o^{\pi-\theta_n} \int_\pi^{2\pi} \sin^2\theta\sin\phi d\theta d\phi = [\pi - \theta_n + \tfrac{1}{2}\sin(2\theta_n)]\, dA \cdot L_- \quad (23)$$

In the same way the total power P_ℓ delivered by L_- onto the lower surface is:

$$P_\ell = dA \cdot L_- \int_B \sin^2\theta\sin\phi d\theta d\phi = [\theta_n - \tfrac{1}{2}\sin(2\theta_n)]\, dA \cdot L_- \quad (24)$$

the total power P_U' delivered by L_+ onto the upper surface is:

$$P_U' = dA \cdot L_+ \int_C \sin^2\theta\sin\phi d\theta d\phi = [\theta_n - \tfrac{1}{2}\sin(2\theta_n)]\, dA \cdot L_+ \quad (25)$$

and the total power P_U' delivered by L_+ one the lower surface is:

$$P_\ell' = dA \cdot L_+ \int_D \sin^2\theta\sin\phi d\theta d\phi = [\pi - \theta_n + \tfrac{1}{2}\sin(2\theta_n)]\, dA \cdot L_+ \quad (26)$$

Hence, the total power intercepted by both sides from L_- is $P_T = P_U + P_\ell = \pi L_- dA$ and the total power from L_+ is:

$$P_T' = P_U' + P_\ell' = \pi L_+ dA$$

Calculation of α_{ij}, i, j=1,2

The portion of E_+ lost over dx because of either absorption or redirection downward of E_+ is equal to $\alpha_{11}E_+$. Therefore $\alpha_{11}E_+$ is the difference of the total upwelling power intercepted by dA minus the amount of power emerging upward from dA.

Similarly, $\alpha_{22}E_-$ is the portion of E_- lost over thickness dx due to absorption or redirection of E_-, $\alpha_{12}E_-$ is the portion added to E_+ over dx due to scattering of E_- into E_+, and $\alpha_{21}E_+$ is the change in E_- due to scattering of E_+ into E_-. So using the previously derived formulas for total power we get:

$$\alpha_{11}E_+ = n(L_+\pi dA - \langle P_+' \rangle)$$

$$\alpha_{22}E_- = n(L_-\pi dA - \langle P_- \rangle)$$

$$\alpha_{21}E_+ = n\langle P_-' \rangle$$

$$\alpha_{12}E_- = \frac{dE_+}{dx} = n \langle P_+ \rangle$$

and since $E_\pm = \pi L_\pm$ we get:

$$\alpha_{11} = \left[n \ dA - \frac{\langle P_+' \rangle}{L_+ \pi} \right] \tag{27}$$

$$\alpha_{12} = \frac{n \langle P_+ \rangle}{L_- \pi} \tag{28}$$

$$\alpha_{21} = \frac{n \cdot \langle P_-' \rangle}{L_+ \pi} \tag{29}$$

$$\alpha_{22} = n \left[dA - \frac{\langle P_- \rangle}{L_- \pi} \right] \tag{30}$$

where $\langle P_\pm \rangle$, $\langle P_\pm' \rangle$ are given in formulas (13), (14), (21), and (22).

The Derivation of α_{13}, α_{23}

The change in upwelling diffuse intensity over dx due to scattering of specular intensity is $\alpha_{13}E(s,o)$, where $E(s,o)$ is the specular flux at the top of the canopy, and is given by:

$$E(s,o) = I(s,o) \cos\theta_s \cdot \Delta\Omega_s$$

In the same way, $\alpha_{23}E(s,o)$ is the change in downwelling diffuse intensity over dx due to scattering of specular intensity.

The scattered intensity from volume element ΔV on which intensity $I(s,o)$ is incident is given by:

$$I_s(\cos\theta,\phi) = \tfrac{1}{4}\pi\, P(\cos\theta,\phi;\ \cos\theta_s,\phi_s)\ I(s,o)\ \frac{\Delta V}{\Delta A}\ \Delta\Omega_s$$

where $P(\cos\theta,\phi;\ \cos\theta_s,\phi_s)$ is the phase function.

The power scattered from volume element ΔV is:

$$P_{\pm} = \Delta A \int_{\pm h} I_s(\cos\theta,\phi)\ d\Omega$$

$$= \tfrac{1}{4}\pi\ \Delta V\ I(s,o)\ \Delta\Omega_s \int_{\pm h} P(\cos\theta,\phi;\ \cos\theta_s,\phi_s)\ d\Omega$$

where + means upwelling and - downwelling power and +h denoted integration over the uppwer hemisphere, -h over the lower hemisphere.

Now since:

$$\frac{P_{\pm}}{\Delta V} = \frac{dE_{\pm}}{dx} \quad \text{and} \quad \frac{E(s,o)}{\cos\theta_s} = I(s,o)\cdot\Delta\Omega_s$$

we have:

$$\frac{dE_{\pm}}{dx} = \frac{E(s,o)}{4\pi\cos\theta_s} \int_{\pm h} P(\cos\theta,\phi;\ \cos\theta_s,\phi_s)d\Omega = \alpha_{i3}E(s,o)$$

Thus:

$$\alpha_{13} = \frac{1}{4\pi\mu_s} \int_{+h} P(\mu_s,\phi_s;\ \mu,\phi)d\Omega \tag{31}$$

$$\alpha_{23} = \frac{1}{4\rho\mu_s} \int_{-h} P(\mu_s,\phi_s;\mu,\phi)d\Omega \tag{32}$$

where $\mu = \cos\theta$, $\mu_s = \cos\theta_s$.

Evaluation of α_{33}

The power intercepted by a component is proportional to the projection of the component in the direction of the beam.

Let $\vec{A}$ be a vector of magnitude equal to the area dA of a component and direction perpendicular to the plane of the component. Let $\vec{R}$ be the unit vector in the direction of the incoming beam.

In a cartesian x,y,z system with z vertical we have:

$$\vec{A} = \sum_i A_i \vec{\varepsilon}_i, \; i=x,y,z, \; \vec{A} \cdot \vec{A} = A^2 = dA$$

$$\vec{R} = \sum_i R_i \vec{\varepsilon}_i, \; i=x,y,z, \; \vec{R} \cdot \vec{R} = 1$$

with $\vec{\varepsilon}_x$, $\vec{\varepsilon}_y$, $\vec{\varepsilon}_z$ unit vectors on x, y, and z axis respectively.

In polar coordinates we have:

$$\vec{A} = |A|(\sin\theta_n\cos\phi_n\vec{\varepsilon}_x + \sin\theta_n\sin\phi_n\vec{\varepsilon}_y + \cos\theta_n\vec{\varepsilon}_z)$$

$$\vec{R} = \sin\theta_s\cos\phi_s\vec{\varepsilon}_x + \sin\theta_s\sin\phi_s\vec{\varepsilon}_y + \cos\theta_s\vec{\varepsilon}_z$$

Thus:

$$|\vec{A} \cdot \vec{R}| = |A|[|\sin\theta_n\sin\theta_s\cos(\phi_n-\phi_s) + \cos\theta_n\cos\theta_s|]$$

By basic algebra we see that if $|\vec{A} \cdot \vec{R}| = |A|\{|F(\phi_n-\phi_s)|\}$ with $F(\phi_n-\phi_s) = \sin\theta_n\sin\theta_s\cos(\phi_n-\phi_s) + \cos\theta_n\cos\theta_s$ then for $\phi_n-\phi_s \leqq \delta_o$: $F(\phi_n-\phi_s) \geqq 0$ and for $\phi_n-\phi_s > \delta_o$: $F(\phi_n-\phi_s) \leqq 0$ where:

$$\delta_o = \begin{cases} \pi, \text{ for } 0 < \theta_n + \theta_s \leqq \frac{\pi}{2} \\ \cos^{-1}[-\cot\theta_n \cot\theta_s], \text{ for } \frac{\pi}{2} \leqq \theta_n + \theta_s < \pi \end{cases}$$

Hence, if we assume that the distribution functio for ϕ_n is $D(\phi_n) = 1$ (i.e., assume azimuthal symmetry), we can calculate the average of $\vec{A} \cdot \vec{R}$ as follows:

$$\langle \vec{A} \cdot \vec{R} \rangle_{\phi_n} = \frac{2A}{\pi}\{\int_o^{\delta_o} [\sin\theta_n \sin\theta_s \cos(\phi_n - \phi_s) +$$

$$+ \cos\theta_n\cos\theta_s] \, d(\phi_n-\phi_s) + \int_{\delta_o}^{\pi} [-\sin\theta_n\sin\theta_s\cos(\phi_n-\phi_s) -$$

$$- \cos\theta_n\cos\theta_s] \, d(\phi_n-\phi_s)\} =$$

$$= \frac{2A}{\pi}\{\sin\theta_n\sin\theta_s\sin\delta_o + (\delta_o - \frac{\pi}{2})\cos\theta_n\cos\theta_s\} S(\theta_n) \, d\theta_n$$

Averaging next over θ_n, we find that the average power for component is:

$$\langle \vec{A} \cdot \vec{R} \rangle_{\theta_n,\phi_n} = \frac{4}{\pi^2} |A| \{\frac{\pi}{2} \cos\theta_s \int_o^{\pi/2-\theta_s} S(\theta_n)\cos\theta_n d\theta_n +$$

$$+ \sin\theta_s \int_{\pi/2-\theta_s}^{\pi/2} \sin\theta_n \sin\delta_o \, S(\theta_n) d\theta_n +$$

$$+ \cos\theta_s \int_{\pi/2-\theta_s}^{\pi/2} (\delta_o - \frac{\pi}{2}) \cos\theta_n \, S(\theta_n) d\theta_n\}$$

where $\delta_o = \cos^{-1}[-\cot\theta_n \cot\theta_s]$. Finally,

$$\alpha_{33} = \frac{n \cdot \langle \vec{A} \cdot \vec{R} \rangle \, \theta_n,\phi_n}{\cos\theta_s} \tag{33}$$

Evaluation of Emergent Intensity in the General Case of Plane Parallel Problems

Let $\mu = \cos\theta$. Then the radiation transfer equation becomes:

$$\mu \frac{dI(\tau,\mu,\phi)}{d\tau} = I(\tau,\mu,\phi) - F(\tau,\mu,\phi)$$

where the optical thickness:

$$\tau = \int_t^\infty k\rho dt$$

k = scattering coefficient and ρ = density of material. If the optical thickness is finite then the solution becomes:

$$I(\tau,\mu,\phi) = I(\tau_1,\mu,\phi)e^{-(\tau_1-\tau)/\mu} + \int_\tau^{\tau_1} F(t,\mu,\phi)e^{-(t-\tau)/\mu} \frac{dt}{\mu}$$

In particular for emergent intensity we have:

$$L(\mu,\phi) = I(o,\mu,\phi) = I(\tau_1,\mu,\phi)e^{-\tau_1/\mu} + \int_o^{\tau_1} e^{-t/\mu} F(t,\mu,\phi) \frac{dt}{\mu} \tag{34}$$

where the source function F is:

$$F(\theta,\phi) = \tfrac{1}{4}\pi \int_o^\pi \int_o^{2\pi} P(\theta,\phi;\, \theta',\phi') \, I(\theta,\phi) \sin\theta' \, d\theta' \, d\phi' \tag{35}$$

To solve (34) we use the following iterative approach:

First we make an initial guess for I, by using the Duntley equations. Then given this initial guess for I, we can calculate F from (35) and then update I.

Now let (μ,ϕ) the view angle, (μ_o,ϕ_o) the direction of coming specular flux, ρ_s = the soil reflectance. Assume components in canopy are Labmertian scatters. Then the upward radiance L of the canopy for the view angle (μ,ϕ) will be:

$$L(\mu,\phi) = I(o,\mu,\phi) = I(\tau_1,\mu,\phi)e^{-\tau_1/\mu} + \frac{1}{\mu}\int_o^{\tau_1} F(t,\mu,\phi)e^{-t/\mu}\,dt$$

Now $I(\tau_1,\mu,\phi)$ is the radiance from the soil that goes through canopy and

$$I(\tau_1,\mu,\phi) = \gamma_s\, I(+d,\tau_1)$$

To find the initial $I(o,\mu,\phi)$ we assume that the medium (canopy) is a conservative case of perfect scattering, i.e., all incident radiation becomes diffuse flux; there is no absorption. In that case the upward radiance will be:

$$I(\tau,\mu_1,\phi_1) = I(+d,\tau) + I(-d,\tau) + I(s,\mu_o,\phi_o)$$

But:

$$E(\pm d,\tau) = \pi L(\pm d,\tau) = \pi\, I(\pm d,\tau)$$

so:

$$I(+d,\tau) = \frac{E(+d,\tau)}{\pi},\quad I(-d,\tau) = \frac{E(-d,\tau)}{\pi}$$

and also:

$$I(s,\tau,\mu_o,\phi_o) = I(s,o,\mu_o,\phi_o)e^{-(\tau-\tau_1)/\mu_o} = \frac{E_s(o)}{\mu_o}\, e^{-(\tau-\tau_1)/\mu_o}$$

Thus:

$$F(\tau,\mu,\phi) = \tfrac{1}{4\pi} \int_{-1}^{1} \int_{o}^{2\pi} P(\mu,\phi,\mu',\phi')\ I(\mu',\phi')d\phi'\ d\mu'$$

$$= \tfrac{1}{4\pi} \int_{-1}^{1} \int_{o}^{2\pi} P(\mu,\phi,\mu',\phi') \left\{\frac{E_+}{\pi} + \frac{E_-}{\pi} + \frac{E_s(o)}{\mu_o}\ e^{-(\tau-\tau_1)/\mu_o}\right\} d\phi'\ d\mu'$$

$$= \frac{E_+}{4\pi^2} \int_{-1}^{1} \int_{o}^{2\pi} P(\mu,\phi,\mu',\phi') + \frac{E_-}{4\pi^2} \int_{-1}^{1} \int_{o}^{2\pi} P(\mu,\phi,\mu',\phi')d\phi'd\mu'$$

$$+ \frac{E_s(o)}{4\pi\mu_o}\ e^{-(\tau-\tau_1)/\mu_o} \int_{-1}^{1} \int_{o}^{2\pi} P(\mu,\phi,\mu',\phi')d\phi'\ d\mu'$$

And so:

$$F(\theta,\phi) = F(\tau,\mu,\phi) = \tfrac{1}{4\pi} \left\{\frac{E(-d,\tau)}{\pi} \int_{o}^{1} \int_{o}^{2\pi} P(\mu,\phi,\mu',\phi')d\mu'\ d\phi'\right.$$

$$\left. + \frac{E(+d,\tau)}{\pi} \int_{-1}^{o} \int_{o}^{2\pi} P(\mu,\phi,\mu',\phi')d\mu'\ d\phi'\right\}$$

$$+ \tfrac{1}{4\pi} \frac{E_o}{\mu_o}\ e^{-(\tau-\tau_1)/\mu_o}\ P(\mu,\phi,\mu_o,\phi_o)$$

Now if we know the phase function we can find $I(o,\mu,\phi) = L(\mu,\phi)$.

Development of a Simplified Model for Lambertian Canopy Components

To simplify the model we assume first that the canopy components are uniformly diffuse Lambertian scatterers (i.e, that the bidirectional scattering functions are constants).

Let $G = \theta_n - \tfrac{1}{2}\sin(2\theta_n)$. Then:

$$\int_A \sin\theta\sin\phi d\Omega = \pi - \theta_n + \tfrac{1}{2}\sin(2\theta_n) = \pi - G$$

$$\int_B \sin\theta\sin\phi d\Omega = \theta_n - \tfrac{1}{2}\sin(2\theta_n) = G$$

$$\int_C \sin\theta\sin\phi d\Omega = \theta_n - \tfrac{1}{2}\sin(2\theta_n) = G$$

$$\int_D \sin\theta\sin\phi d\Omega = \pi - G$$

Now since $\hat{n} \cdot \hat{K} = \sin\theta\sin\phi$, using relations (5) - (8) for L_-, we get:

$$I_{\gamma_U}(\theta,\phi) = \frac{L_-}{\pi} \int_A \rho_U\ \hat{n} \cdot \hat{K} d\Omega = \frac{L_-\rho_U}{\pi} \int_A \sin^2\theta\sin\phi d\theta d\phi = \frac{L_-\rho_U}{\pi}\ (\pi - G)$$

$$I_{\tau_\upsilon}(\theta,\phi) = \frac{L_-\tau_\upsilon}{\pi}(\pi - G)$$

$$I_{\gamma_\ell}(\theta,\phi) = \frac{L_-\rho_\ell}{\pi} G$$

$$I_{\tau_\ell}(\theta,\phi) = \frac{L_-\tau_\ell}{\pi} G$$

Similarly using relation (15) - (18) for L_+, we get:

$$I'_{\gamma_\upsilon} = \frac{L_+}{\pi} \int_C \rho_\upsilon \hat{n} \cdot \hat{K}\, d\Omega = \frac{L_+\rho_\upsilon}{\pi} G$$

$$I'_{\tau_\upsilon}(\theta,\phi) = \frac{L_+\tau_\upsilon}{\pi} G$$

$$I'_{\gamma_\ell}(\theta,\phi) = \frac{L_+\rho_\ell}{\pi}(\pi - G)$$

$$I'_{\tau_\ell}(\theta,\phi) = \frac{L_+\tau_\ell}{\pi}(\pi - G)$$

Using the above equations in relations (11) and (12) we get that the power due to downwelling intensity is:

$$P_+ = \frac{dAL_-}{\pi}[\rho_\upsilon(\pi - G)^2 + \tau_\ell G(\pi - G) + \rho_\ell G^2 + \tau_\upsilon(\pi - G)G]$$

$$P_- = \frac{dAL_-}{\pi}[\rho_\upsilon(\pi - G)G + \tau_\ell G^2 + \rho_\ell G(\pi - G) + \tau_\upsilon(\pi - G)^2]$$

Similarly the power due to upwelling intensity L_+ is:

$$P'_+ = \frac{dAL_+}{\pi}[\rho_\upsilon G(\pi - G) + \tau_\ell(\pi - G)^2 + \rho_\ell(\pi - G)G + \tau_\upsilon G^2]$$

$$P'_- = \frac{dAL_+}{\pi}[\rho_\upsilon G^2 + \tau_\ell(\pi - G)G + \rho_\ell(\pi - G)^2 + \tau_\upsilon(\pi - G)G]$$

where $G = \theta_n = \frac{1}{2}\sin(2\theta_n)$. Thus averaging over θ_n and using relations (13) and (14), we get:

$$\langle P_+ \rangle = \pi d A L_- \left[D(\rho_u - \tau_\ell + \rho_\ell - \tau_u) + R(-2\rho_u + \tau_\ell + \tau_u) + \rho_u\right]$$

$$\langle P_- \rangle = \pi d A L_- \left[D(-\rho_u - \rho_\ell + \tau_\ell + \tau_u) + R(\rho_u + \rho_\ell - 2\tau_u) + \tau_u\right]$$

$$\langle P_+' \rangle = \pi d A L_+ \left[D(-\rho_u - \rho_\ell + \tau_u + \tau_\ell) + R(\rho_u + \rho_\ell - 2\tau_\ell) + \tau_\ell\right]$$

$$\langle P_-' \rangle = \pi d A L_+ \left[D(\rho_u + \rho_\ell - \tau_\ell - \tau_u) + R(\tau_u + \tau_\ell - 2\rho_\ell) + \rho_\ell\right]$$

where:

$$R = \frac{2}{\pi^2} \int_o^{\pi/2} \left[\theta_n - \tfrac{1}{2}\sin(2\theta_n)\right] S(\theta_n)\, d\theta_n$$

$$D = \frac{2}{\pi^3} \int_o^{\pi/2} \left[\theta_n - \tfrac{1}{2}\sin(\theta_n)\right]^2 S(\theta_n)\, d\theta_n$$

Now, relations (27) - (30) give:

$$\alpha_{11} = n\left[dA - \frac{\langle P_+' \rangle}{L_+ \pi}\right] = ndA\left[1 - (\tau_u+\tau_\ell-\rho_u-\rho_\ell)D - (\rho_u+\rho_\ell-2\tau_\ell)R - \tau_\ell\right]$$

$$\alpha_{12} = \frac{n\langle P_+ \rangle}{\pi L_-} = ndA\left[(\rho_u + \ell_\ell + \tau_u - \tau_\ell)D + (\tau_u + \tau_\ell - 2\rho_u)R + \rho_u\right]$$

$$\alpha_{21} = \frac{n\langle P_-' \rangle}{\pi L_+} = ndA\left[(\rho_u + \rho_\ell - \tau_\ell - \tau_u)D + (\tau_u + \tau_\ell - 2\rho_\ell)R + \rho_\ell\right]$$

$$\alpha_{22} = n\left[dA - \frac{\langle P_- \rangle}{\pi L_-}\right] = ndA\left[1 - \tau_u - (\tau_\ell+\tau_u-\rho_\ell-\rho_u)D - (\rho_u+\rho_\ell-2\tau_u)R\right]$$

Assuming that $\rho_u = \rho_\ell$ and $\tau_u = \tau_\ell$ we get:

$$\alpha_{11} = ndA\left[1 + 2(\tau-\rho)D + 2(\rho-\tau)R - \tau\right] = \alpha_{22}$$

$$\alpha_{12} = ndA\left[2(\rho-\tau)D + 2(\tau-\rho)R + \rho\right] = \alpha_{21}$$

with

$$R = \frac{2}{\pi^2} \int_o^{\pi/2} G(\theta_n)\, S(\theta_n)\, d\theta_n$$

$$D = \frac{2}{\pi^3} \int_o^{\pi/2} G^2(\theta_n)\, S(\theta_n)\, d\theta_n$$

$$G(\theta_n) = \theta_n - \tfrac{1}{2}\sin(2\theta_n)$$

Evaluation of α_{13}, α_{23} for case $\rho_u = \rho_\ell$, $\tau_u = \tau_\ell$

The intensity due to reflection from upper surface is:

$$I_{\gamma_u} = \frac{I_o\, \Delta\Omega_o \rho_u}{\pi} \left| \hat{K} \cdot \hat{n} \right| \tag{37}$$

The intensity due to transmission from the upper surface to the lower surface is:

$$I_{\tau_u} = \frac{I_o\, \Delta\Omega_o\, \tau_u}{\pi} \left| \hat{K} \cdot \hat{n} \right| \tag{38}$$

The intensity due to reflection from lower surface is:

$$I_{\gamma_\ell} = \frac{I_o\, \Delta\Omega_o\, \rho_\ell}{\pi} \left| \hat{K} \cdot \hat{n} \right| \tag{39}$$

The intensity due to transmission from lower to upper surface is:

$$I_{\tau_\ell} = \frac{I_o\, \Delta\Omega_o\, \tau_\ell}{\pi} \left| \hat{K} \cdot \hat{n} \right| \tag{40}$$

where $\left| \hat{K} \cdot \hat{n} \right| = \cos\gamma_o = \sin\theta_s \sin\theta_n \cos(\phi_s - \phi_n) + \cos\theta_s \cos\theta_n$ and γ_o is the angle between $\hat{\nu}$ and $\hat{n}$.

The conditions for upper and lower incidence can be seen to be the following:

$\cos\gamma_o$ is positive if $(0 < \theta_n < \frac{\pi}{2} - \theta_s$ and $0 < \phi_n < 2\pi)$

or if $(\frac{\pi}{2} - \theta_s < \theta_n < \frac{\pi}{2}$ and $\phi_s - \delta_o < \phi_n < \phi_s + \delta_o)$

Also $\cos\gamma_o < 0$ if $(\frac{\pi}{2} - \theta_s < \theta_n < \frac{\pi}{2}$ and $\phi_s + \delta_o < \phi_n < \phi_s + 2\pi - \delta_o)$

where $\delta_o = \cos^{-1}(-\cot\theta_s \cot\theta_n)$

The upwelling power reflected from upper side is

$$P^+_{\gamma_\upsilon} = I_{\gamma_\upsilon} \, dA \int_A \sin\theta \sin\phi \, d\Omega$$

Similarly

$$P^-_{\gamma_\upsilon} = I_{\gamma_\upsilon} \, dA \int_C \sin\theta \sin\phi \, d\Omega$$

$$P^-_{\tau_\upsilon} = I_{\tau_\upsilon} \, dA \int_D \sin\theta \sin\phi \, d\Omega \qquad (41)$$

$$P^+_{\tau_\upsilon} = I_{\tau_\upsilon} \, dA \int_B \sin\theta \sin\phi \, d\Omega$$

Using (37) and (41) we get:

$$P^+_\upsilon(\theta_n,\phi_n) = \frac{I_o \, \Delta\Omega_o \cos\gamma_o \, dA}{\pi} [\rho_\upsilon\pi + (\tau_\upsilon - \rho_\upsilon) G]$$

$$= \frac{E_s(0)}{\cos\theta_s} \frac{\cos\gamma_o}{\pi} dA \, [\rho_\upsilon\pi + (\tau_\upsilon - \rho_\upsilon) G]$$

$$P^-_\upsilon(\theta_n,\phi_n) = \frac{I_o \, \Delta\Omega_o \cos\gamma_o \, dA}{\pi} [\tau_\upsilon\pi + (\rho_\upsilon - \tau_\upsilon) G]$$

$$= \frac{E_s(0)}{\cos\theta_s} \frac{\cos\gamma_o}{\pi} dA \, [\tau_\upsilon\pi + (\rho_\upsilon - \tau_\upsilon) G]$$

Similarly for elements illuminated on the lower side we have:

$$P_{\ell}^{+}(\theta_n,\phi_n) = \frac{I_o\,\Delta\Omega_o\,\cos\gamma_o\,dA}{\pi}\,[\tau_{\ell}\pi + (\rho_{\ell} - \tau_{\ell})\,G]$$

$$= \frac{E_s\,(0)\,\cos\gamma_o\,dA}{\pi\,\cos\theta_s}\,[\tau_{\ell}\pi + (\rho_{\ell} - \tau_{\ell})\,G]$$

$$P_{\ell}^{-}(\theta_n,\phi_n) = \frac{I_o\,\Delta\Omega_o\,\cos\gamma_o\,dA}{\pi}\,[\rho_{\ell}\pi + (\tau_{\ell} - \rho_{\ell})\,G]$$

$$= \frac{E_s\,(0)\,\cos\gamma_o\,dA}{\pi\,\cos\theta_s}\,[\rho_{\ell}\pi + (\tau_{\ell} - \rho_{\ell})\,G]$$

Thus the total upwelling power by all elements in ΔV is given by:

$$P^{+} = \frac{n\Delta V}{\pi^2}\int_o^{\pi/2-\theta_s}\int_o^{2\pi} S(\theta_n)\,D(\phi_n)\,P_{U}^{+}(\theta_n,\phi_n)\,d\phi_n\,d\theta_n$$

$$+ \int_{\pi/2-\theta_s}^{\pi/2}\int_{\phi_s-\delta_o}^{\phi_s+\delta_o} S(\theta_n)\,D(\phi_n)\,P_{U}^{+}(\theta_n,\phi_n)\,d\phi_n\,d\theta_n$$

$$+ \int_{\pi/2-\theta_s}^{\pi/2}\int_{\phi_s+\delta_o}^{\phi_s+2\pi-\delta_o} S(\theta_n)\,D(\phi_n)\,P_{\ell}^{+}(\theta_n,\phi_n)\,d\phi_n\,d\theta_n \qquad (42)$$

and the total downwelling power is given by:

$$P^{-} = \frac{n\Delta V}{\pi^2}\int_o^{\pi/2-\theta_s}\int_o^{2\pi} S(\theta_n)\,D(\phi_n)\,P_{U}^{-}(\theta_n,\phi_n)\,d\phi_n\,d\theta_n$$

$$+ \int_{\pi/2-\theta_s}^{\pi/2}\int_{\phi_s-\delta_o}^{\phi_s+\delta_o} S(\theta_n)\,D(\phi_n)\,P_{U}^{-}(\theta_n,\phi_n)\,d\phi_n\,d\theta_n$$

$$+ \int_{\pi/2-\theta_s}^{\pi/2}\int_{\phi_s+\delta_o}^{\phi_s+2\pi-\delta_o} S(\theta_n)\,D(\phi_n)\,P_{\ell}^{-}(\theta_n,\phi_n)\,d\phi_n\,d\theta_n \qquad (43)$$

Now as before $\alpha_{13} = \dfrac{P^{+}}{\Delta V E_s\,(0)}$, $\alpha_{23} = \dfrac{P^{-}}{\Delta V E_s\,(0)}$

Assuming that the distribution function $D(\phi_n)$ of the azimuths of the leaves is equal to 1 we get:

$$\alpha_{13} = \frac{ndA}{\pi^3 \cos\theta_s} \int_o^{\pi/2-\theta_s} S(\theta_n)[\pi\rho + (\tau - \rho)\, G]\, (2\pi \cos\theta_s \cos\theta_n)\, d\theta_n$$

$$+ \int_{\pi/2-\theta_s}^{\pi/2} S(\theta_n)[\pi\rho+(\tau-\rho)G](2\sin\theta_s\sin\theta_n\sin\delta_o+2\delta_o \cos\theta_s \cos\theta_n)\, d\theta_n$$

$$+ \int_{\pi/2-\theta_s}^{\pi/2} S(\theta_n)[\pi\tau+(\rho-\tau)G](2(\pi-\delta_o) \cos\theta_s\cos\theta_n-2\sin\theta_s\sin\theta_n\sin\delta_o)d\theta_n$$

Also

$$\alpha_{23} = \frac{ndA}{\pi^3 \cos\theta_s} \int_o^{\pi/2-\theta_s} S(\theta_n)[\pi\tau + (\rho - \tau)\, G]\, 2\pi \cos\theta_s \cos\theta_n\, d\theta_n$$

$$+ \int_{\pi/2-\theta_s}^{\pi/2} S(\theta_n)[\pi\tau+(\rho-\tau)G](2\sin\theta_s \sin\theta_n \sin\delta_o + 2\delta_o \cos\theta_s \cos\theta_n)\, d\theta_n$$

$$+ \int_{\pi/2-\theta_s}^{\pi/2} S(\theta_n)[\pi\rho+(\tau-\rho)G](2(\pi-\delta_o) \cos\theta_s \cos\theta_n - 2\sin\theta_s \sin\theta_n \sin\delta_o)\, d\theta_n$$

Evaluation of α_{33}

In the same way as in previous section we find that $\alpha_{33} = n \cdot \langle \vec{A}\cdot\vec{R} \rangle_{\theta_n,\phi_n/\cos\theta_s}$ where

$$\langle \vec{A}\cdot\vec{R} \rangle_{\theta_n,\phi_n} = \frac{2}{\pi}\, dA \Big\{ \frac{\pi}{2} \cos\theta_s \int_o^{\pi/2-\theta_s} S(\theta_n) \cos\theta_n\, d\theta_n$$

$$+ \sin\theta_s \int_{\pi/2-\theta_s}^{\pi/2} \sin\theta_n \sin\delta_o\, S(\theta_n)\, d\theta_n + \cos\theta_s$$

$$\int_{\pi/2-\theta_s}^{\pi/2} (\delta_o - \tfrac{\pi}{2}) \cos\theta_n\, S(\theta_n)\, d\theta_n \Big\}$$

and $\delta_o = \cos^{-1}(-\cot\theta_n \cot\theta_s)$.

Calculation of the Bidirectional Reflectance Distribution Function of the Canopy

Due to the difficulties involved in using the phase functions to calculate the bidirectional reflectance, we will use here an approach similar to that used in the SRVC Model (Smith and Oliver, 1972).

We have that the reflected and transmitted radiation in direction θ due to incident flux is: (see Goudriaan, 1973, p. 48).

(i) Due to specular flux E_s, the radiance is:

$$L_{E_S} = E_S \{(\rho + \tau) \frac{4}{2\pi^2} [\alpha_1 (2\alpha_c \alpha_c' - \pi\alpha_c - \pi\alpha_c') + \alpha_2 \sin\alpha_c' (2\alpha_c - \pi) + \alpha_3 \sin\alpha_c (2\alpha_c' - \pi) + 2\alpha_4 \sin\alpha_c \sin\alpha_c'] + 2\alpha_1\rho\} \sin\theta \quad (44)$$

(ii) Due to downwelling irradiance $E(-d)$:

$$L_{E(-d)} = E(-d) \{(\rho + \tau) \frac{4}{2\pi^2} \frac{2}{\pi} \int_o^{\pi/2} [\alpha_1 (2\alpha_c \alpha'_c - \pi\alpha_c - \pi\alpha_c') + \alpha_2 \sin\alpha_c' (2\alpha_c - \pi) + \alpha_3 \sin\alpha_c (2\alpha_c - \pi) + 2\alpha_4 \sin\alpha_c \sin\alpha_c'] d\theta + 2\rho \frac{2}{\pi} \int_o^{\pi/2} \alpha_1 d\theta\} \sin\theta \quad (45)$$

(iii) Due to upwelling irradiance $E(+d)$:

$$L_{E(+d)} = E(+d) \{(\rho + \tau) \frac{4}{2\pi^2} \frac{2}{\pi} \int_o^{\pi/2} [\alpha_1 (2\alpha_c \alpha_c' - \pi\alpha_c - \pi\alpha_c') + \alpha_2 \sin\alpha_c' (2\alpha_c - \pi) + \alpha_3 \sin\alpha_c (2\alpha_c' - \pi) + 2\alpha_4 \sin\alpha_c \sin\alpha_c'] d\theta + 2\tau \frac{2}{\pi} \int_o^{\pi/2} \alpha_1 d\theta\} \sin\theta \quad (46)$$

where,
$$\alpha_1 = \cos\theta_s \cos\theta \cos^2\theta_n$$
$$\alpha_2 = \cos\theta_s \sin\theta \sin\theta_n \cos\theta_n$$
$$\alpha_3 = \sin\theta_s \cos\theta \sin\theta_n \cos\theta_n \quad (47)$$
$$\alpha_4 = \sin\theta_s \sin\theta \sin^2\theta_n$$
$$\alpha_c = \begin{cases} \cos^{-1}(-\cot\theta_n \cot\theta_s), & \text{if } \frac{\pi}{\pi} - \theta_n < \theta_s \\ \pi, & \text{if } \theta_s \leq \frac{\pi}{2} - \theta_n \end{cases}$$

$$\alpha_c' = \begin{cases} \cos^{-1}(-\cot\theta_n \cot\theta), & \text{if } \theta > \frac{\pi}{\pi} - \theta_n \\ \pi, & \text{if } \theta \leq \frac{\pi}{2} - \theta_n. \end{cases}$$

Thus the total radiance emitted from a component of inclination θ_n will be:

$$\Delta L(\theta_n) = L_{E_S} + L_{E(+d)} + L_{E(-d)} = \frac{u_1}{\pi} E(+d) + \frac{v_1}{\pi} E(-d) + \frac{w_1}{\pi} E_S \quad (48)$$

where u_1, v_1, w_1 are functions of θ, θ_s, α_i, α_c, α_c'. For exact expression of u_1, v_1, w_1 see Appendum A.

Now if $\theta_s \geq \theta$, then $\pi/2 - \theta_s \leq \pi/2 - \theta$ and in averaging $\Delta L(\theta_n)$ over θ_n, we need to subdivide the interval $(0, \pi/2)$ into the subintervals $(0, \pi/2 - \theta_s)$, $(\pi/2 - \theta_s, \pi/2 - \theta)$, $(\pi/2 - \theta, \pi/2)$. Then the values of α_c, α_c' in the expressions of u_1, v_1, w_1 become:

in $w_1(\alpha_c, \alpha_c')$ we have:

(i) $\alpha_c = \pi$, $\alpha_c' = \pi$, if $0 \leq \theta_n \leq \frac{\pi}{2} - \theta_s$

(ii) $\alpha_c = \cos^{-1}(-\cot\theta_s \cot\theta_n)$, $\alpha_c' = \pi$, if $\frac{\pi}{2} - \theta_s \leq \theta_n \leq \frac{\pi}{2} - \theta$

(iii) $\alpha_c = \cos^{-1}(-\cot\theta_s \cot\theta_n)$, $\alpha_c' = \cos^{-1}(-\cot\theta \cot\theta_n)$,

if $\frac{\pi}{2} - \theta < \tau_n < \frac{\pi}{2}$

in $u_1(\alpha_c')$ we have:

(i) $\alpha_c' = \pi$, if $0 \leq \theta_n \leq \frac{\pi}{2} - \theta$

(ii) $\alpha_c' = \cos^{-1}(-\cot\theta \cot\theta_n)$, if $\frac{\pi}{2} - \theta \leq \theta_n \leq \frac{\pi}{2}$

in $v_1(\alpha_c')$ we have:

(i) $\alpha_c' = \pi$, if $0 \leqq \theta_n \leqq \frac{\pi}{2} - \theta$

(ii) $\alpha_c' = \cos^{-1}(-\cot\theta \cot\theta_n)$, if $\frac{\pi}{2} - \theta \leqq \theta_n \leqq \frac{\pi}{2}$.

Similarly for $\theta_s < \theta$.

Let $S(\theta_n)$ be the distribution function of the leaf inclination. Averaging over θ_n we get that:

$$\Delta L(\text{layer}) = \frac{2}{\pi} dA \left\{ \frac{E_S}{\pi} w + \frac{E(+d)}{\pi} u + \frac{E(-d)}{\pi} v \right\}, \quad \text{if} \quad \theta_s \geqq \theta$$

and

$$\Delta L(\text{layer}) = \frac{2}{\pi} dA \left\{ \frac{E_S}{\pi} w' + \frac{E(+d)}{\pi} u + \frac{E(-d)}{\pi} v \right\}, \quad \text{if} \quad \theta_s < \theta$$

and the exact expressions of w, w', u, v are given in the Appendum B. The probability of achieving line of sight through the canopy is e^{Kx}, where

$$K = \frac{2}{\pi} \int_o^{\pi/2} S(\theta_n) \left| \vec{A} \cdot \vec{r} \right| d\theta_n$$

where $\vec{A}$ is a perpendicular to the leaf vector and $\vec{r}$ is a unit vector in the direction of view. Thus in the same way as for α_{33} we get that

$$K = \frac{n \cdot \langle \vec{A} \cdot \vec{r} \rangle_{\theta_n, \phi_n}}{\cos\theta} ,$$

where

$$\langle \vec{A} \cdot \vec{r} \rangle_{\theta_n, \phi_n} = \frac{2}{\pi} dA \left[\frac{\pi}{2} \cos\theta_o \int_o^{\pi/2-\theta} S(\theta_n) \cos\theta_n \, d\theta_n \right.$$

$$+ \sin\theta_o \int_{\pi/2-\theta}^{\pi/2} \sin\theta_n \sin\delta_o \, S(\theta_n) \, d\theta_n + \cos\theta_o$$

$$\left. \int_{\pi/2-\theta}^{\pi/2} (\delta_o - \frac{\pi}{2}) \cos\theta_n \, S(\theta_n) \, d\theta_n \right]$$

and

$$\delta_o = \cos^{-1} (-\cot\theta_n \cot\theta).$$

Hence $\Delta L_\lambda (x) = \Delta L_\lambda (\text{layer})\ e^{Kx}$

and so $\Delta L_\lambda (\text{outside}) = \int_{-1}^{0} \Delta L_\lambda (\text{layer})\ e^{Kx}\ dx.$

The solution to the system of differential equations (1) is:

$$E (+d,x) = A\ e^{mx} + B\ e^{-mx} + C\ e^{kx}$$

$$E (-d,x) = N_1\ A\ e^{mx} + N_2\ B\ e^{-mx} + D\ e^{kx}$$

$$E_s (x) = E_s (0)\ e^{kx} = e^{kx}$$

where A, B, C, D, N_1, and N_2 are defined earlier in terms of α_{ij}. Thus the outgoing irradiance from depth x is

$$\Delta L(\text{layer}) (x) = \frac{E (+d,x)}{\pi} u + \frac{E (-d,x)}{\pi} v + \frac{E_s (x)}{\pi} w \quad e^{Kx} \qquad (49)$$

where u, v, and w are given previously and e^{Kx} is the probability that the light will go through the canopy. To get the total ΔL we integrate with respect to x

$$\Delta L(\text{layer}) = \int_{-1}^{0} \Delta L(\text{layer}) (x) = \frac{u}{\pi} \int_{-1}^{0} E (+d,x)\ e^{Kx}\ dx$$

$$+ \frac{v}{\pi} \int_{-1}^{0} E (-d,x)\ e^{Kx}\ dx + \frac{w}{\pi} \int_{-1}^{0} E_s (x)\ e^{Kx}\ dx$$

$$= \frac{u}{\pi} \left\{ \frac{A (1 - e^{-(K + m)})}{K + m} + \frac{B (1 - e^{-(K - m)})}{K - m} + \frac{C (1 - e^{-(K + k)})}{K + k} \right\}$$

$$+ \frac{v}{\pi} \left\{ \frac{N1\ A (1 - e^{-(K + m)})}{K + m} \quad \frac{N_2\ B (1 - e^{-(K - m)})}{K - m} \quad \frac{D (1 - e^{-(K + k)})}{K + k} \right\}$$

$$+ \frac{w}{\pi} \frac{1 - e^{-(K + k)}}{K + k} \qquad (50)$$

Now the radiance contribution from the soil can be calculated using the hemispherical reflectance ρ_s of the soil and the flux values of E (-d,-1), E_S (-1):

$$\pi L_{soil} = e^{-K} \rho_S (E_S (-1) + E (-d,-1)) \quad (51)$$

Thus the total directional radiance of the canopy is

$$\pi L (\theta,\theta_s) = \pi L \text{ (layer)} + \pi L_{soil}$$

Let $E_1 (\theta_s) = E (-d,o) + E_s (o) \cos\theta_s$

Then the directional reflectance is:

$$R (\theta,\theta_s) = \pi L (\theta,\theta_s)/E_1 (\theta_s). \quad (52)$$

APPENDUM A

EXPRESSIONS FOR u_1, v_1, and w_1

$$\Delta L\ (\theta_n) = L_{E_S} + L_{E(+d)} + L_{E(-d)} = \frac{u_1}{\pi} E(+d) + \frac{v_1}{\pi} E(-d) + \frac{w_1}{\pi} E_S\ .$$

We give below the exact expressions of u_1, v_1, and w_1.

$$u_1 = [(\rho + \tau)(\tfrac{2}{\pi})^2 \{\pi \cos^2\theta_n\ [(\alpha_c' - \pi) \cos\theta \cos\theta_n + \sin\alpha_c' \sin\theta \sin\theta_n]$$

$$+ ((2\alpha_c' - \pi \cos\theta \cos^2\theta_n + 2\sin\alpha_c' \sin\theta \sin\theta_n \cos\theta_n).$$

$$\int_{\frac{\pi}{2} - \theta_n}^{\frac{\pi}{2}} \cos\theta \cos^{-1}(-\cot\theta \cot\theta_n)\, d\theta + ((2\alpha_c' \pi) \cos\theta \cos\theta_n \sin\theta_n$$

$$+ 2\sin\alpha_c' \sin\theta \sin^2\theta_n) \int_{\frac{\pi}{2} - \theta_n}^{\frac{\pi}{2}} \sqrt{1 - \frac{\cos^2\theta}{\sin^2\theta_n}}\, d\theta$$

$$- (1 - \cos\theta_n)\, \pi \cos\theta_n\, (\alpha_c' \cos\theta \cos\theta_n + \sin\alpha_c' \sin\theta \sin\theta_n)\}$$

$$+ 2\cos\theta \cos^2\theta_n\, \tau]\, \sin\theta$$

$$v_1 = [(\rho + \tau)(\tfrac{2}{\pi})^2 \{\pi \cos^2\theta_n\ [(\alpha_c' - \pi) \cos\theta \cos\theta_n + \sin\alpha_c' \sin\theta \sin\theta_n]$$

$$+ ((2\alpha_c' - \pi) \cos\theta \cos^2\theta_n + 2\sin\alpha_c' \sin\theta \sin\theta_n \cos\theta_n)$$

$$\int_{\frac{\pi}{2} - \theta_n}^{\frac{\pi}{2}} \cos\theta \arccos(-\cot\theta \cot\theta_n)\, d\theta + ((2\alpha_c' - \pi) \cos\theta \sin\theta_n \cos\theta_n$$

$$+ 2\sin\alpha_c' \sin\theta \sin^2\theta_n) \int_{\frac{\pi}{2} - \theta_n}^{\frac{\pi}{2}} \sqrt{1 - \frac{\cos^2\theta}{\sin^2\theta_n}}\, d\theta$$

$$- (1 - \cos\theta_n)\, \pi \cos\theta_n\, (\alpha_c' \cos\theta \cos\theta_n + \sin\alpha_c' \sin\theta \sin\theta_n)\}$$

$$+ 2\cos\theta \cos^2\theta_n\, \rho]\, \sin\theta$$

and

$$w_1 = [(\rho + \tau)\frac{2}{\pi}\{\cos\theta_s \cos\theta \cos^2\theta_n (2\alpha_c\alpha_c' - \pi\alpha_c - \pi\alpha_c')$$

$$+ \cos\theta_s \sin\theta \sin\theta_n \cos\theta_n \sin\alpha_c' (2\alpha_c - \pi) + \sin\theta_s \cos\theta \sin\theta_n \cos\theta_n$$

$$\sin\alpha_c (2\alpha_c' - \pi) + 2\sin\theta_s \sin\theta \sin^2\theta_n \sin\alpha_c \sin\alpha_c'\}$$

$$+ 2\cos\theta_s \cos\theta \cos^2\theta_n \rho] \sin\theta$$

APPENDUM B

EXPRESSIONS FOR w, w', u, v

$$\Delta L \text{ (layer)} = \frac{2}{\pi} dA \left\{ \frac{E_S}{\pi} w + \frac{E(+d)}{\pi} u + \frac{E(-d)}{\pi} v \right\}$$

We explicitly give the coefficients w, w', u, v.

$$w = 2\pi \cos\theta_s \cos\theta \sin\theta \rho \int_0^{\frac{\pi}{2} - \theta_s} S(\theta_n) \cos^2\theta_n \, d\theta_n$$

$$+ \sin\theta_o \left(2 (\rho + \tau) \cos\theta_s \cos\theta_o \int_{\frac{\pi}{2} - \theta_s}^{\frac{\pi}{2} - \theta_o} S(\theta_n) \cos^2\theta_n \cos^{-1} (-\cot\theta_s \cot\theta_n) \, d\theta_n - 2 (\rho + \tau) \pi \cos\theta_s \cos\theta_o \int_{\frac{\pi}{2} - \theta_s}^{\frac{\pi}{2} - \theta_o} S(\theta_n) \cos^2\theta_n \, d\theta_n \right.$$

$$+ (\rho + \tau) 2 \sin\theta_s \cos\theta_o \int_{\frac{\pi}{2} - \theta_s}^{\frac{\pi}{2} - \theta_o} S(\theta_n) \sin\theta_n \cos\theta_n \sin \{\cos^{-1} (-\cot\theta_n \cot\theta_s)\} \, d\theta_n$$

$$\left. + 2\pi \cos\theta_s \cos\theta_o \rho \int_{\frac{\pi}{2} - \theta_s}^{\frac{\pi}{2} - \theta_o} S(\theta_n) \cos^2\theta_n \, d\theta_n \right)$$

$$+ (\rho + \tau) \frac{2}{\pi} \sin\theta_o \left(2 \cos\theta_s \cos\theta_o \int_{\frac{\pi}{2} - \theta_o}^{\frac{\pi}{2}} S(\theta_n) \cos^{-1} (-\cot\theta_n \cot\theta_s) \cos^{-1} (-\cot\theta_n \cot\theta_o) \cos^2\theta_n \, d\theta_n \right.$$

$$\left. - \pi \cos\theta_s \cos\theta_o \int_{\frac{\pi}{2} - \theta_o}^{\frac{\pi}{2}} S(\theta_n) \cos^2\theta_n \cos^{-1} (-\cot\theta_n \cot\theta_s) \, d\theta_n \right.$$

$$\left. - \pi \cos\theta_s \cos\theta_o \int_{\frac{\pi}{2} - \theta_o}^{\frac{\pi}{2}} S(\theta_n) \cos^2\theta_n \cos^{-1} (-\cot\theta_n \cot\theta_o) \, d\theta_n \right.$$

$$+ 2 \cos\theta_s \sin\theta_o \int_{\frac{\pi}{2} - \theta_o}^{\frac{\pi}{2}} S(\theta_n) \sin\theta_n \cos\theta_n \sin(\cos^{-1}(-\cot\theta_n \cot\theta_o))$$

$$\cos^{-1}(-\cot\theta_n \cot\theta_s)\, d\theta_n - \pi \cos\theta_s \sin\theta_o \int_{\frac{\pi}{2} - \theta_o}^{\frac{\pi}{2}} S(\theta_n) \sin\theta_n \cos\theta_n$$

$$\sin(\cos^{-1}(-\cot\theta_n \cot\theta_o))\, d\theta_n$$

$$+ 2 \sin\theta_s \cos\theta_o \int_{\frac{\pi}{2} - \theta_o}^{\frac{\pi}{2}} S(\theta_n) \sin\theta_n \cos\theta_n \sin(\cos^{-1}(-\cot\theta_n \cot\theta_s))$$

$$\cos^{-1}(-\cot\theta_n \cot\theta_o)\, d\theta_n$$

$$- \pi \sin\theta_s \cos\theta_o \int_{\frac{\pi}{2} - \theta_o}^{\frac{\pi}{2}} S(\theta_n) \sin\theta_n \cos\theta_n \sin(\cos^{-1}(-\cot\theta_n \cot\theta_s))\, d\theta_n$$

$$+ 2 \sin\theta_s \sin\theta_o \int_{\frac{\pi}{2} - \theta_o}^{\frac{\pi}{2}} S(\theta_n) \sin^2\theta_n \sin(\cos^{-1}(-\cot\theta_n \cot\theta_s)) \sin$$

$$(\cos^{-1}(-\cot\theta_n \cot\theta_o))\, d\theta_n) + 2\pi \cos\theta_s \cos\theta_o \rho \sin\theta_o \int_{\frac{\pi}{2} - \theta_o}^{\frac{\pi}{2}}$$

$$S(\theta_n) \cos^2\theta_n\, d\theta_n.$$

$$u = \sin\theta_o \left[\frac{4}{\pi^2}(\rho + \tau)\left(\pi \cos\theta_o \int_0^{\frac{\pi}{2} - \theta_o} \int_{\frac{\pi}{2} - \theta_n}^{\frac{\pi}{2}} S(\theta_n) \cos^2\theta_n \cos\theta\right.\right.$$

$$\cos^{-1}(-\cot\theta \cot\theta_n)\, d\theta\, d\theta_n$$

$$+ \pi \cos\theta_o \int_0^{\frac{\pi}{2} - \theta_o} \int_{\frac{\pi}{2} - \theta_n}^{\frac{\pi}{2}} S(\theta_n) \sin\theta_n \cos\theta_n \sqrt{1 - \frac{\cos^2\theta}{\sin^2\theta_n}}\, d\theta\, d\theta_n$$

$$\left.\left. - \pi^2 \cos\theta_o \int_0^{\frac{\pi}{2} - \theta_o} S(\theta_n)(1 - \cos\theta_n) \cos^2\theta_n\, d\theta_n\right)\right.$$

$$+ 4 \cos\theta_o \tau \int_0^{\frac{\pi}{2} - \theta_o} S(\theta_n) \cos^2\theta_n \, d\theta_n$$

$$+ \frac{4}{\pi^2} (\rho + \tau)(\pi \cos\theta_o \int_{\frac{\pi}{2} - \theta_o}^{\frac{\pi}{2}} S(\theta_n) \cos^3\theta_n \cos^{-1} (-\cot\theta_n \cot\theta_o) \, d\theta_n$$

$$- \pi^2 \cos\theta_o \int_{\frac{\pi}{2} - \theta_o}^{\frac{\pi}{2}} S(\theta_n) \cos^3\theta_n \, d\theta_n$$

$$+ \pi \sin\theta_o \int_{\frac{\pi}{2} - \theta_o}^{\frac{\pi}{2}} S(\theta_n) \sin\theta_n \sin (\cos^{-1} (-\cot\theta_n \cot\theta_o)) \cos^2\theta_n \, d\theta_n$$

$$+ 2 \cos\theta_o \int_{\pi}^{\frac{\pi}{2}} \int_{\frac{\pi}{2} - \theta_n}^{\frac{\pi}{2}} S(\theta_n) \cos^2\theta_n \cos^{-1} (-\cot\theta_n \cot\theta) \cos\theta$$

$$\cos^{-1} \qquad \theta_n) \, d\theta \, d\theta_n$$

$$- \pi \cos\theta_o \int_{\frac{\pi}{2} - \theta_o}^{\frac{\pi}{2}} \int_{\frac{\pi}{2} - \theta_n}^{\frac{\pi}{2}} S(\theta_n) \cos^2\theta_n \cos\theta \cos^{-1} (-\cot\theta \cot\theta_n) \, d\theta \, d\theta_n$$

$$+ 2 \sin\theta_o \int_{\frac{\pi}{2} - \theta_o}^{\frac{\pi}{2}} \int_{\frac{\pi}{2} - \theta_n}^{\frac{\pi}{2}} S(\theta_n) \sin\theta_n \cos\theta_n \sin(\cos^{-1} (\cot\theta_n \cot\theta_o))$$

$$\cos^{-1} (-\cot\theta \cot\theta_n) \, d\theta \, d\theta_n$$

$$+ 2 \cos\theta_o \int_{\frac{\pi}{2} - \theta_o}^{\frac{\pi}{2}} \int_{\frac{\pi}{2} - \theta_n}^{\frac{\pi}{2}} S(\theta_n) \sin\theta_n \cos\theta_n \cos^{-1} (-\cot\theta_n \cot\theta_o)$$

$$\sqrt{1 - \frac{\cos^2\theta}{\sin^2\theta_n}} \, d\theta \, d\theta_n$$

$$- \pi \cos\theta_o \int_{\frac{\pi}{2} - \theta_o}^{\frac{\pi}{2}} \int_{\frac{\pi}{2} - \theta_n}^{\frac{\pi}{2}} S(\theta_n) \sin\theta_n \cos\theta_n \sqrt{1 - \frac{\cos^2\theta}{\sin^2\theta_n}} \, d\theta \, d\theta_n$$

$$+ 2 \sin\theta_o \int_{\frac{\pi}{2} - \theta_o}^{\frac{\pi}{2}} \int_{\frac{\pi}{2} - \theta_n}^{\frac{\pi}{2}} S(\theta_n) \sin^2\theta_n \sin(\cos^{-1}(-\cot\theta_n \cot\theta_o)$$

$$\sqrt{1 - \frac{\cos^2\theta}{\sin^2\theta_n}}\, d\theta\, d\theta n$$

$$- \pi \cos\theta_o \int_{\frac{\pi}{2} - \theta_o}^{\frac{\pi}{2}} S(\theta_n)\,(1 - \cos\theta_n) \cos^2\theta_n \cos^{-1}(-\cot\theta_n \cot\theta_o)\, d\theta_n$$

$$- \pi \sin\theta \int_{\frac{\pi}{2} - \theta_s}^{\frac{\pi}{2}} S(\theta_n) \sin\cos^{-1}(-\cot\theta_n \cot\theta_o) \sin\theta_n \cos\theta_n$$

$$(1 - \cos\theta_n)\, d\theta_n$$

$$+ 4 \cos\theta_o\, \tau \int_{\frac{\pi}{2} - \theta_o}^{\frac{\pi}{2}} S(\theta_n) \cos^2\theta_n\, d\theta_n] \,.$$

$$v = \sin\theta_o \left[\frac{4}{\pi^2}(\rho + \tau)\left(\pi \cos\theta_o \int_0^{\frac{\pi}{2} - \theta_o} \int_{\frac{\pi}{2} - \theta_n}^{\frac{\pi}{2}} S(\theta_n) \cos^2\theta_n \cos\theta\right.\right.$$

$$\cos^{-1}(-\cot\theta \cot\vartheta_n)\, d\theta\, d\theta_n$$

$$+ \pi \cos\theta_o \int_o^{\frac{\pi}{2} - \theta_o} \int_{\frac{\pi}{2} - \theta_n}^{\frac{\pi}{2}} S(\theta_n) \sin\theta_n \cos\theta_n \sqrt{1 - \frac{\cos^2\theta}{\sin^2\theta_n}}\, d\theta\, d\theta_n$$

$$\left. - \pi^2 \cos\theta_o \int^{\frac{\pi}{2} - \theta_o} S(\theta_n)\,(1 - \cos\theta_n) \cos^2\theta_n\, d\theta_n\right)$$

$$+ 4 \cos\theta_o\, \rho \int_0^{\frac{\pi}{2} - \theta_o} S(\theta_n) \cos^2\theta_n\, d\theta_n$$

$$+ (\rho + \tau)\frac{4}{\pi^2}\left(\pi \cos\theta_o \int_{\frac{\pi}{2} - \theta_o}^{\frac{\pi}{2}} S(\theta_n) \cos^3\theta_n \cos^{-1}(-\cot\theta_o \cot\theta_n)\, d\theta_n\right.$$

$$- \pi^2 \cos\theta_o \int_{\frac{\pi}{2} - \theta_o}^{\frac{\pi}{2}} S(\theta_n) \cos^3\theta_n \, d\theta_n + \pi \sin\theta_o \int_{\frac{\pi}{2} - \theta_o}^{\frac{\pi}{2}} S(\theta_n) \sin\theta_n$$

$$\cos^2\theta_n \sin\left(\cos^{-1}\left(-\cot\theta_n \cot\theta_o\right)\right) d\theta_n$$

$$+ 2 \cos\theta_o \int_{\frac{\pi}{2} - \theta_o}^{\frac{\pi}{2}} \int_{\frac{\pi}{2} - \theta_n}^{\frac{\pi}{2}} S(\theta_n) \cos^2\theta_n \cos^{-1}\left(-\cot\theta_n \cot\theta_o\right)$$

$$\cos\theta \cos^{-1}\left(-\cot\theta_n \cot\theta\right) d\theta \, d\theta_n$$

$$- \pi \cos\theta_o \int_{\frac{\pi}{2} - \theta_o}^{\frac{\pi}{2}} \int_{\frac{\pi}{2} - \theta_n}^{\frac{\pi}{2}} S(\theta_n) \cos^2\theta_n \cos\theta \cos^{-1}\left(-\cot\theta \cot\theta_n \, d\theta \, d\theta_n\right.$$

$$+ 2 \sin\theta_o \int_{\frac{\pi}{2} - \theta_o}^{\frac{\pi}{2}} \int_{\frac{\pi}{2} - \theta_n}^{\frac{\pi}{2}} S(\theta_n) \sin\left(\cos^{-1}\left(-\cot\theta_o \cot\theta_n\right)\right) \sin\theta_n \cos\theta_n$$

$$\cos\theta \cos^{-1}\left(-\cot\theta \cot\theta_n\right) d\theta \, d\theta_n$$

$$+ 2 \cos\theta_o \int_{\frac{\pi}{2} - \theta_o}^{\frac{\pi}{2}} \int_{\frac{\pi}{2} - \theta_n}^{\frac{\pi}{2}} S(\theta_n) \sin\theta_n \cos\theta_n \cos^{-1}\left(-\cot\theta_o \cot\theta_n\right)$$

$$\sqrt{1 - \frac{\cos^2\theta}{\sin^2\theta_n}} \, d\theta \, d\theta_n$$

$$- \pi \cos\theta_o \int_{\frac{\pi}{2} - \theta_o}^{\frac{\pi}{2}} \int_{\frac{\pi}{2} - \theta_n}^{\frac{\pi}{2}} S(\theta_n) \sin\theta_n \cos\theta_n \sqrt{1 - \frac{\cos^2\theta}{\sin^2\theta_n}} \, d\theta \, d\theta_n$$

$$+ 2 \sin\theta_o \int_{\frac{\pi}{2} - \theta_o}^{\frac{\pi}{2}} \int_{\frac{\pi}{2} - \theta_n}^{\frac{\pi}{2}} S(\theta_n) \sin^2(\theta_n) \sin\left(\cos^{-1}\left(-\cot\theta_o \cot\theta_n\right)\right)$$

$$\sqrt{1 - \frac{\cos^2\theta}{\sin^2\theta_n}} \, d\theta \, d\theta n$$

$$- \pi \cos\theta_o \int_{\frac{\pi}{2} - \theta_o}^{\frac{\pi}{2}} S(\theta_n) (1 - \cos\theta_n) \cos^2\theta_n \cos^{-1} (-\cot\theta_o \cot\theta_n) \, d\theta_n$$

$$- \pi \sin\theta_o \int_{\frac{\pi}{2} - \theta_o}^{\frac{\pi}{2}} S(\theta_n) (1 - \cos\theta_n) \cos\theta_n \sin\theta_n \sin (\cos^{-1}$$

$$(-\cot\theta_o \cot\theta_n)) \, d\theta_n$$

$$+ 4 \rho \cos\theta_o \int_{\frac{\pi}{2} - \theta_o}^{\frac{\pi}{2}} S(\theta_n) \cos^2\theta_n \, d\theta_n].$$

and

$$w' = 2 \rho \cos\theta_s \cos\theta_o \sin\theta_o \int_0^{\frac{\pi}{2} - \theta_o} S(\theta_n) \cos^2\theta_n \, d\theta_n$$

$$+ \sin\theta_o (2 (\rho + \tau) \cos\theta_s \cos\theta_o \int_{\frac{\pi}{2} - \theta_o}^{\frac{\pi}{2} - \theta_s} S(\theta_n) \cos^2\theta_n \cos^{-1}$$

$$(-\cot\theta_o \cot\theta_n) \, d\theta_n$$

$$- 2 \pi (\rho + \tau) \cos\theta_s \cos\theta_o \int_{\frac{\pi}{2} - \theta_o}^{\frac{\pi}{2} - \theta_s} S(\theta_n) \cos^2\theta_n \, d\theta_n$$

$$+ 2 (\rho + \tau) \cos\theta_s \sin\theta_o \int_{\frac{\pi}{2} - \theta_o}^{\frac{\pi}{2} - \theta_s} S(\theta_n) \sin\theta_n \cos\theta_n \sin (\cos^{-1}$$

$$(-\cot\theta_o \cot\theta_n)) \, d\theta_n$$

$$+ 2 \pi \cos\theta_s \cos\theta_o \rho \int_{\frac{\pi}{2} - \theta_o}^{\frac{\pi}{2} - \theta_s} S(\theta_n) \cos^2\theta_n \, d\theta_n$$

$$+ \frac{2}{\pi} (\rho + \tau) \sin\theta_o (2 \cos\theta_s \cos\theta_o \int_{\frac{\pi}{2} - \theta_s}^{\frac{\pi}{2}} S(\theta_n) \cos^{-1} (-\cot\theta_s \cot\theta_n)$$

$$\cos^{-1} (-\cot\theta_o \cot\theta_n) \cos^2\theta_n \, d\theta_n$$

$$- \pi \cos\theta_s \cos\theta_o \int_{\frac{\pi}{2} - \theta_s}^{\frac{\pi}{2}} S(\theta_n) \cos^2\theta_n \cos^{-1}(-\cot\theta_n \cot\theta_s)\, d\theta_n$$

$$- \pi \cos\theta_s \cos\theta_o \int_{\frac{\pi}{2} - \theta_s}^{\frac{\pi}{2}} S(\theta_n) \cos^2\theta_n \cos^{-1}(-\cot\theta_n \cot\theta_o)\, d\theta_n$$

$$+ 2 \cos\theta_s \sin\theta_o \int_{\frac{\pi}{2} - \theta_s}^{\frac{\pi}{2}} S(\theta_n) \sin\theta_n \cos\theta_n \sin(\cos^{-1}(-\cot\theta \cot\theta_n)$$

$$\cos^{-1}(-\cot\theta_s \cot\theta_n)\, d\theta_n$$

$$- \pi \cos\theta_s \sin\theta_o \int_{\frac{\pi}{2} - \theta_s}^{\frac{\pi}{2}} S(\theta_n) \sin\theta_n \cos\theta_n \sin(\cos^{-1}(-\cot\theta \cot\theta_n))\, d\theta_n$$

$$+ 2 \sin\theta_s \cos\theta_o \int_{\frac{\pi}{2} - \theta_s}^{\frac{\pi}{2}} S(\theta_n) \sin\theta_n \cos\theta_n \sin(\cos^{-1}(-\cot\theta_s \cot\theta_n))$$

$$\cos^{-1}(-\cot\theta_o \cot\theta_n)\, d\theta_n$$

$$- \pi \sin\theta_s \cos\theta_o \int_{\frac{\pi}{2} - \theta_s}^{\frac{\pi}{2}} S(\theta_n) \sin\theta_n \cos\theta_n \sin(\cos^{-1}(-\cot\theta_s \cot\theta_n))\, d\theta_n$$

$$+ 2 \sin\theta_s \sin\theta_o \int_{\frac{\pi}{2} - \theta_s}^{\frac{\pi}{2}} S(\theta_n) \sin^2\theta_n \sin(\cos^{-1}(-\cot\theta_s \cot\theta_n))$$

$$\sin(\cos^{-1}(-\cot\theta_o \cot\theta_n))\, d\theta_n)$$

$$+ 2 \pi \cos\theta_s \cos\theta_o \sin\theta_o \rho \int_{\frac{\pi}{2} - \theta_s}^{\frac{\pi}{2}} S(\theta_n) \cos^2\theta_n\, d\theta_n \,.$$

REFERENCES

Allen, W. A., T. V. Gayle, and A. J. Richardson. 1970. Plant-Canopy Irradiance Specified by the Duntley Equations. J. Opt. Soc. Am. 60(3):372-376.

Anderson, M. C. 1966. Stand Structure and Light Penetration. II: A Theoretical Analysis. J. Appl. Ecol. 3:41-54.

Balick, L. K., R. K. Scoggins, and L. E. Link. 1981. Inclusion of a Simple Vegetation Layer in Terrain Temperature Models for Thermal IR Signature Prediction. IEEE Trans. on Geosc. and Rem. Sens. GE-19:143.

Bunnik, N. J. J. 1978. The Multispectral Reflectance of Short-wave Radiation by Agricultural Crops in Relation with Their Morphological and Optical Properties. Thesis, H. Veemann en Zonen, Wageningen, The Netherlands.

Burden, R. L., J. D. Faires, and A. C. Reynolds. 1978. Numerical Analysis. Prindle, Weber an Schmidt, 579 p.

Colwell, J. E. 1974. Vegetation Canopy Reflectance. Rem. Sens. Environ. 3:175-183.

Cooper, K., J. A. Smith, and D. Pitts. 1982. Reflectance of a Vegetation Canopy Using the Adding Method. Appl. Opt. 21:4112.

Cowan, I. R. 1968. The Interception and Absorption of Radiation in Plant Stands. J. Appl. Ecol. 5:367-379.

DeWit, C. T. 1965. Photosynthesis of Leaf Canopies. Agr. Res. Report 663, Center for Agricultural Publications and Documentation, Wageningen, The Netherlands.

Donohoe, P. A. 1981. Abstract Measurement and Analysis of Solar Radiation in Forest Stands: A New Approach. Thesis, Yale University, 117 p.

Duntley, S. Q. 1942. The Optical Properties of Diffusing Material. J. Opt. Soc. Am. 32(2):61-70.

Goudriaan, J. 1973. A Calculation Model and Descriptive Formulas for the Extinction and Reflection of Radiation in Leaf Canopies. Proc. The Sun in Service of Mankind. Paris.

Impens, I. and R. Lemeur. 1969. Extinction of Net Radiation in Different Crop Canopies. Arch. Met. Geoph. Biokl., Ser. B. 17:403-412.

Isobe, S. 1962. Preliminary Studies on Physical Properties of Plant Communities. Bull. Nat. Inst. Agric. Sci., Tokyo, Ser. A, 9:29-67.

Kimes, D. S. and J. A. Smith. 1980. Simulation of Solar Radiation Absorption in Vegetation Canopies. Appl. Opt. 19:2801.

Kimes, D. S., J. A. Smith, and L. E. Link. 1981. Thermal IR Exitance Model of a Plant Canopy. Appl. Opt. 20:623.

Kimes, D. S., J. A. Smith, and K. J. Ranson. 1982. Vegetation Reflectance Measurements as a Function of Solar Zenith Angle. Photog. Eng. and Rem. Sens. 46:1563.

Kimes, D. S. and J. A. Kirchner. 1982. Radiative Transfer Model for Heterogeneous 3D Scenes. Appl. Opt. 21:4119.

Kirchner, J. A., S. Youkhana, and J. A. Smith. 1982. Influence of Sky Radiance Distribution on the Ratio Technique for Estimating Bidirectional Reflectance. Photog. Eng. and Rem. Sens. 48:995.

Landsberg, J. J., R. G. Jarvis and M. B. Slater. 1973. The Radiation Regime of a Spruce Forest. In. Plant Response to Climatic Factors, Proc. Uppsala Symp., UNESCO, Paris, pp. 411-418.

Lemeur, R. and B. L. Blad. 1974. A Critical Review of Light Models for Estimating the Shortwave Radiation Regime of Plant Canopies. Agricultural Meteorology 14:255-286.

McCree, K. J. and R. S. Loomis. 1969. Photosynthesis in Fluctuating Light. Ecology, 50(3):422-428.

Miller, P. C. 1967. Leaf Orientation and Energy Exchange in Quaking Aspen (Populus tremuloids) and Gambell's Oak (Quercus gambellii) in Central Colorado. Oecol. Plant. 2:241-270

Monsi, M. and T. Saeki. 1953. Über den Lichtfaktor in den Pflanzengesellschaften und seine Boedeutung für die Stoffproducktion. Jap. J. Bot. 14:22-52.

Norman, J. M. 1980. Interfacing Leaf and Canopy Light Interception Models in Predicting Photosynthesis for Ecosystem Models. CRC Press, Inc. Boca Raton, Florida, Vol. 2, 279 p.

Ranson, K. J., V. D. Vanderbilt, L. L. Biehl, B. F. Robinson, and M. E. Bauer. Soybean Canopy Reflectance as a Function of View and Illumination Geometry. 1981. Proc. 15th Int'l. Symp. Rem. Sens. Environ., Ann Arbor, Michigan.

Smith, J. A. 1980. Vegetation Canopy Thermal Model. Presentation to Extraordinary Meeting, Working Group D, NATO Special Group of Experts on Concealment, Camouflage, and Deception. U. S. Army Engineer, Waterways Experiment Station (WES).

Smith, J. A. 1982. Reflectance Models and Field Measurements: Some Issues. Proc. 26th Int'l. SPIE symposium. San Diego, CA.

Smith, J. A., J. K. Berry, and F. J. Heimes. 1976. Signature Extension for Sun Angle. Final Report, NASA/JSC, NAS9-14467.

Smith, J. A. and R. E. Oliver. 1972. Plant Canopy Models for Simulating Composite Scene Spectroradiance. Proc. 8th Symp. Rem. Sens. Environ., Ann Arbor, Michigan, 2:1333-1353.

Smith, J. A., K. J. Ranson, D. Nguyen, L. Balick, L. E. Link, L. Fritschen, and B. Hutchison. 1981. Thermal Vegetation Canopy Model Studies. Rem. Sens. of Environ. 11:311.

Suits, G. H. 1972. The Calculation of the Directional Reflectance of a Vegetation Canopy. Rem. Sens. of Environ. 2:117-125.

Verhoef, W. and N. J. J. Bunnik. 1981. Influence of Crop Geometry on Multispectral Reflectance Determined by the Use of Canopy Reflectance Models. Symposium on Signatures Spectrales d'objects, en te'le'de'tection, held in Avigon, France, September 8-11, 1981. pp. 273-290.

Warren, Wilson J. 1967. Stand Structure and Light Penetration. III. Sunlit Foliage Area. J. Appl. Eco. 4(1):159-165.

APPENDIX A: ABSTRACTS OF PUBLISHED PAPERS AND RELATED PRESENTATIONS

Contributions representing direct funding by ARO

Contributions representing cooperative efforts

Extraordinary Meeting, Working Group D
NATO SPECIAL GROUP OF EXPERTS ON CONCEALMENT,
CAMOUFLAGE, AND DECEPTION

U. S. Army Engineer Waterways Experiment Station (WES)
Vicksburg, Mississippi
14-18 January 1980

AGENDA

Modelling/Simulation Techniques
Monday, 14 January

0830-0845	Welcome	COL Nelson Conover Commander and Director WES
0845-0900	Administrative Matters	Dr. L. E. Link Environmental Laboratory WES
0900-0930	Terrain Surface Thermal Model	Dr. L. Balick and Mr. R. Scoggins Environmental Laboratory WES
0930-1000	Vegetation Canopy Thermal Model	Dr. J. Smith Colorado State University
1000-1030	Break	
1030-1100	Finite Element Models for Camouflage	Dr. G. Huebner West Germany
1100-1130	Camouflage Effectiveness Evaluation Procedure	Dr. K. Vattrodt West Germany
1130-1230	Image Modification Concepts	Dr. L. E. Link
1230-1330	Lunch	
1330-1500	Application of Models and Image Modification Techniques	Mr. Curt Gladen and Mr. Randy Scoggins WES
1500-1530	Break	
1530-1630	Discussion	

Reprinted from APPLIED OPTICS, Vol. 19, page 2801, August 15, 1980

Simulation of solar radiation absorption in vegetation canopies

D. S. Kimes and J. A. Smith

A solar radiation canopy absorption model, including multiple scattering effects, was developed and tested for a lodgepole pine (*Pinus contorta*) canopy. Reflectance above the canopy, spectral transmittance to the ground layer, and geometric and spectral measurements of canopy elements were made. Relatively large differentials occurred in spectral absorption by canopy layers, especially in the photosynthetically active region, as a function of solar zenith angle. In addition, the proportion of total global irradiance absorbed by individual layers varied greatly as a function of solar zenith angle. However, absorption by the entire canopy system remained relatively constant.

I. Introduction

The manner in which a vegetation canopy absorbs solar radiation has an important effect on both the thermal properties and the photosynthetic efficiency of the canopy. Thus, an understanding of these principles is important in remote sensing with respect to military, agricultural, forestry, and ecological applications. In recent years the thermal region of the electromagnetic spectrum has received keen interest in the field of remote sensing. This region may add valuable additional information to make inferences concerning the characteristics of vegetation canopies. However, before the thermal emission characteristics of a canopy can be understood, the manner in which the canopy absorbs solar radiation must be studied. In the field of agriculture, there is strong evidence that the solar radiation distribution within a canopy as a function of canopy structure strongly affects the productivity of the canopy.[1-3]

Physically based mathematical models serve as convenient tools for studying the complex radiation–vegetation interactions. The objective of this investigation was to develop a model to study spectral and total solar radiation absorption in vegetation canopies as a function of solar zenith angle. The following describes the absorption model and the application of the model to a lodgepole pine (*Pinus contorta*) canopy at Leadville, Colorado, for which a data base was collected during 1977.[4] A complete study site description is given by Ranson *et al.*[4] The specific canopy modeled consisted of a cluster of four lodgepole pine trees with these mean statistics: 6.0-m height, 30-yr age, 13.2-cm diam breast height, and a surrounding stand of 102-m^2/ha basal area.

II. Solar Radiation Canopy Models

Several deterministic models have been developed to study the interactions of solar radiation within vegetation canopies. Allen and Richardson,[5] Alderfer and Gates,[6] and Suits[7] have adapted a system of simultaneous differential equations, developed by Kubelka and Munk,[8] in various ways to vegetation canopies. The Suits model includes geometric effects and predicts non-Lambertian characteristics of vegetation canopies. Chance and LeMaster[9] derived a light absorption model for vegetative plant canopies from the Suits reflectance model.

Another approach developed by Oliver and Smith[10] is the solar radiation vegetation canopy (SRVC) model. This model simulates the solar radiation flow through the canopy by using Monte Carlo techniques. This stochastic model predicted the diurnal apparent directional spectral reflectance of a vegetation canopy.

The ray tracing technique used in the SRVC model is advantageous when applied to solar radiation interactions within vegetation canopies for several reasons.

(1) The model can accept any relevant parameter, such as the number of components, the optical properties of the components, and the spatial dispersion and density of the components.

(2) Diffuse skylight is treated as a set of independent source vectors.

D. S. Kimes is with NASA Goddard Space Flight Center, Earth Resources Branch, Greenbelt, Maryland 20771, and J. A. Smith is with Colorado State University, College of Forestry & Natural Resources, Fort Collins, Colorado 80523.

Received 21 January 1980.
0003-6935/80/162801-11$00.50/0.

Reprinted from APPLIED OPTICS, Vol. 20, page 623, February 15, 1981

Thermal IR exitance model of a plant canopy

D. S. Kimes, J. A. Smith, and L. E. Link

A thermal IR exitance model of a plant canopy based on a mathematical abstraction of three horizontal layers of vegetation was developed. Canopy geometry within each layer is quantitatively described by the foliage and branch orientation distributions and number density. Given this geometric information for each layer and the driving meteorological variables, a system of energy budget equations was determined and solved for average layer temperatures. These estimated layer temperatures, together with the angular distributions of radiating elements, were used to calculate the emitted thermal IR radiation as a function of view angle above the canopy. The model was applied to a lodgepole pine (*Pinus contorta*) canopy over a diurnal cycle. Simulated vs measured radiometric average temperatures of the midcanopy layer corresponded within 2°C. Simulation results suggested that canopy geometry can significantly influence the effective radiant temperature recorded at varying sensor view angles.

I. Introduction

The thermal IR region (3–20 μm) of the electromagnetic spectrum may provide valuable information about the characteristics of natural or man-made targets. With the advent of satellite thermal sensor systems (e.g., the Heat Capacity Mapping Mission and the proposed Thematic Mapper on Landsat D as well as multispectral aircraft scanners), it is becoming more important to relate underlying scene phenomena to the remote sensing observables.[1] In both the design and utilization of electrooptical sensors it is important to be able to estimate the statistical characteristics of the target and background as a function of sensor parameters. Often empirical methods are used to obtain these required data.[2,3]

An alternative approach is to employ a physically based or process-oriented model of the scene.[4,5] This latter approach is particularly useful and often required when detailed or subtle characteristics of a target need to be enhanced.

Many thermal models exist for different nonvegetated targets of interest and for planar solid objects. For example, Watson[6] developed a thermal model for predicting the diurnal surface temperature variation of the ground, and the University of Michigan[7] developed a model for the prediction of time-dependent temperatures and radiance of planar targets and backgrounds. However, few thermal models exist for plant canopies; and in agriculture and forestry applications, vegetation is the primary target of interest.

Gates[8] presented an energy budget for a single plant leaf isolated in space, as did Kimes *et al.*[9] and Wiebelt and Henderson.[10] Other investigators have modeled the thermal dynamics of vegetation canopies assuming a simplistic single homogeneous layer abstraction. For example, vegetation was treated as a single homogeneous layer with an associated transmission factor for solar radiation in the University of Michigan model.[7] Heilman *et al.*[11] used thermal scanning data to measure crop effective radiant temperatures and used an evapotranspiration (ET) equation to estimate crop ET. They assumed that the sensor was viewing only the top layer of the crop, and they ignored the effects of canopy geometry on sensor response.

It is known that vegetation canopies are non-Lambertian at optical wavelengths primarily due to canopy geometry.[12] Similarly, in the thermal region, it is believed that while individual canopy elements are isotropic radiators, the response from the canopy may also be non-Lambertian, because canopy geometry causes spatial variations in many energy flow processes.

A primary objective of this paper is to describe a thermal IR exitance model of a plant canopy, which includes a detailed accounting of vegetation structure. The model was applied to a lodgepole pine canopy over a diurnal cycle. This treatment is then shown to result in angular variations in predicted thermal radiance.

D. S. Kimes is with NASA Goddard Space Flight Center, Earth Resources Branch, Greenbelt, Maryland 20771; J. A. Smith is with Colorado State University, Department of Forest & Wood Sciences, Fort Collins, Colorado 80523; and L. E. Link is with U.S.A.E. Waterways Experiment Station, Environmental Laboratory, Vicksburg, Mississippi 39180.

Received 7 March 1980.
0003-6935/81/040623-10$00.50/0.

REMOTE SENSING OF ENVIRONMENT 11:311-326(1981)

Thermal Vegetation Canopy Model Studies

J. A. SMITH, K. J. RANSON, D. NGUYEN, L. BALICK,

College of Forestry and Natural Resources, Colorado State University, Fort Collins, Colorado 80523

L. E. LINK,

Environmental Laboratory, U.S. Army Corps of Engineers Waterways Experiment Station, Vicksburg, Mississippi 39180

L. FRITSCHEN,

College of Forest Resources, University of Washington, Seattle, Washington 98115

and

B. HUTCHISON

Atmospheric Turbulence and Diffusion Laboratory, Oak Ridge, Tennessee 37830

An iterative-type thermal model applicable to forest canopies was tested with data from two diverse forest types. The model framework consists of a system of steady-state energy budget equations describing the interactions of short- and long-wave radiation within three horizontally infinite canopy layers. A state-space formulation of the energy dynamics within the canopy is used which permits a factorization of canopy geometrical parameters from canopy optical and thermal coefficients as well as environmental driving variables. Two sets of data characterizing a coniferous (Douglas-fir) and deciduous (oak-hickory) canopy were collected to evaluate the thermal model. The results show that the model approximates measured mean canopy temperatures to within 2°C for relatively clear weather conditions and deviates by a maximum of 3°C for very hazy or foggy conditions.

Introduction

Rapid and accurate assessment of renewable resources is an increasingly important task facing remote sensing specialists. Mathematical abstraction of energy processes of vegetation canopies is a useful technique for relating sensor response to environment–canopy interactions. Such an understanding is required in order to make timely inferences about the condition of forestry and agricultural resources from remote sensors. In the thermal regime, several authors have reported success in estimating evapotranspiration of crops from thermal sensor data (Heilman et al., 1976; Reginato et al., 1976; and Soer, 1980). Several models have been reported that describe the energy balance of vegetation either in terms of a single leaf (Gates, 1968; Wiebelt and Henderson, 1977; and Kimes et al., 1978), or an abstract layered canopy (Alderfer and Gates, 1971; and Deardorff, 1978). Few models have been described that characterize the energy flows within vegetation canopies as a function of the canopy geometry (Goudriaan, 1977; Norman, 1979; and Kimes et al., 1981).

52 Vanderbilt Ave., New York, NY 10017

0034-4257/81/040311+16$02.50

Reflectance of a vegetation canopy using the Adding method

K. Cooper, J. A. Smith, and D. Pitts

The Adding method has been used to calculate vegetation canopy bidirectional reflectance. Appropriate reflection and transmission matrices for canopy and underlying soil layers are developed in terms of canopy geometry and basic optical properties. The model is illustrated by comparisons with field reflectance measurements for blue grama (*Bouteloua gracilis*) and soybeans (Calahan 9250). Calculations using the Suits model are also included for comparison.

I. Introduction

The interaction of electromagnetic radiation with vegetation canopies is an intriguing problem and an understanding of such interactions has application to the remote sensing of renewable resources. During the past ten years several investigators have applied modeling techniques to predict vegetation reflectance or as an aid in interpreting remotely sensed data. The modeling problem generally separates into two parts. The first part is the selection of an appropriate mathematical solution technique to describe the radiative transfer interactions within the canopy. The second requirement is the development of appropriate abstractions of a canopy which permit the determination of electromagnetic parameters in terms of biophysical attributes.

Existing models which have been applied to the 1-D canopy case include the Allen *et al.*,[1] Suits,[2] and Park and Deering,[3] models based on the Duntley approach, the Monte Carlo approach of Smith and Oliver,[4] the application of first-order scattering theory by Ross and Nilson,[5] and the method of discrete ordinates used by Weinman and Guetter.[6] Models based solely on geometric optics are being evaluated for selected terrain materials; for example, Richardson *et al.*,[7] Egbert,[8] Jackson, *et al.*,[9] and Strahler and Li.[10] Finally, combined geometric optics and radiative transfer formulations of the canopy reflectance problem are being attempted, most notably by Verhoef and Bunnik[11] and Welles and Norman.[12]

In this paper we describe a new vegetation reflectance model based on the Adding method of van de Hulst.[13] The technique has been modified slightly to adapt it to the interaction of shortwave radiation within a vegetation canopy. The required scattering matrices for the canopy layers are developed using an abstraction of the canopy similar to that of the model of Smith and Oliver; that is, reflecting and transmitting leaf facets whose orientations may be described by a leaf-slope distribution. Example comparisons of the model with field measurements and with the Suits model are also given.

II. Adding Method

Consider two arbitrary horizontal layers X_i and X_{i-1} of a scattering medium so that X_i lies above X_{i-1}, with the following properties: (1) all radiation incident from above on X_{i-1} is either absorbed or scattered back upward; and (2) radiation incident on X_i may be reflected, transmitted, or absorbed. Let s_i describe flux incident on X_i from above and define R_i and T_i to be operators for layer i so that the flux from s_i reflected back upward is $R_i s_i$ and that transmitted toward layer $i-1$ is $T_i s_i$. If R_{i-1} describes the response of X_{i-1} to incident radiation, the flux scattered back from X_{i-1} to X_i is given by $R_{i-1}(T_i s_i)$. Finally, define two additional operators R_i' and T_i' for X_i which describe how layer i responds to flux incident from below. The flux reflected from X_{i-1} and transmitted through X_i is given by $T_i'(R_{i-1}T_i s_i)$, while that reflected back toward X_{i-1} is $R_i'(R_{i-1}T_i s_i)$.

The scattering of flux back and forth between the two layers is indicated schematically in Fig. 1 and leads to a series to describe the total flux s_i' escaping X_i upward:

$$s_i' = [R_i + T_i' R_{i-1} T_i + T_i' R_{i-1} R_{i-1}' R_{i-1} T_i + \ldots] s_i,$$

$$s_i' = \left[R_i + T_i' R_{i-1} \left[\sum_{n=0}^{\infty} (R_i' R_{i-1})^n\right] T_i\right] s_i.$$

D. Pitts is with NASA Lyndon B. Johnson Space Center, Earth Resources Branch, Houston, Texas 77058; the other authors are with Colorado State University, College of Forestry Natural Resources, Fort Collins, Colorado 80523.

Received 1 February 1982.

AD-A122 940 MATHEMATICAL STRUCTURE OF ELECTROMAGNETIC TERRAIN FEATURE CANOPY MODELS(U) COLORADO STATE UNIV FORT COLLINS COLL OF FORESTRY AND NATURAL.. J A SMITH

UNCLASSIFIED NOV 82 ARO-16628.5-GS DAAG29-79-C-0199 F/G 12/1 NL

2/2

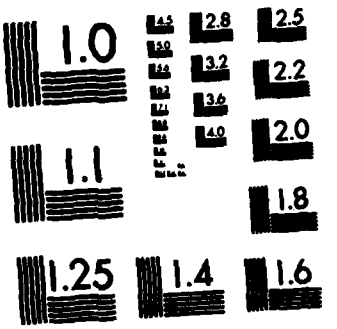

D. S. Kimes
NASA Goddard Space Flight Center
Greenbelt, MD 20771
J. A. Smith
K. J. Ranson*
College of Forestry and Natural Resources
Colorado State University
Fort Collins, CO 80523

Vegetation Reflectance Measurements as a Function of Solar Zenith Angle

The wide variability in diurnal reflectance is caused by variations in anisotropic sky irradiance, canopy component geometry and optical properties, and type of reflectance measurement.

Abstract: *An understanding of the behavior of vegetation canopy reflectance as a function of solar zenith angle is important to several remote sensing applications. Spectral hemispherical-conical reflectances of a nadir looking sensor were taken throughout the day of a lodgepole pine and two grass canopies. Mathematical simulations of both a spectral hemispherical-conical reflectance factor and a spectral bi-hemispherical reflectance were performed for two theoretical canopies of contrasting geometric structure. These results and results from literature studies showed a great amount of variability of vegetation canopy reflectances as a function of solar zenith angle. Explanations for this variability are discussed and recommendations for future measurements are proposed.*

Introduction

An understanding of solar radiation interaction with vegetation canopies is necessary for accurately interpreting remotely sensed data. Broad- and narrow-band spectral reflectance measurements of vegetation canopies are often used to characterize this interaction. Measured reflectance, however, is a complex function of canopy constituent optical properties (Gates, 1970; Knipling, 1970), canopy geometry (Ross, 1976; Kimes *et al.*, 1979b) optical properties of the ground, atmospheric conditions (Kriebel, 1976; Ross, 1976), solar zenith angle (Smith *et al.*, 1974; Kriebel, 1975; Jarvis *et al.*, 1976), and sensor inclination and azimuthal view angles (Smith and Oliver, 1974; Kriebel, 1978; Smith *et al.*, 1979).

Understanding variations in canopy reflectance as a function of solar zenith angle is important for several remote sensing applications. For example, such knowledge can improve multitemporal vegetation classification by using sun-angle signature extension techniques (Smith *et al.*, 1975). At higher latitudes low sun-angles predominate and an understanding of the reflectance changes at low sun-angles would be beneficial. Diurnal reflectance trends are also important in photosynthetic and productivity studies (Kimes *et al.*, 1980).

To better understand these relationships, spectral reflectance measurements were obtained for several solar zenith angles for a lodgepole pine

* Now with the Laboratory for Applications of Remote Sensing (LARS), Purdue University, 1220 Potter Drive, West Lafayette, IN 47906.

Photogrammetric Engineering and Remote Sensing, Vol. 46, No. 12, December 1980, pp. 1563-1573.

J. A. KIRCHNER
Earth Resources Branch
NASA Goddard Space Flight Center
Greenbelt, MD 20771
S. YOUKHANA
J. A. SMITH
College of Forestry and Natural Resources
Colorado State University
Fort Collins, CO 80523

Influence of Sky Radiance Distribution on the Ratio Technique for Estimating Bidirectional Reflectance

The error induced in the estimation of bidirectional reflectance factors using the standard ratio technique is less than five percent for zenith view and sun angles less than 55 degrees.

ABSTRACT: *The technique of ratioing scene radiance to the radiance obtained from standard Lambertian reference panels in order to estimate bidirectional reflectance factors may depend on the angular distribution of the diffuse irradiance field as well as the direct solar irradiance. A simulation study was performed to estimate the magnitude of this effect for differing clear sky irradiance distributions for a variety of vegetated surfaces. For the seven surfaces and wavelengths analyzed, the error induced in the estimation of bidirectional reflectance factors using the standard ratio technique was less than 5 percent for zenith view and sun angles less than 55 degrees.*

INTRODUCTION

THE BIDIRECTIONAL reflectance distribution function, BRDF, of a surface is an intrinsic property of the material and is independent of incident irradiance (Kriebel, 1976). In reality, one generally utilizes the average of the BRDF over finite solid angles of incidence and exitance. This average quantity is termed the (bidirectional) reflectance factor, R, and is also defined to be the ratio of the radiant flux reflected by the surface to that which similarly would be reflected by a Lambertian surface under the same viewing and illumination geometries (Robinson and Biehl, 1979). A commonly used measurement method to estimate (bidirectional) reflectance factors is to ratio the radiance of a target to the radiance of a standard Lambertian reference panel for varying view and sun angles.

Several authors have recently highlighted the potential errors induced in this method by a time varying irradiance field and have suggested potential improvements in the measurement procedures (Duggin, 1980; Duggin, 1981; Milton, 1981; Richardson, 1981). A second potential source of error is that induced by the diffuse sky radiance field. The interaction of the angular sky irradiance distribution with target reflectance anisotropies yields contributions to the target radiance in addition to that induced by the direct solar term. In order to yield a bidirectional reflectance factor corresponding to the solar incidence direction, these contributions of the sky radiance distribution are implicitly assumed to be negligible. For

PHOTOGRAMMETRIC ENGINEERING AND REMOTE SENSING,
Vol. 48, No. 6, June 1982, pp. 955-959.

0099-1112/82/4806-0955$02.25/0

556-42

Reflectance models and field measurements: some issues

James A. Smith

College of Forestry and Natural Resources, Colorado State University
Fort Collins, Colorado 80523

Abstract

Electro-optical field measurements of scene reflectance, together with appropriate target characterization, will play an increasingly important role in the testing, intercomparison, and extension of scene radiation models. Such models, in turn, will serve to extrapolate the range of applicability of field measurements to a wider set of environmental conditions and sensor/source viewing geometries than could practically be obtained by direct measurement. This paper presents several issues which must be addressed before such a symbiotic relationship between modeling and measurement approaches can be achieved. The direct comparison of model predictions with field measurements is seen to be a somewhat more subtle task than might be suspected.

Introduction

In order to intelligently design sensor systems operating in the optical reflective regime to extract or identify earth surface terrain features, one must have an understanding of the basic electro-optical properties of such features. With our increased capability to measure radiation patterns at varying spatial and temporal scales, the limiting factor now appears not so much how to construct such devices, but rather what their operating parameters should be. In the remote sensing field, similar comments are also applicable to our data processing capabilities. We have the technological capability to process large data volumes in a timely fashion, but still need to utilize fundamental understanding of terrain element behavior in the design of appropriate algorithms. Smith gave a recent overview of the role of scene radiation models in remote sensing applications.[1] It is evident from the review that in the past 20 years several candidate calculational procedures and media abstractions have been developed to relate reflectance behavior to intrinsic target characteristics. In order to effectively utilize these candidate tools, the system designer must have a feeling for their relative trade-offs and range of applicability to his particular problem areas. To achieve this goal, the models must be subjected to field measurement comparisons. The purpose of this paper is to raise some issues that should be considered in such modeling/measurement comparisons and to point out some potential pitfalls to be avoided. It should become evident that field measurement experiments developed in support of modeling activities must consider additional factors than those programs whose primary mission is to develop empirical characterizations of overall terrain element electro-optical behavior.

In this paper, a brief overview of some broad issues is first given, followed by an example illustrating some of the issues raised.

Issues

The fundamental intrinsic physical property governing the reflectance behavior of a scene element is its bidirectional reflectance distribution function, BRDF[2]. An objective of reflectance modeling is typically to develop relationships between the BRDF and biophysical or other meaningful attributes of the terrain element under study. In a strict sense, the BRDF is unmeasureable and more commonly, it is the integration of this quantity over finite solid angles of incidence and exitance yielding the reflectance factor[3] which is actually estimated in field measurements. Both of these quantities are precisely defined, but the fact that they vary spectrally, directionally, and that it is, in practice, difficult to develop precise and distict definitions of target categories, leads to considerable pragmatic confusion as is evident in the literature. In the natural world, these quantities must really be considered stochastic variables which means that one is always sampling from a distribution whose properties are really presently poorly understood. Also, since the quantity directly measured by radiometers is the radiance, which is a convolving of the bidirectional reflectance distribution function with the radiance field and instrument characteristics, indirect experimental techniques, subject to all their whimsy, are actually employed.

In this paper the following problem is analyzed: "What are some of the issues that must be considered when electro-optical field measurements are obtained in support of physical oriented reflectance models (or, perhaps, vice-versa)?" Three broad issues are considered, to wit:

Inclusion of a Simple Vegetation Layer in Terrain Temperature Models for Thermal IR Signature Prediction

LEE K. BALICK, R. K. SCOGGINS, AND L. E. LINK

Abstract—A time-dependent energy budget model was designed to enable the prediction of the temperature of terrain scene elements that contain a simple layer of vegetation and to diagnose the effect of vegetation on remotely sensed temperatures. The model was developed for use as a module in conjunction with existing nonvegetated-terrain temperature models. Vegetation was assumed to be a horizontally homogeneous but porous layer partially covering a specified ground surface. Energy budgets for the foliage and the ground were evaluated separately but are interdependent.

The sensitivity of the vegetation module (VEGIE), to its input variables when used in tandem with a bare-ground model, TSTM, was examined and found to be most strongly dependent on the degree of foliage cover. The model results were verified against measurements made on two moderate days for a 10-cm high-grass canopy in Germany and were compared to results from a complex vegetation model. Results were highly satisfactory and similar for both models. Both models were also applied to forest canopies where assumptions of the simple model were not valid. As expected, the simple model did not perform well, but the complex model was satisfactory. The VEGIE/TSTM system was then applied to diagnosing the effects of various amounts of foliage cover over low emittance soil, with and without reflection of sky thermal IR energy.

I. Introduction

A. Background

RECENT ANALYTICAL and theoretical studies of the thermal infrared (IR) emission characteristics of terrain surfaces have generally ignored the effects of vegetation on thermal IR signatures [1]-[3]. This seems to be due, in part, to the lack of a usable tool for examining the effects of vegetation in real-world situations. In truth the problem is very complex. Models of vegetation temperature which can be directly applied to remote sensing problems [4]-[6] are complex and require careful specification of intracanopy meteorological conditions, canopy structure, and biophysical characteristics which are not often available. Observational and analytical studies are consistent with the models in detailing the complexity of the problem [7]-[15].

A major goal of ongoing work at the U.S. Army Engineer Waterways Experiment Station (WES) is to develop the ability to predict realistic thermal signatures of natural and cultural terrain features for any time-of-day and weather conditions. Work on models for complex vegetation canopies and for planar unvegetated surfaces has pointed to the need to fill the gap between these extremes. A model for predicting the time-varying temperature for an unvegetated planar surface using material thermophysical properties and meteorological conditions was developed under previous WES research [16]. This model, the terrain surface temperature model (TSTM), is briefly discussed in Part II of this paper. Logically, the next step was to develop a module, or submodel, for use in conjunction with the TSTM to account for the dominant effects of a simple layer of vegetation on thermal IR signatures of the terrain surface. Such a capability would be useful even if it only applied to the simplest of canopies in nonextreme environments. It would allow the TSTM to be extended to areas of lawn, pasture, and perhaps rangelands. The module developed in this context was named VEGIE and is described in this paper.

B. Objectives and Scope

The specific objectives of the work presented herein were to develop the capability to predict the temperature of terrain scene elements that contain a simple layer of vegetation and to diagnose the effect of vegetation on remotely sensed temperatures of terrain elements. VEGIE was designed for immediate application to thermal IR signature prediction and analytical studies while more complete and theoretical treatments of the problem were under way. It was also required that VEGIE maintain the operational flexibility and simplicity of the planar surface model, TSTM. Some of the more important of the TSTM characteristics are:

1) time dependence and fast response to environmental changes;
2) air temperature considered a state variable;
3) materials treated as horizontally and vertically homogeneous layers;

Manuscript received February 27, 1981. This work was supported by the Department of the Army under Project 4A762730AT42, Task 4A, Terrain/Operations Simulation, Work Unit 003, Electromagnetic Target Surround Characteristics in Natural Terrains, and the Department of the Army Project No. 4A762719AT40, Task CO, Theather of Operations Construction, Work Unit 006, Fixed Installations Camoflage.

The authors are with USAE Waterways Experiment Station, Environmental Laboratory, P.O. Box 631, Vicksburg, MS 39180.

0196-2892/81/0700-0143$00.75

Radiative transfer model for heterogeneous 3-D scenes

D. S. Kimes and J. A. Kirchner

A general mathematical framework for simulating processes in heterogeneous 3-D scenes is presented. Specifically, a model was designed and coded for application to radiative transfers in vegetative scenes. The model is unique in that it predicts (1) the directional spectral reflectance factors as a function of the sensor's azimuth and zenith angles and the sensor's position above the canopy, (2) the spectral absorption as a function of location within the scene, and (3) the directional spectral radiance as a function of the sensor's location within the scene. The model was shown to follow known physical principles of radiative transfer. Initial verification of the model as applied to a soybean row crop showed that the simulated directional reflectance data corresponded relatively well in gross trends to the measured data. However, the model can be greatly improved by incorporating more sophisticated and realistic anisotropic scattering algorithms.

I. Introduction

Understanding the nature of the interactions between electromagnetic radiation and terrestrial scenes is necessary to utilize remotely sensed data effectively. Mathematical models which simulate these radiant interactions are valuable quantitative tools for relating the physical features of the terrestrial scene and radiant sources to the radiant response of the scene. In some cases these models can be used to infer underlying scene attributes using remotely sensed data. Presently, most models are one-dimensional in that they treat one or more layers of spatially homogeneous material that extends infinitely in the horizontal direction.

There is a need for a general modeling framework for complex scenes which are spatially heterogeneous in three dimensions. A number of important scenes are extremely variable spatially and cannot be treated by 1-D models. For example, forest canopies often have large natural openings between the tree crowns; incomplete row crop canopies show an extreme spatial variation between rows; military detection and camouflage problems within clumps of vegetation are 3-D problems; and urban scenes are also complex 3-D scenes.

The difficulty in modeling any complex 3-D structure is accounting for the many phenomena that occur with variable intensities throughout the scene. The following proposed 3-D model may provide a general accounting framework for many 3-D modeling problems where processes vary in intensity and direction of movement as a function of spatial location. Specifically, the model described in this study was designed and coded for application to radiative transfers in vegetative scenes. However, the basic principles of the model may provide a general framework for other 3-D scenes and other processes.

Several mathematical models have been developed for vegetation canopies in the optical wavelengths. Most of these models treat homogeneous canopies which vary structurally only with height (1-D models) and are reviewed by Cooper *et al.*[1] Exceptions include geometric optic models for row crops developed by both Richardson *et al.*[2] and Jackson *et al.*[3] and for forest canopies by Strahler and Li.[4] In addition, several models combine both radiative transfer and geometric optic techniques as are the extended versions of the 1-D Suits model[5] for row crops developed by Verhoef and Bunnik,[6] the more general extension of the Suits 1-D model for row crops by Suits,[7] and the 3-D reflectance model based on an array of ellipsoids by Welles and Norman.[8] Several other models with more simplistic assumptions and/or empirical characterizations are reviewed by Smith and Ranson.[9]

In this paper we present the concepts of a general mathematical framework for simulating processes in heterogeneous 3-D scenes. Specifically, in this study the model is applied to radiant transfers (reflective wavelengths—visible and near IR) in vegetation canopies with both homogeneous structure and row crop structure. The model simulates the multiple scattering which occurs within the scene given the global distribution of solar irradiance conditions and the optical properties and spatial structure of the scene components. The model predicts (1) the directional spectral reflectance factors as a function of the sensor's azimuth

The authors are with NASA Goddard Space Flight Center, Earth Resources Branch, Greenbelt, Maryland 20771.

Received 7 August 1982.